

The dynamical and magnetized interstellar medium

François LEVRIER

Soutenance d'Habilitation à Diriger des Recherches



Laboratoire d'Étude du Rayonnement et de la Matière en Astrophysique





About me...

« Maître de conférences » (Assistant Professor) at ENS Paris since September 2008
LERMA, LRA, ENS Paris, Observatoire de Paris, UPMC

Former positions

- 2007-2008 : Postdoc at the University of Oxford (SKADS FP7 European program)
- 2004-2007 : Postdoc as « Agrégé-préparateur » at LERMA/ENS
- 2000-2004 : PhD thesis and teaching assistant at LERMA/University Paris VII

Teaching activities

- « Préparation à l'agrégation de physique » [mostly laboratory work, M2 level]
- « Formation interuniversitaire de Physique » [Introductory Astrophysics, L3 level]
- Master « Astronomie, Astrophysique et Ingénierie Spatiale » [Radiative transfer, M2 level]

Pedagogical responsibilities

- Deputy-director for « Préparation à l'agrégation de physique »
- ENS representative for Master « Astronomie, Astrophysique et Ingénierie Spatiale »
- Jury member for ENS admission

Committee memberships

- Member of Planck-HFI's Core Team and Planck Scientist
- Elected member of LERMA laboratory council
- Elected member of ENS Physics Department council
- Appointed member of CNU section 34
- Member of IRAM's Program Committee

Publications

- 92 since 2001 (shown as Planck Collaboration I (2016))
- 26 as first author or major contributor (shown as Planck Collaboration Int. XIX (2015))

Student and post-doc supervision

- Post-docs : Jérémie Neveu [ENS, 2014-2015]
- PhD students : Manuel Berthet [ENS, 2013-2017]
- PhD jurys : Jean-François Robitaille [Université Laval, Québec, 2014]
- M2 students : Rémy Paulin [2011], Manuel Berthet [2012], Bilal Ladjelate [2013]
- M1 students : Brice Poillot [2011]
- Tutoring at ENS : Rémy Paulin, Sandrine Codis, Pierre Mourier, Félix Driencourt-Mengin, Jan Orkisz, Paul Caucal, Jordan Philidet
- Internship jurys : 46 internship jurys [L3 to M2 level]

Talk outline

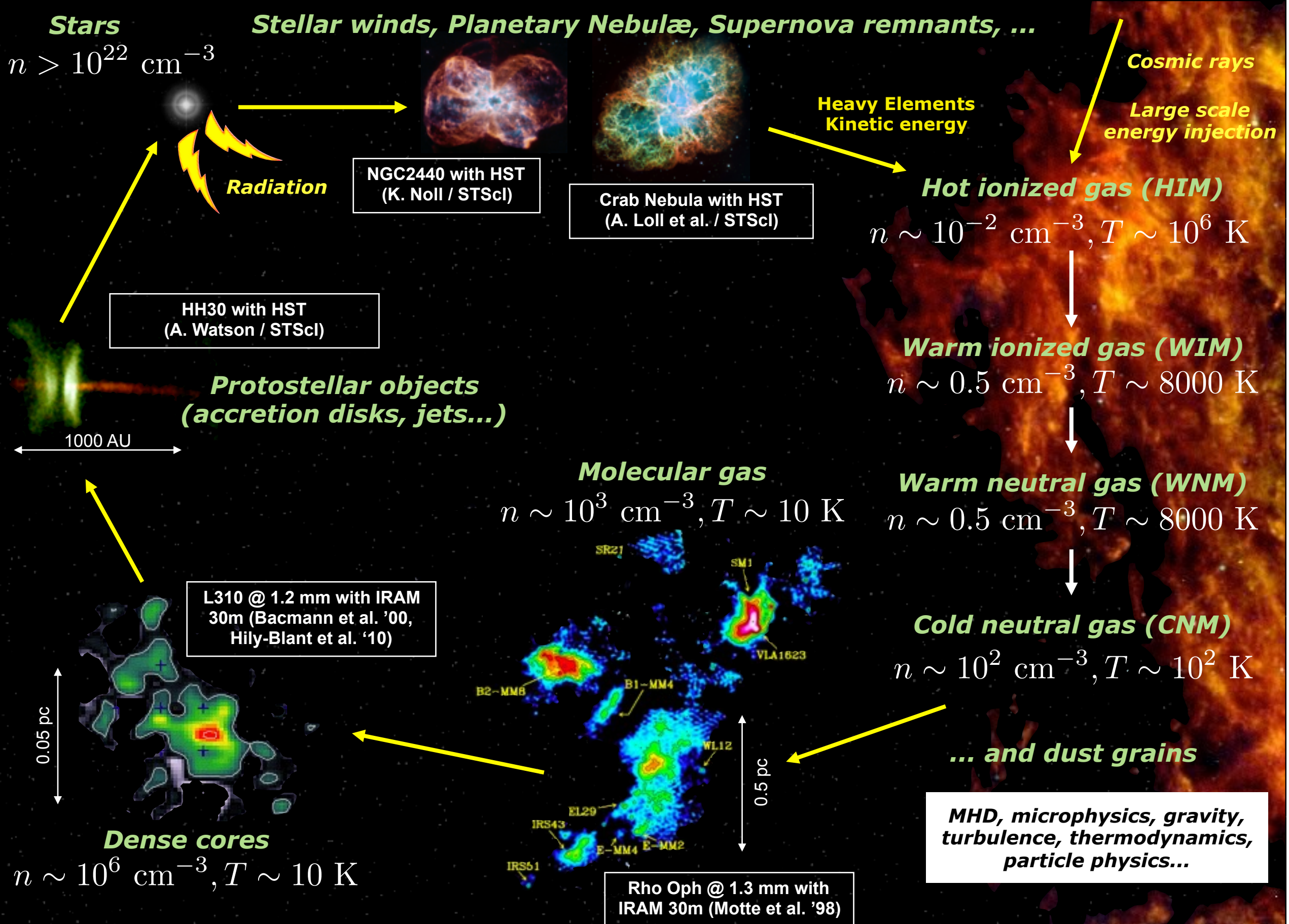
- The turbulent and magnetized interstellar medium : an overview
- The Planck mission
- Main Planck results on the turbulent and magnetized ISM
- Perspectives

The interstellar medium (ISM)

Image credit: Robert Gendler (www.robgendlerastropics.com)

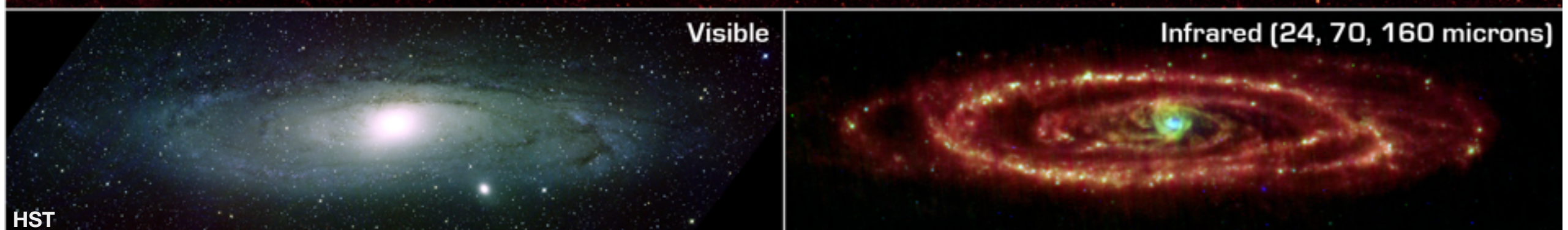
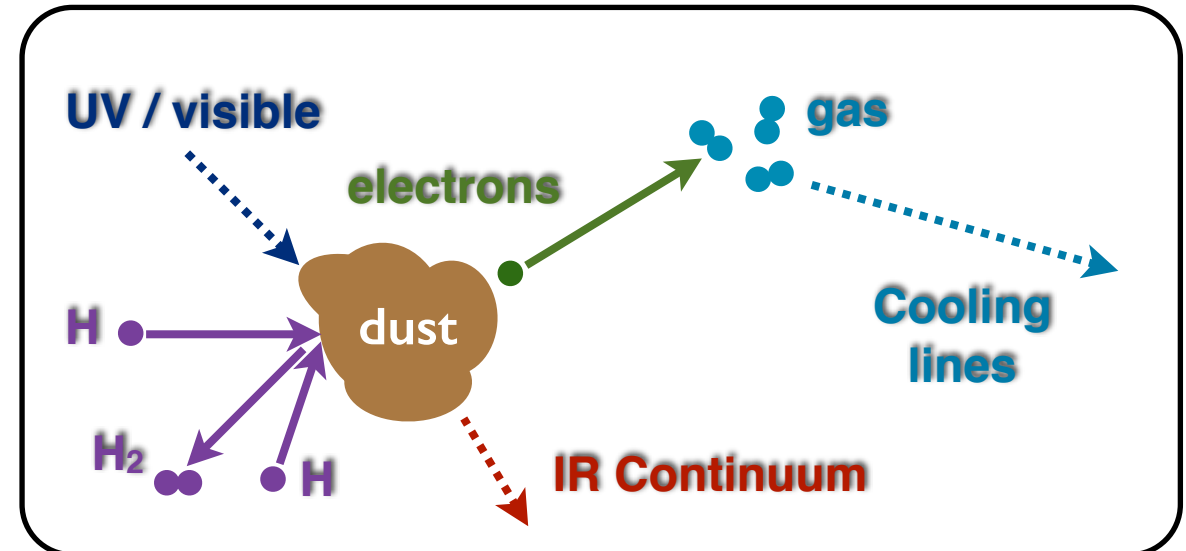
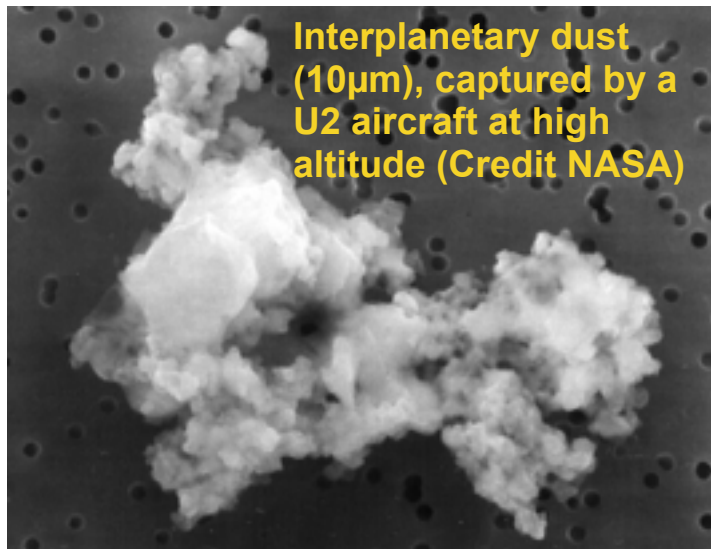
- 1% of the total mass of the Galaxy
- Gas (mainly hydrogen) and dust particles
- The locus of star formation
- Mechanical processes : turbulence and shocks
- Thermodynamical processes : gas heating and cooling
- Electromagnetic processes : radiative transfer, magnetic field
- Quantum processes : Species excitation, radiative transfer
- Chemical processes : in the gas phase and on grain surfaces

Star formation and the cycle of interstellar matter



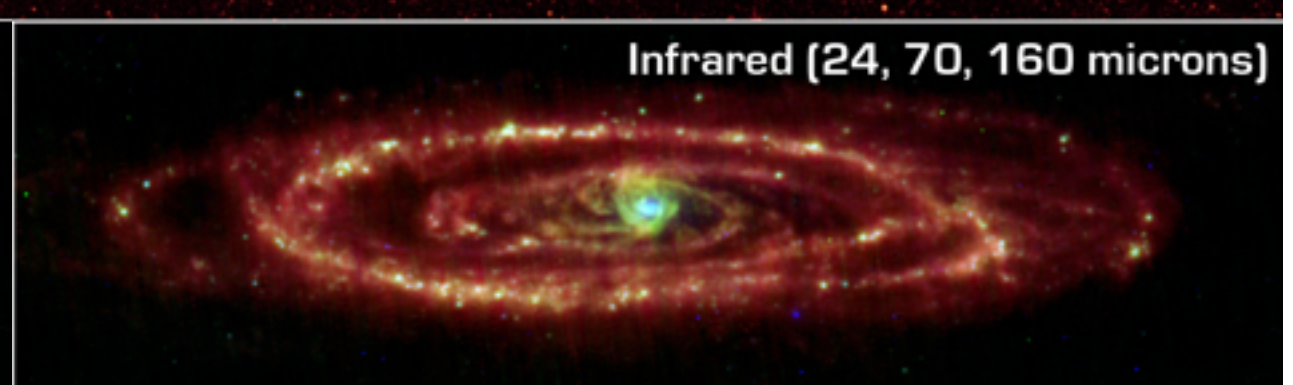
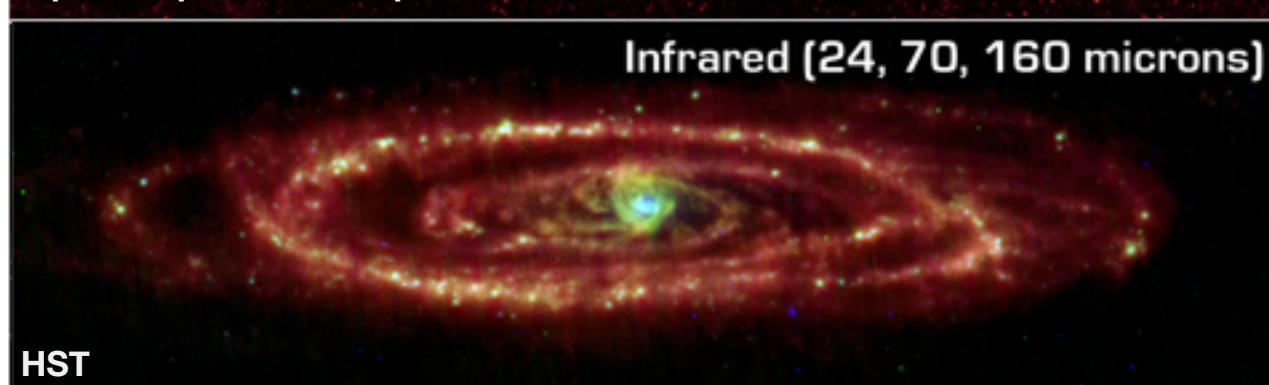
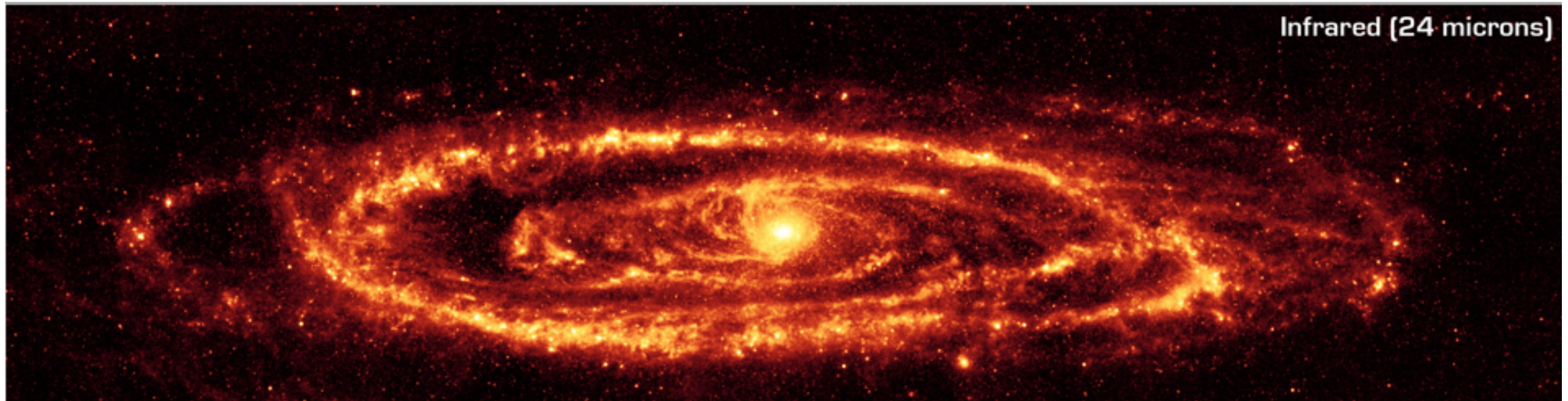
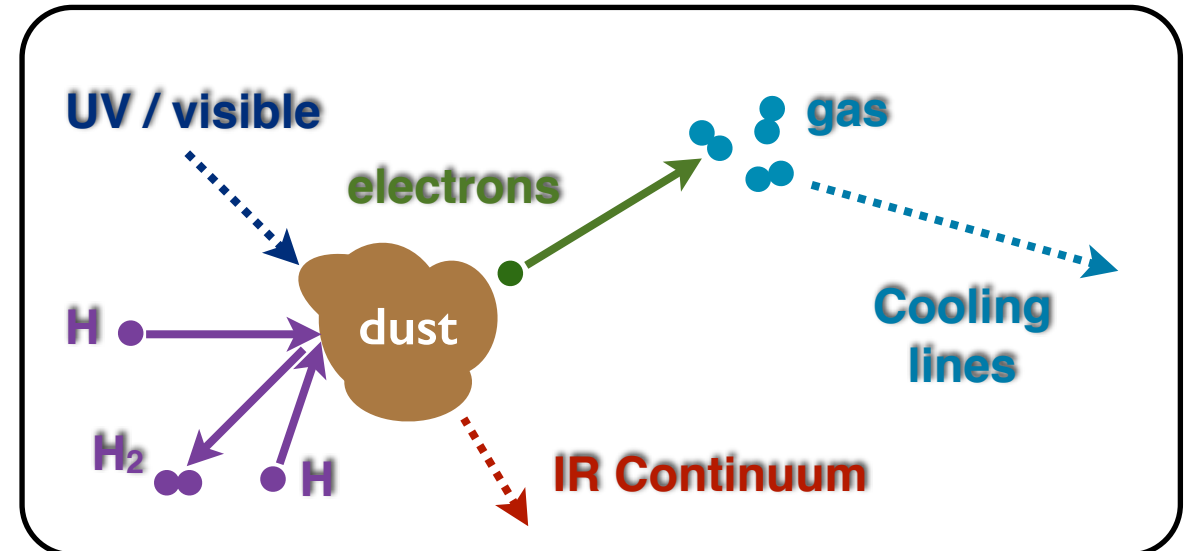
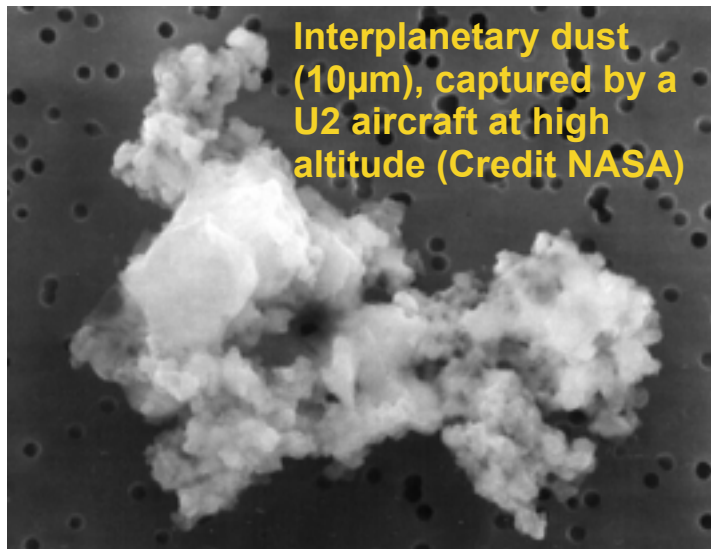
Interstellar dust grains

- Carbonaceous and silicate aggregates (1 nm to 10 μm)
- Starlight reprocessing from visible/UV to IR
- Chemical processes on grain surfaces
- Gas heating via photoelectric effect



Interstellar dust grains

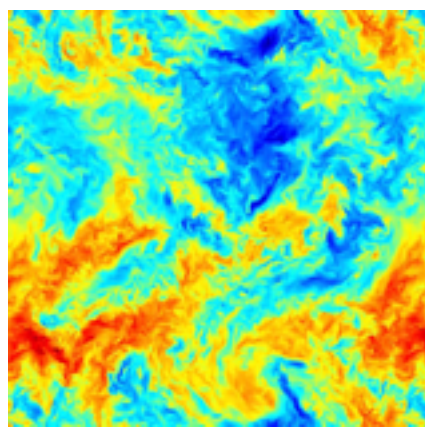
- Carbonaceous and silicate aggregates (1 nm to 10 μm)
- Starlight reprocessing from visible/UV to IR
- Chemical processes on grain surfaces
- Gas heating via photoelectric effect



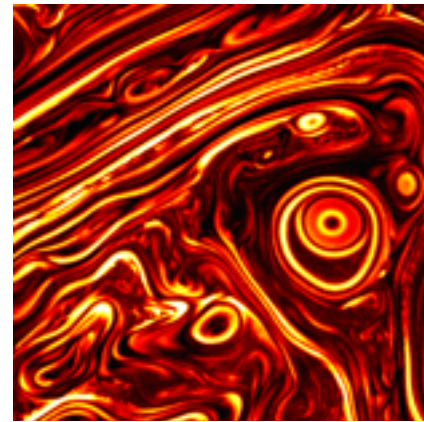
Turbulence

*« Big whirls have little whirls
that feed on their velocity,
and little whirls have lesser whirls
and so on to viscosity. »*

Lewis Fry Richardson (1920)

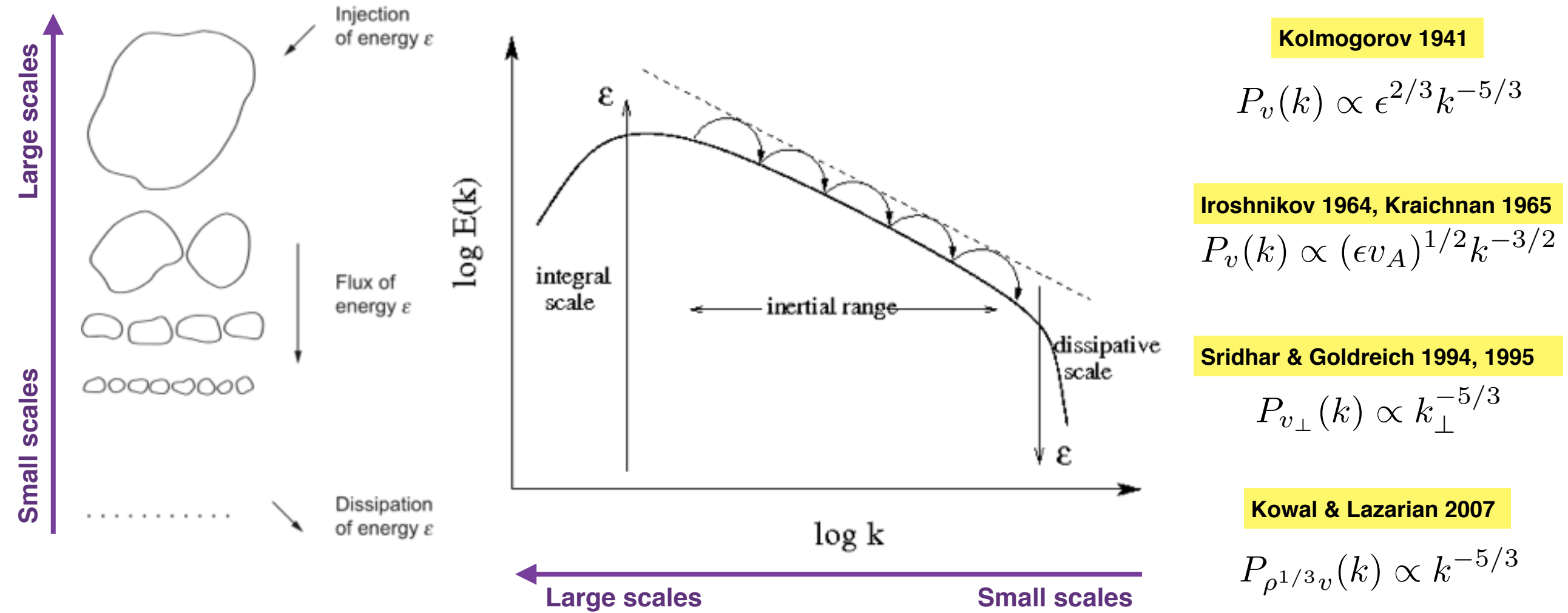


Vorticity (JHU)



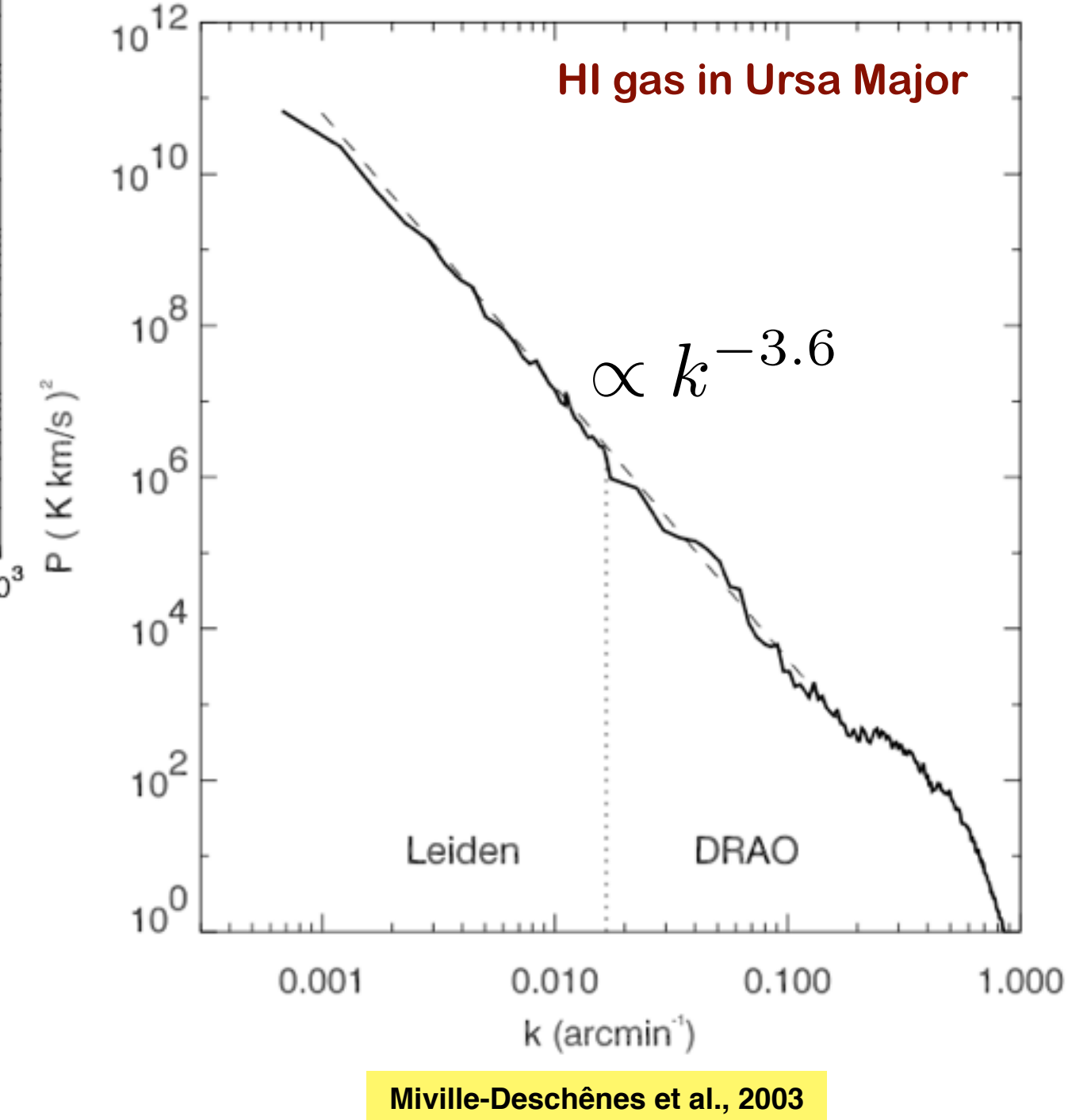
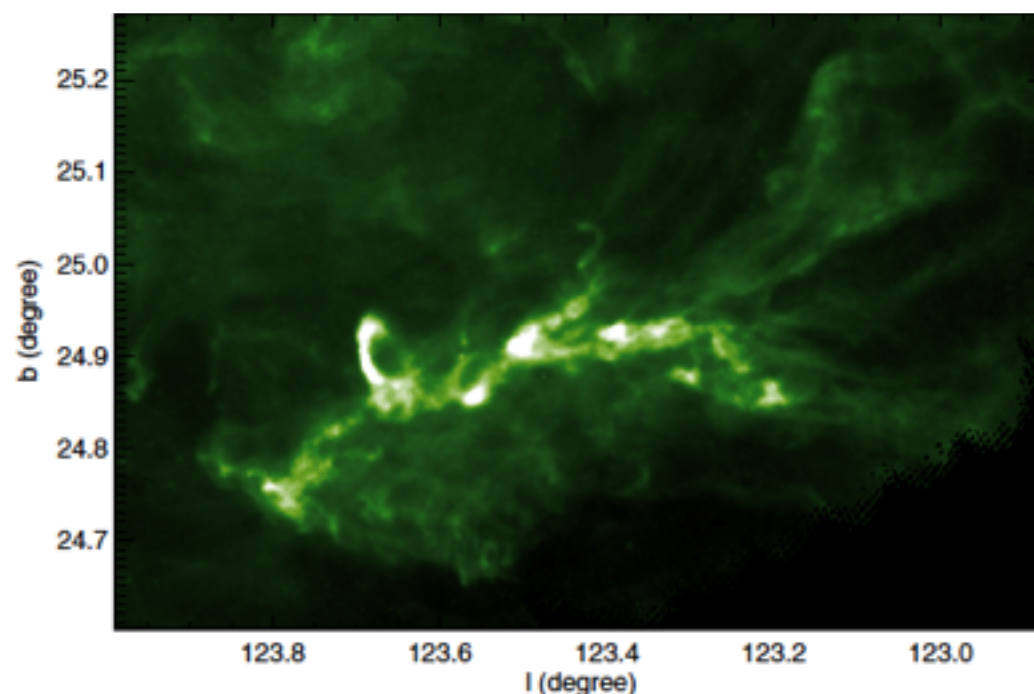
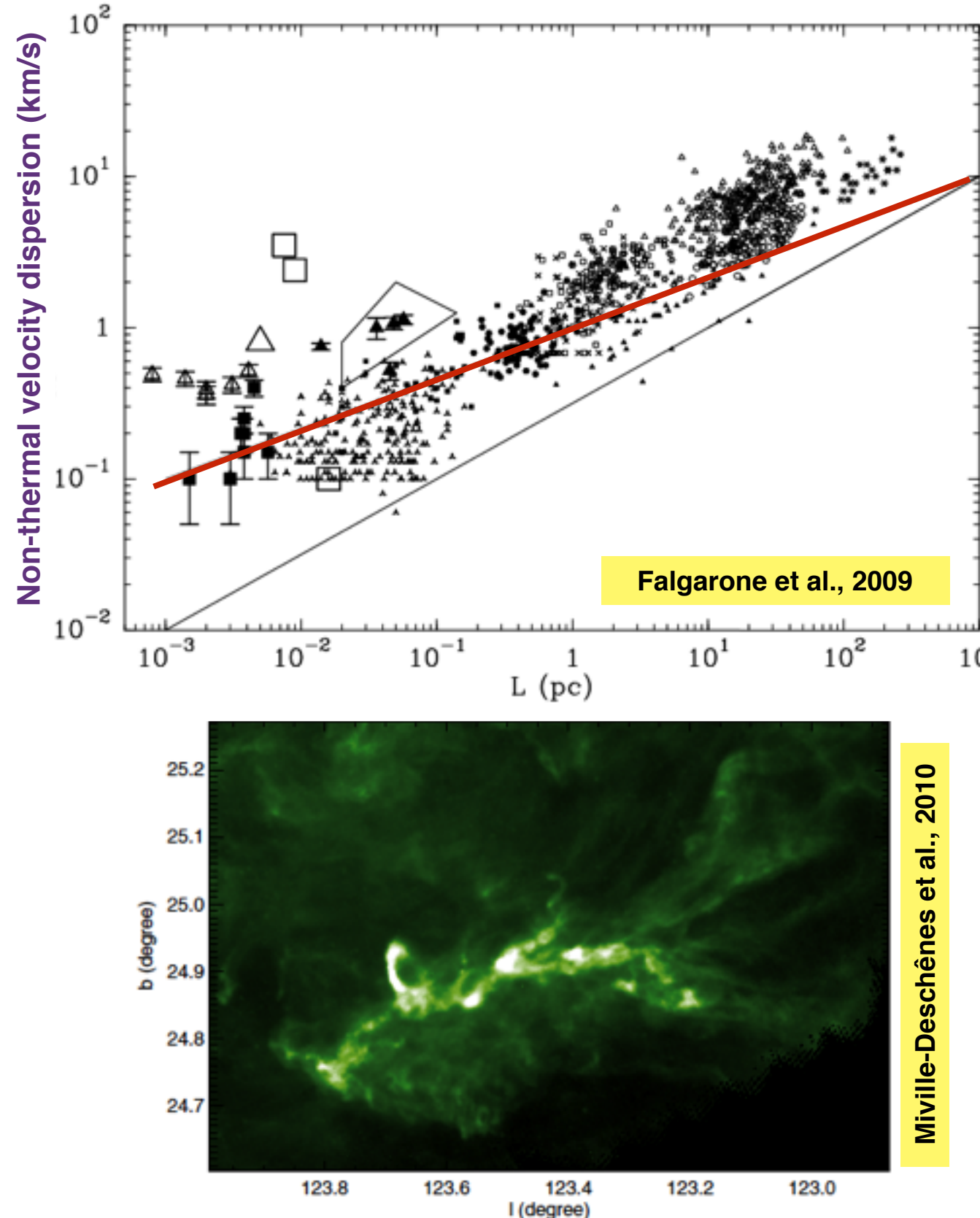
Current (UCSD, Berkeley Lab)

- Kolmogorov's K41 theory : incompressible, homogeneous, isotropic cascade of energy
- Scaling laws and self-similarity
- Intermittency : dissipation of energy occurs in bursts, localized in time and space
- Modification of scaling laws from compressibility and magnetic fields (MHD turbulence)



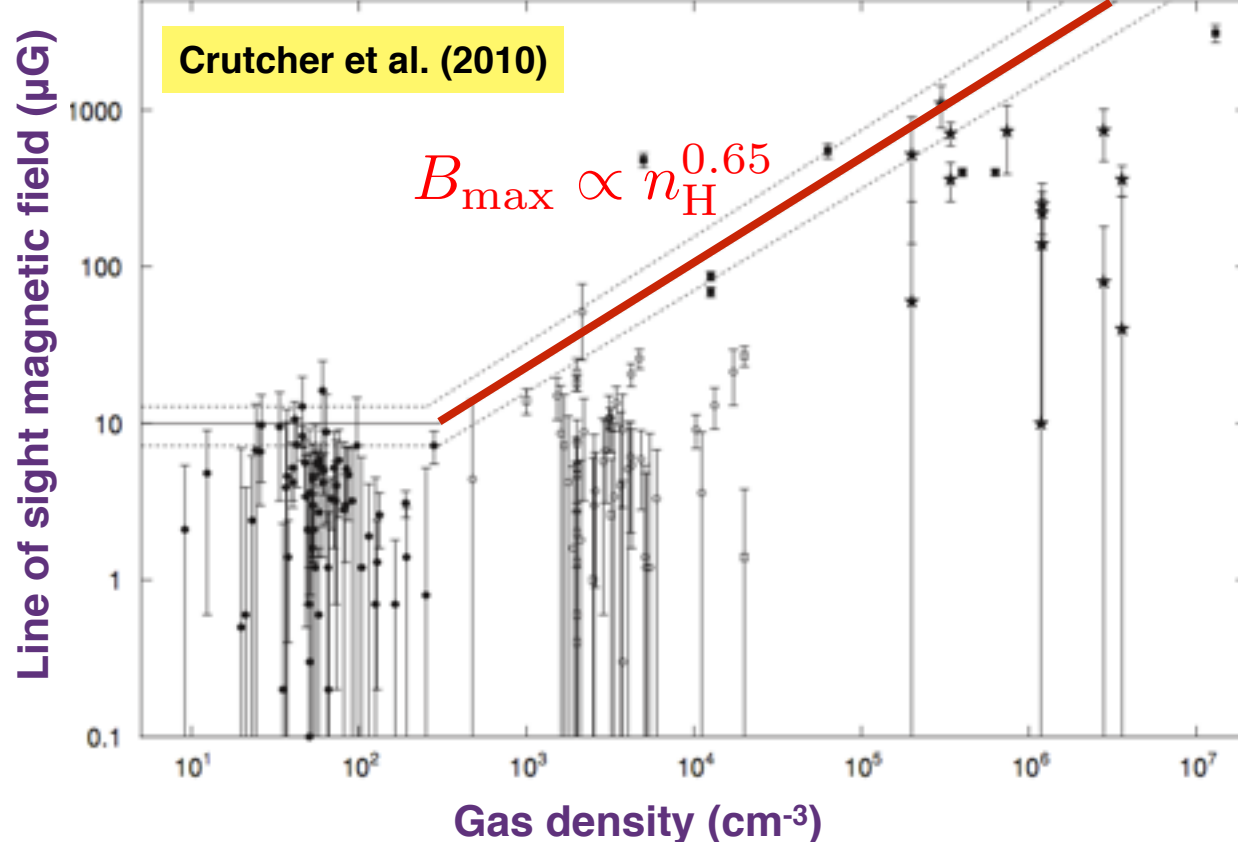
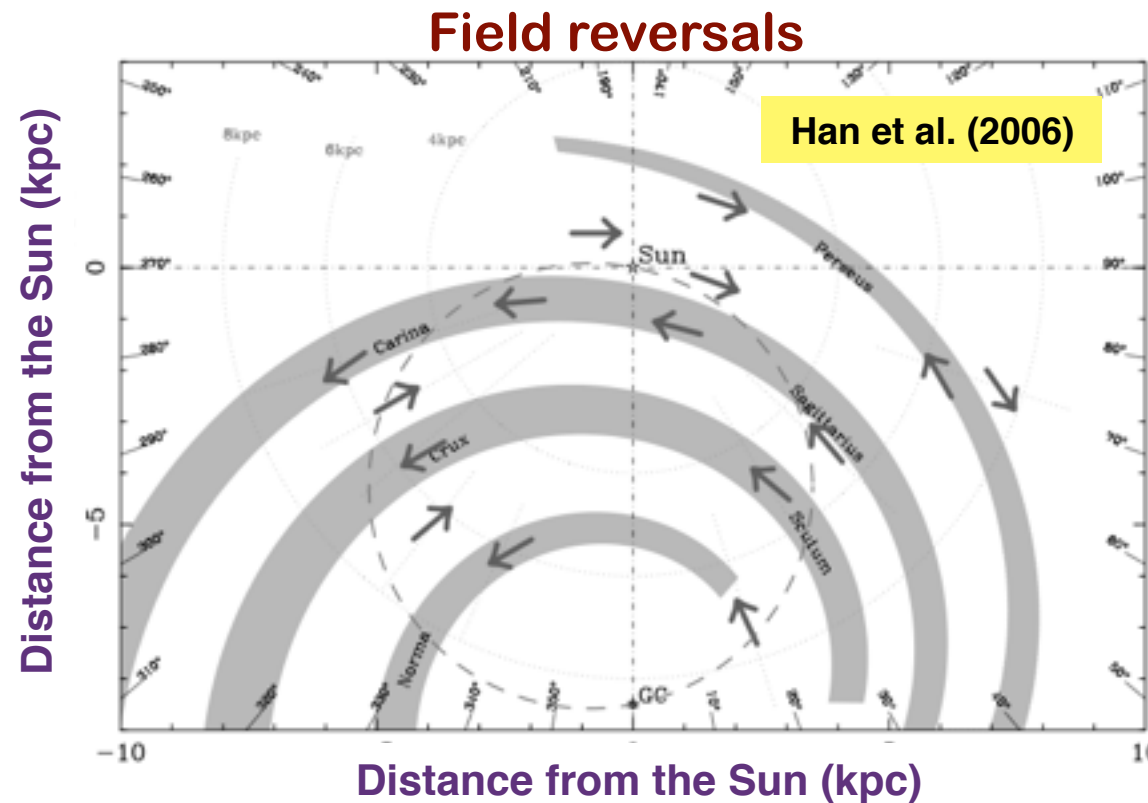
Turbulence in the ISM

- Suprathermal linewidths, scaling with the size of structures
- Self-similarity of structures across many scales
- Intermittency at small scales : non-Gaussian wings in distributions of centroid velocity increments



Magnetic fields in the Milky Way

- Coupled to the gas, provides balance with gravity, controls the propagation of cosmic rays
- Generated from primordial seed fields via a coupling of differential rotation and Coriolis force
- Superposition of a large-scale field following spiral arms and of a turbulent component



$$\mathbf{B} = \mathbf{B}_0 + \mathbf{B}_t$$

$\sim \text{a few } \mu\text{G}$ $\sim \text{a few } \mu\text{G}$

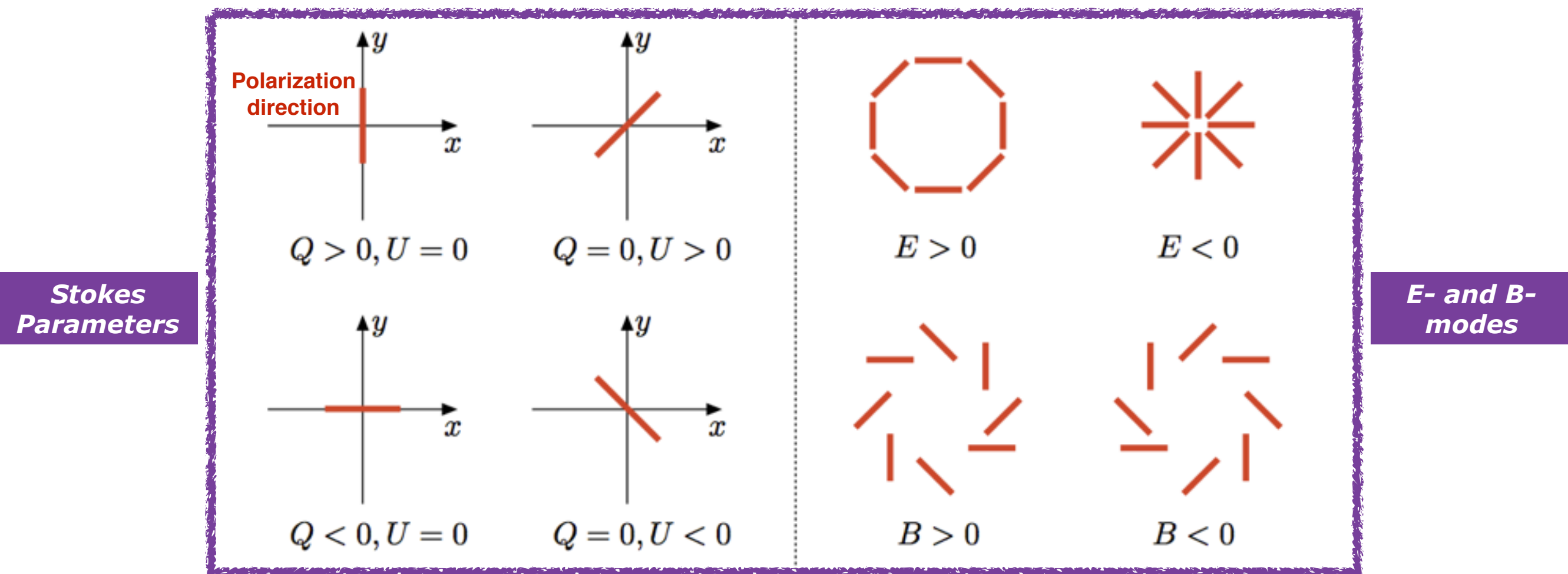
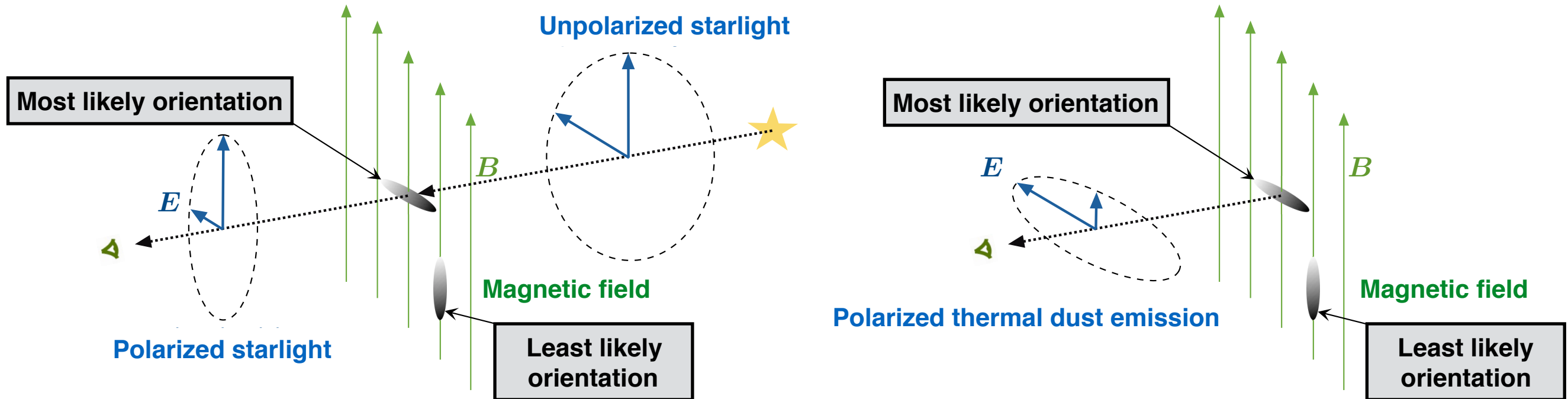
Haverkorn et al. (2008)

Measurement methods

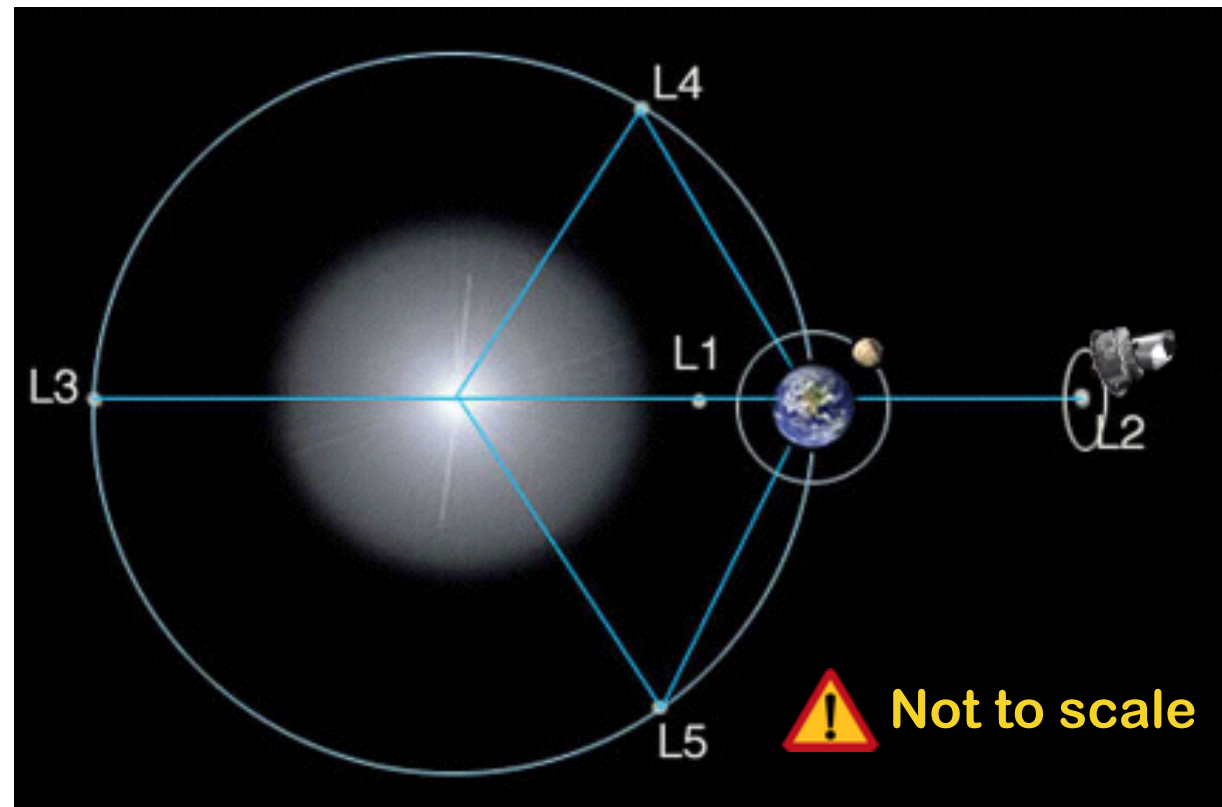
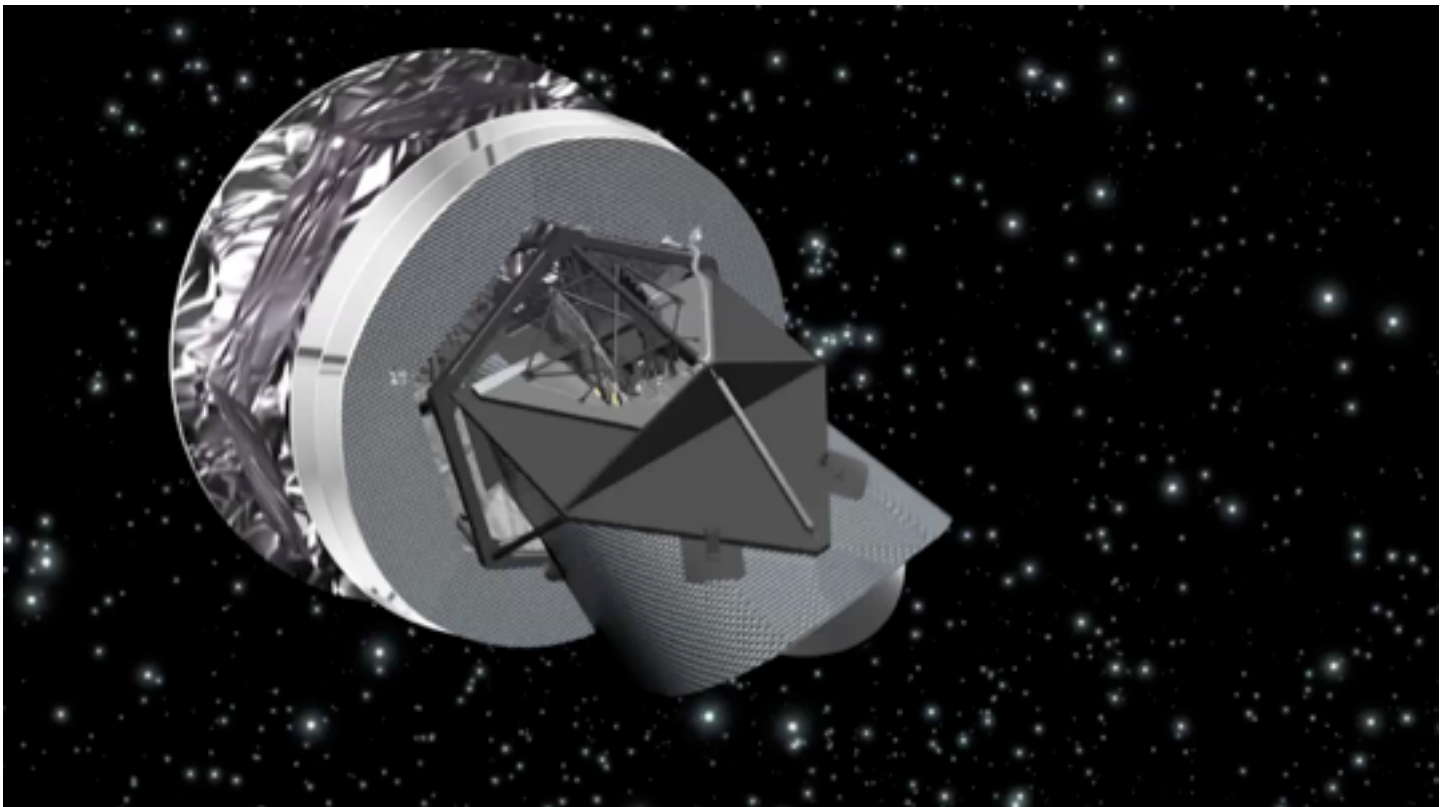
Notation	Observational signatures
$B_{\text{tot},\perp}^2 = B_{\text{turb},\perp}^2 + B_{\text{reg},\perp}^2$	Total synchrotron intensity
$B_{\text{turb},\perp}^2 = B_{\text{iso},\perp}^2 + B_{\text{aniso},\perp}^2$	Total synchrotron emission, partly polarized
$B_{\text{iso},\perp}$ ($= \sqrt{2/3} B_{\text{iso}}$)	Unpolarized synchr. intensity, beam depolarization, Faraday depolarization
$B_{\text{iso},\parallel}$ ($= \sqrt{1/3} B_{\text{iso}}$)	Faraday depolarization
$B_{\text{ord},\perp}^2 = B_{\text{aniso},\perp}^2 + B_{\text{reg},\perp}^2$	Intensity and vectors of radio, optical, IR & submm pol.
$B_{\text{aniso},\perp}$	Intensity and vectors of radio, optical, IR & submm pol., Faraday depolarization
$B_{\text{reg},\perp}$	Intensity and vectors of radio, optical, IR & submm pol., Goldreich-Kylafis effect
$B_{\text{reg},\parallel}$	Faraday rotation + depol., longitudinal Zeeman effect

Dust, magnetic fields and polarization

- Aspherical, charged, rotating dust grains statistically align in the local magnetic field
- Background starlight emerges polarized parallel to the magnetic field
- Polarized thermal dust emission arises perpendicularly to the magnetic field

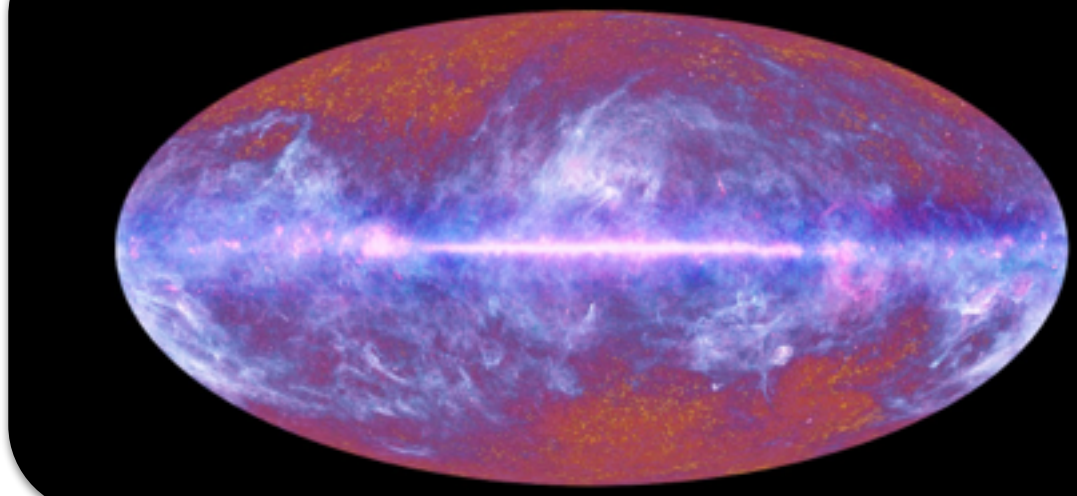


The Planck mission

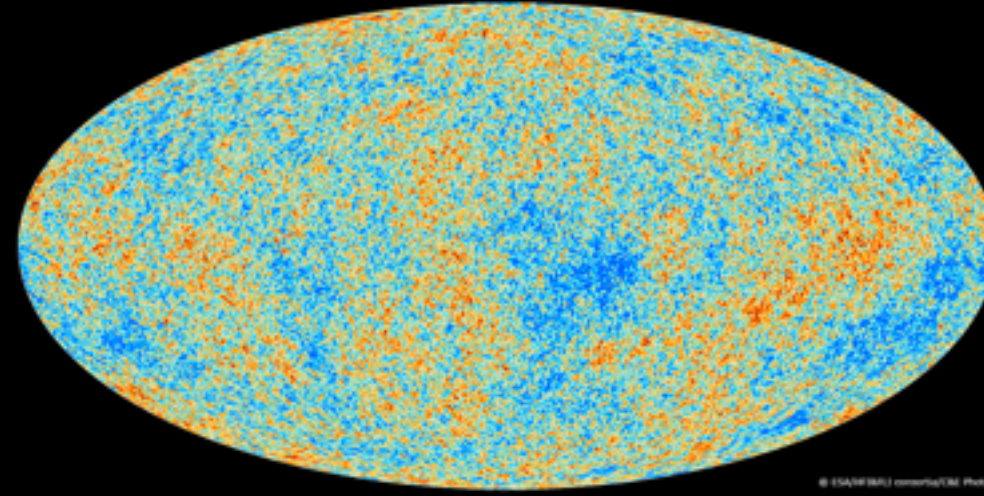


- 2009-2013 European space mission : Full survey of the microwave sky
- 30 - 857 GHz coverage in nine bands
- Measurement of Cosmic Microwave Background (CMB) anisotropies
- Mapping of the cold, dusty Milky Way
- First full-sky survey in microwave polarization

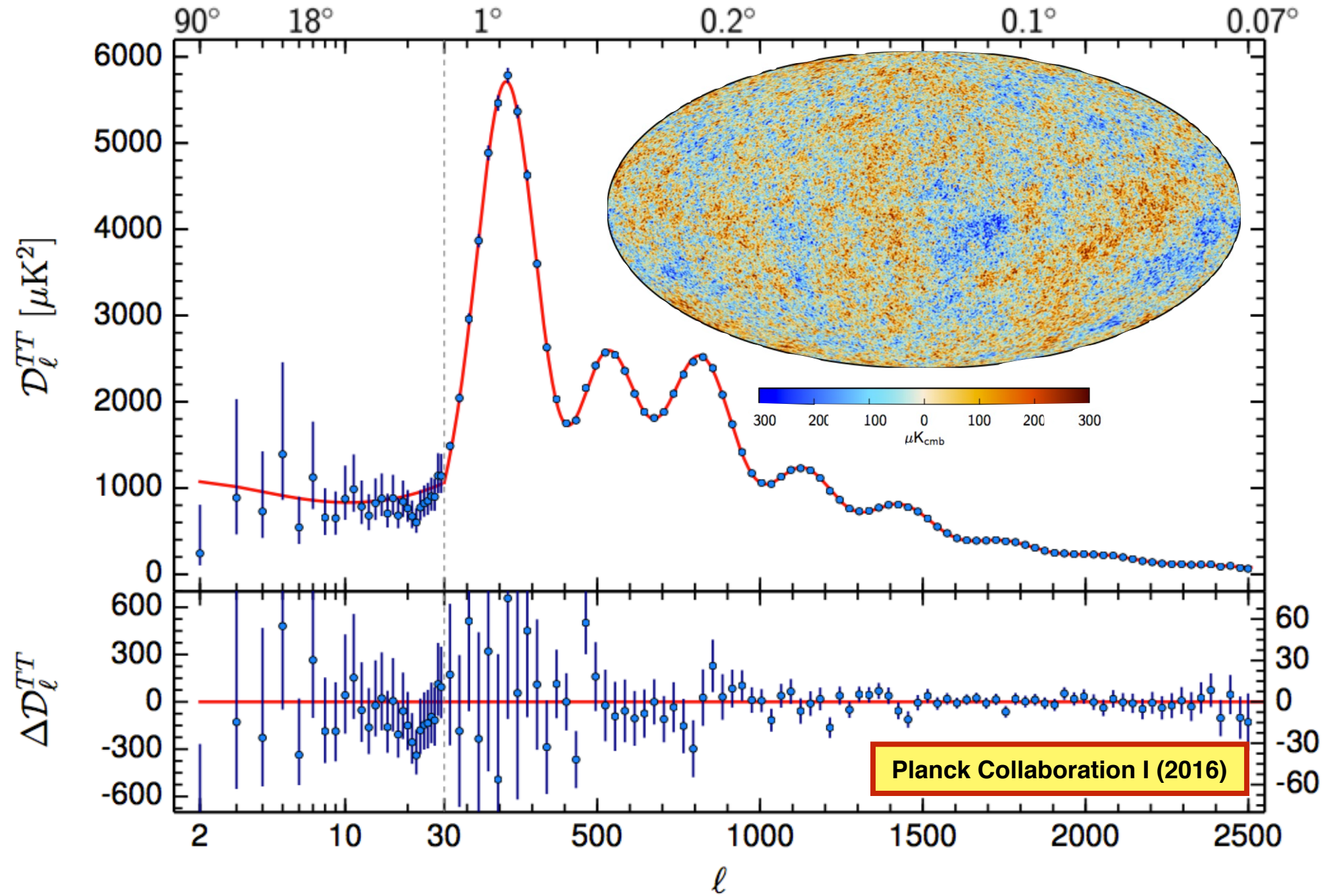
The Planck 1-year survey (2011)



The Planck CMB temperature map (2013)



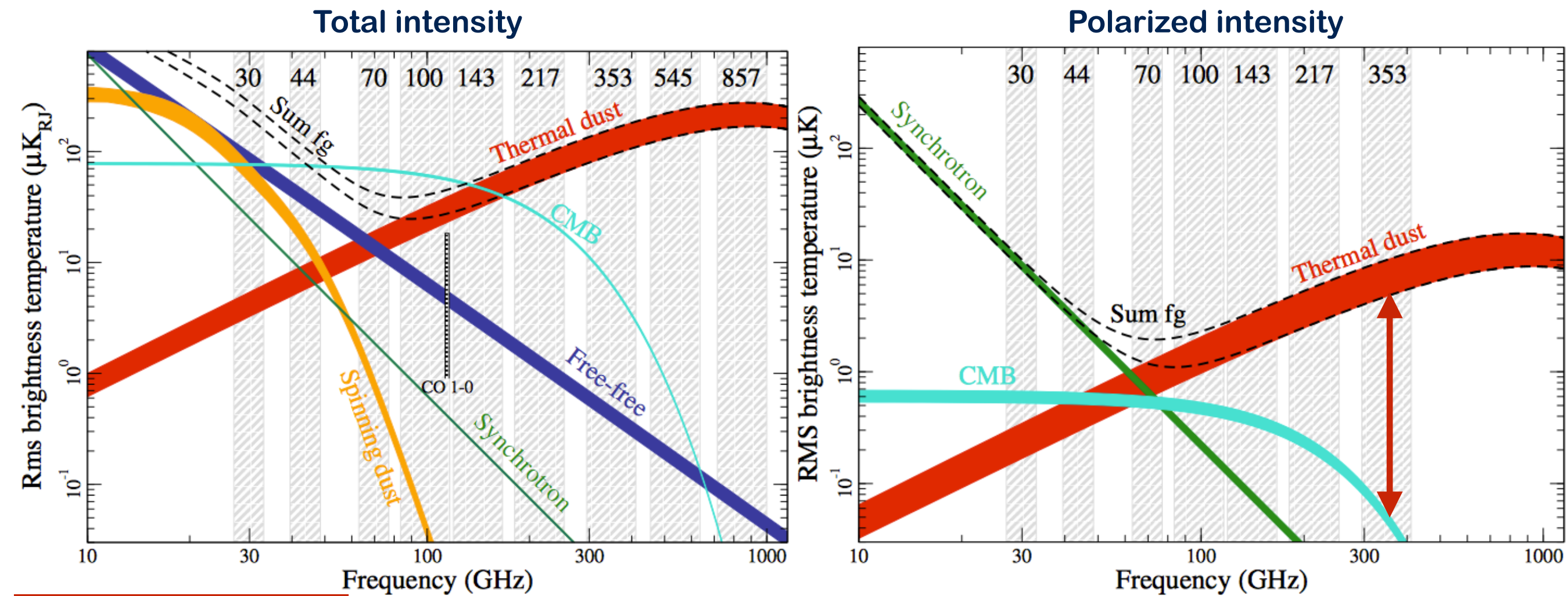
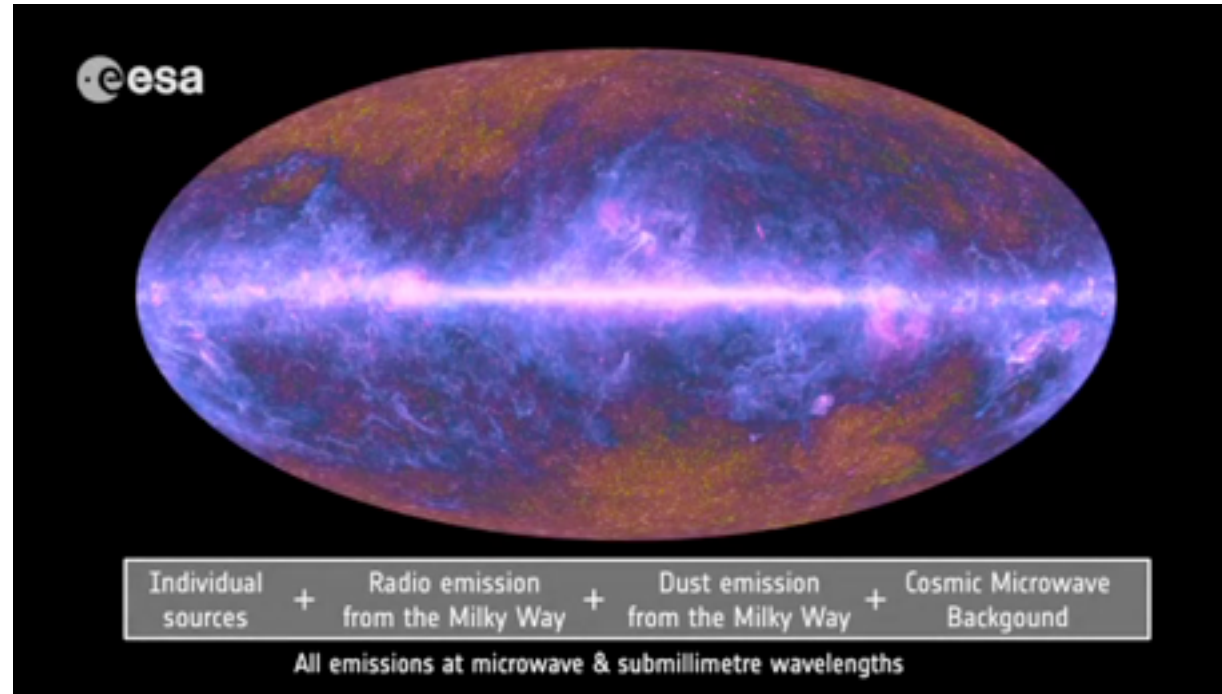
The « ultimate » CMB temperature mission



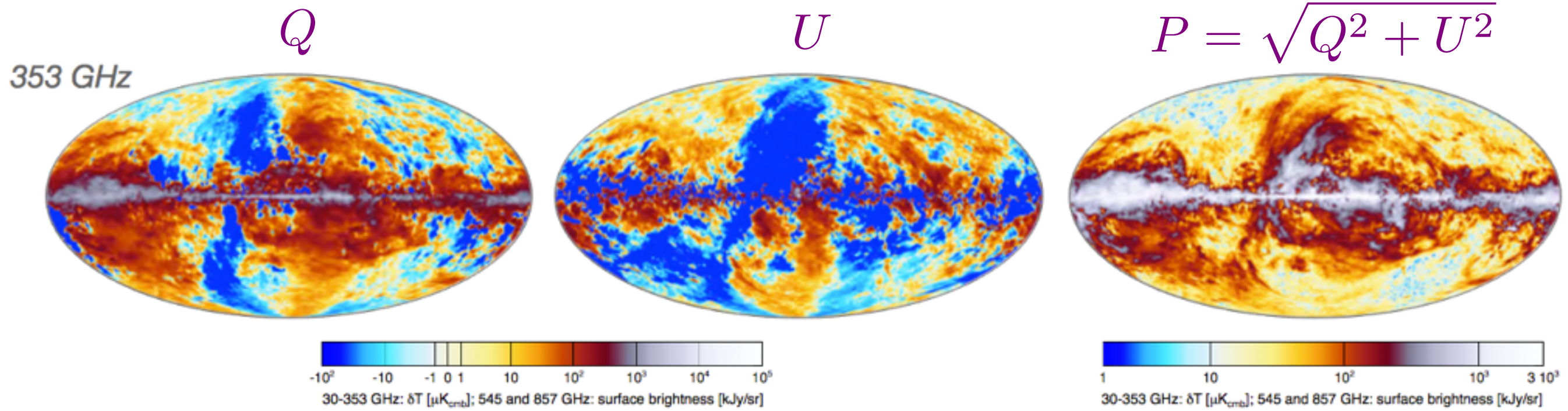
- Mapping of CMB anisotropies of order 10^{-5}
 - Measurement of the power as a function of angular scale
 - Excellent agreement with the 6-parameter Λ -CDM model
 - No hint for a necessity to extend the model

$\Omega_b h^2$	0.02230 ± 0.00014
$\Omega_c h^2$	0.1188 ± 0.0010
$100\theta_{\text{MC}}$	1.04093 ± 0.00030
τ	0.066 ± 0.012
$\ln(10^{10} A_s)$	3.064 ± 0.023
n_s	0.9667 ± 0.0040

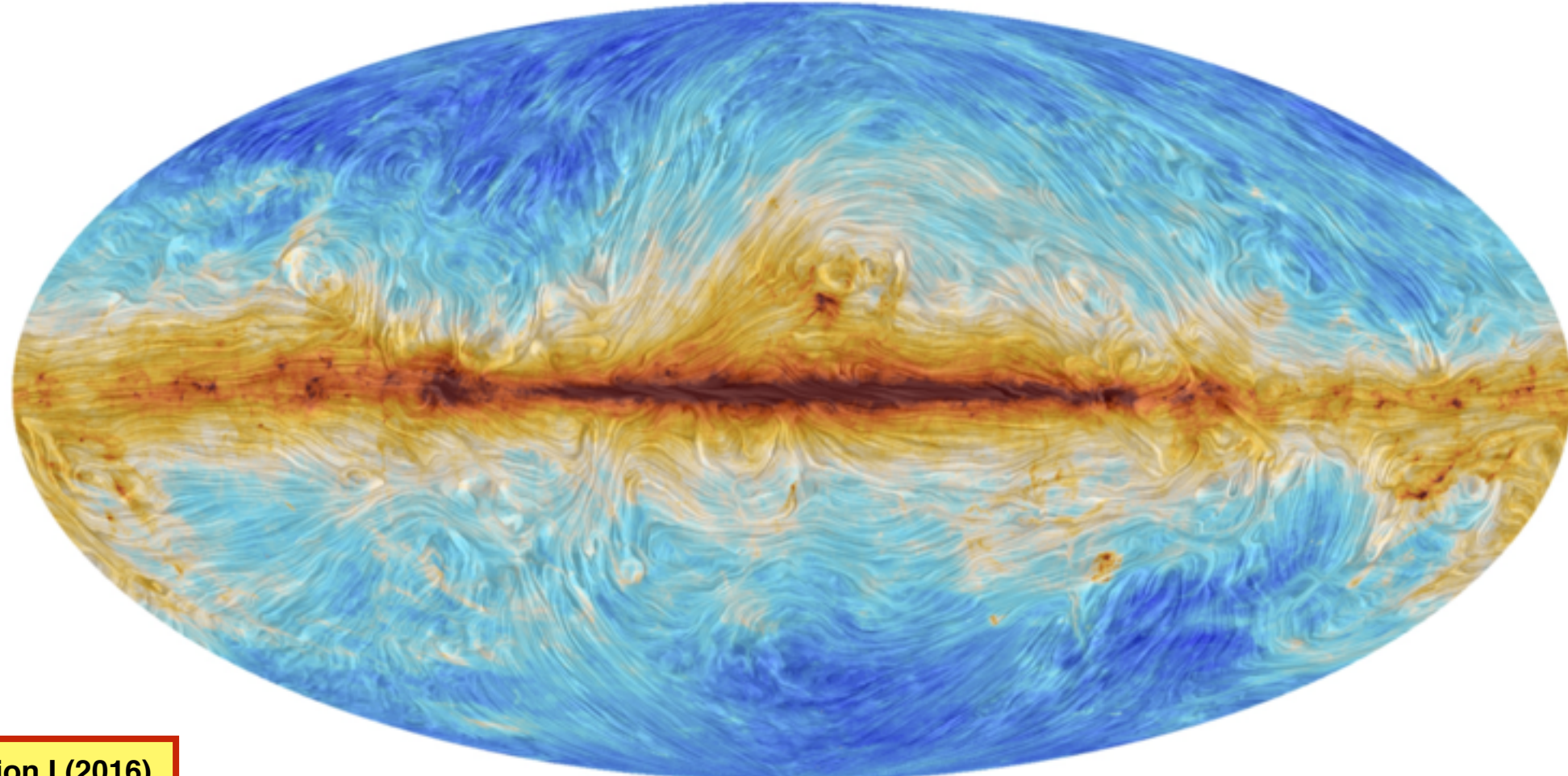
Galactic dust emission : a foreground to the CMB



The Planck view of the Galactic magnetic field



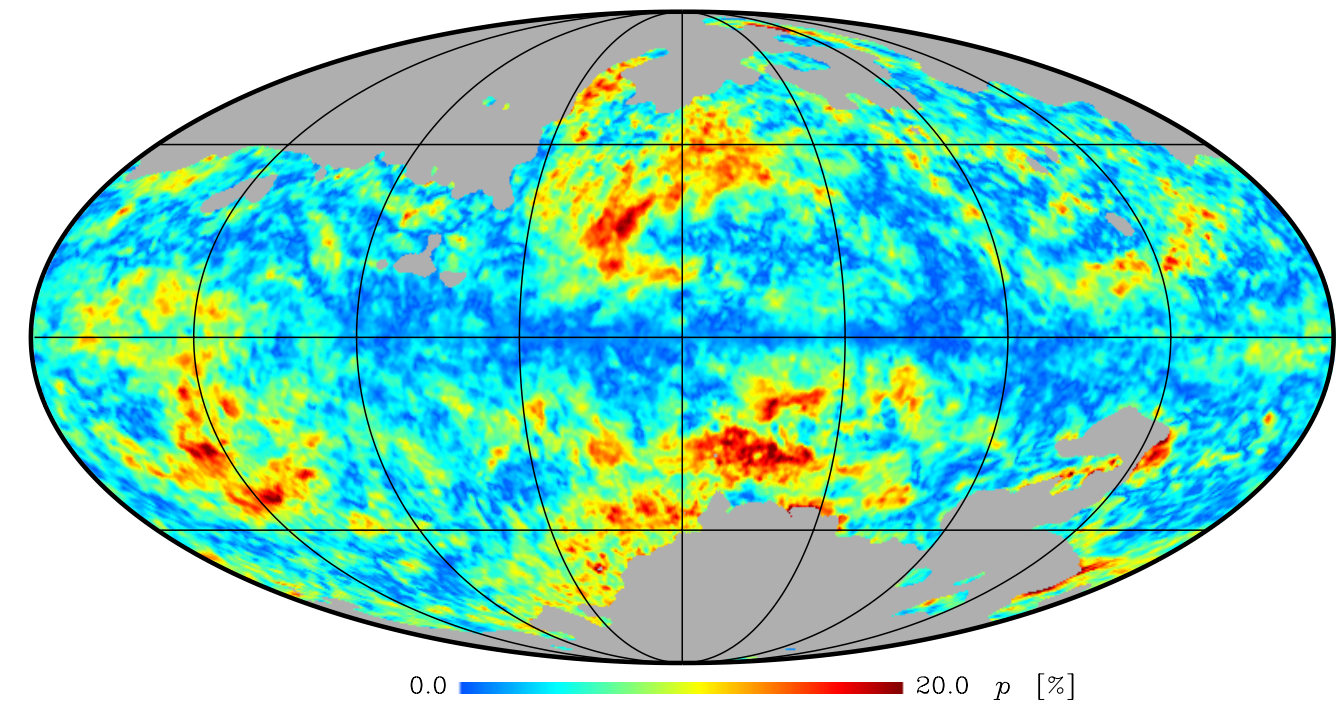
Total intensity and « drapery » showing the direction of the magnetic field



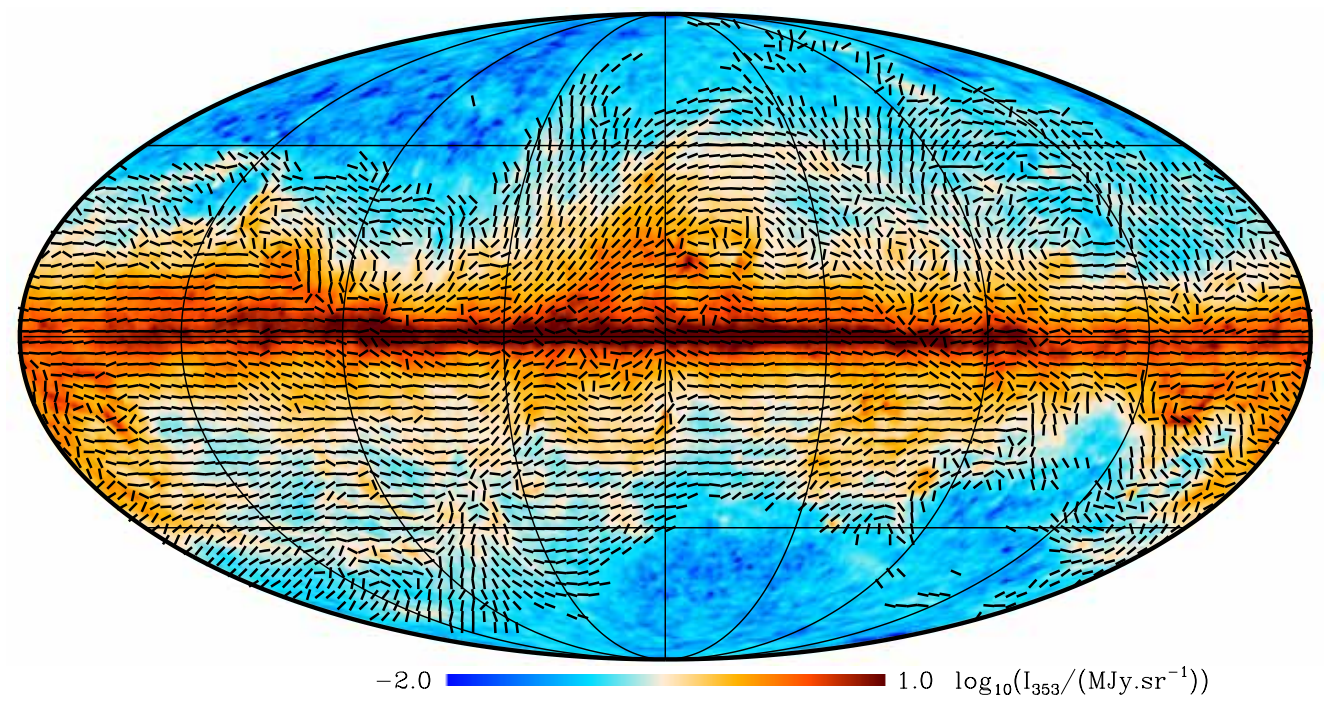
Properties of large-scale thermal dust polarization

- Low polarization fractions in the Galactic Plane and some highly polarized regions
- Thin filamentary structures of low polarization with no material counterpart

Polarization fraction $p = \frac{P}{I}$



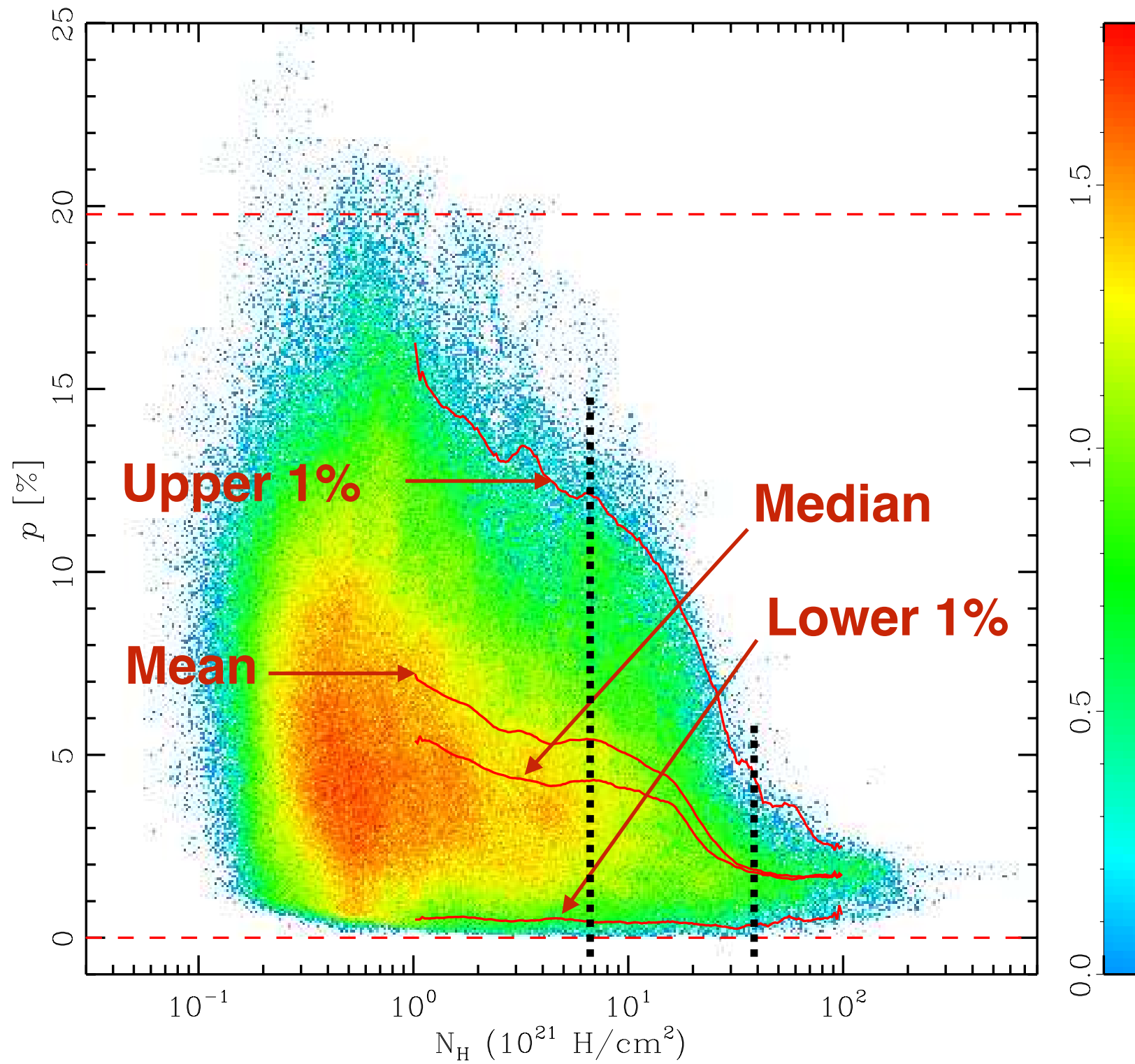
Polarization angle $\psi = \frac{1}{2}\text{atan}(U, Q)$



Update in early 2017...

Polarization fraction vs. column density

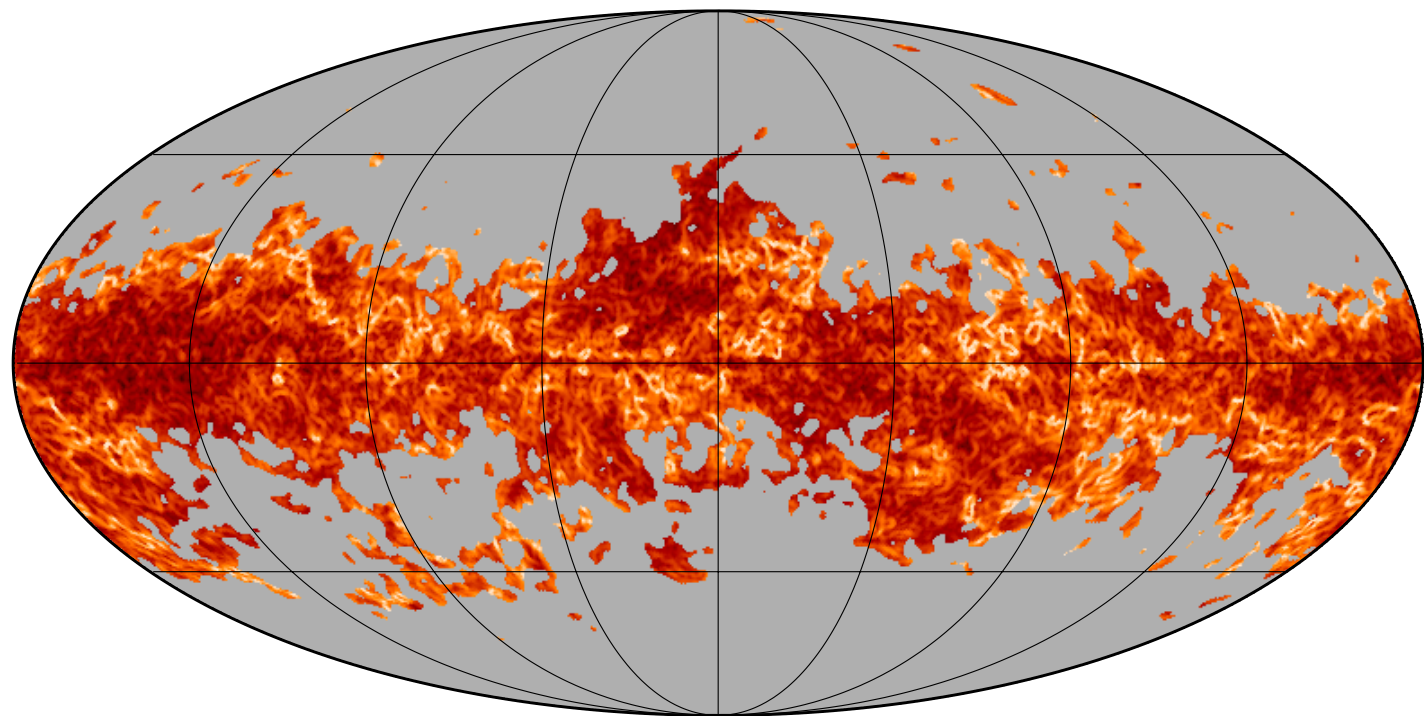
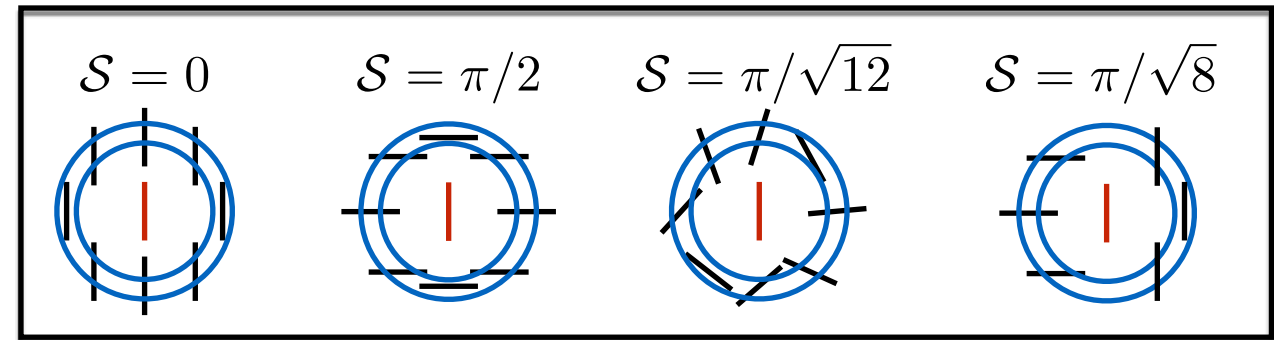
- Intrinsic dust polarization at least of order 20%
- Decrease of the maximum polarization fraction with increasing column density



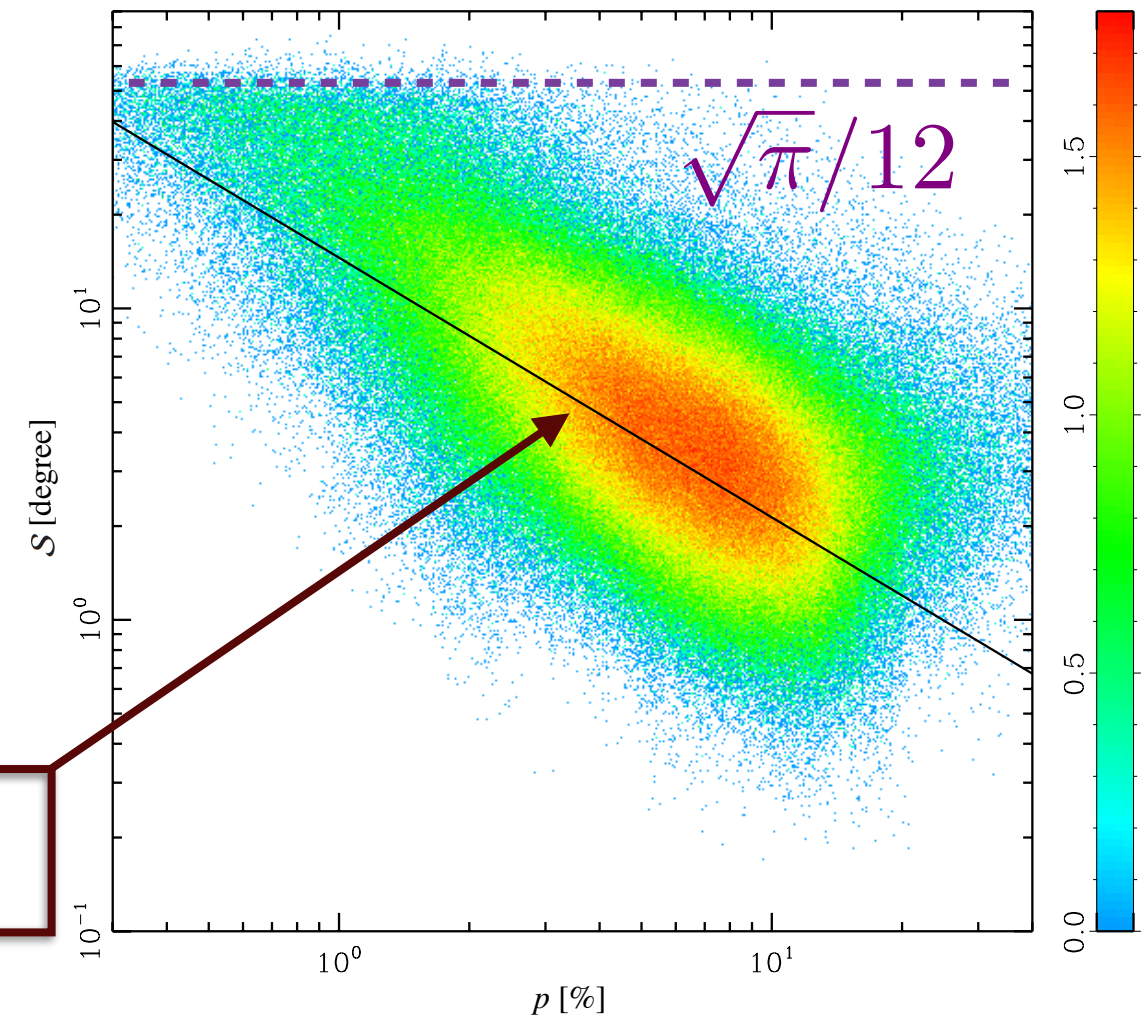
Spatial structure of the polarization angle map

Polarization angle dispersion function

$$\mathcal{S}(r, \delta) = \sqrt{\frac{1}{N} \sum_{i=1}^N [\psi(\mathbf{r} + \boldsymbol{\delta}_i) - \psi(\mathbf{r})]^2}$$



$$\log(\mathcal{S}/\text{deg}) = -0.834 \log p - 0.504$$

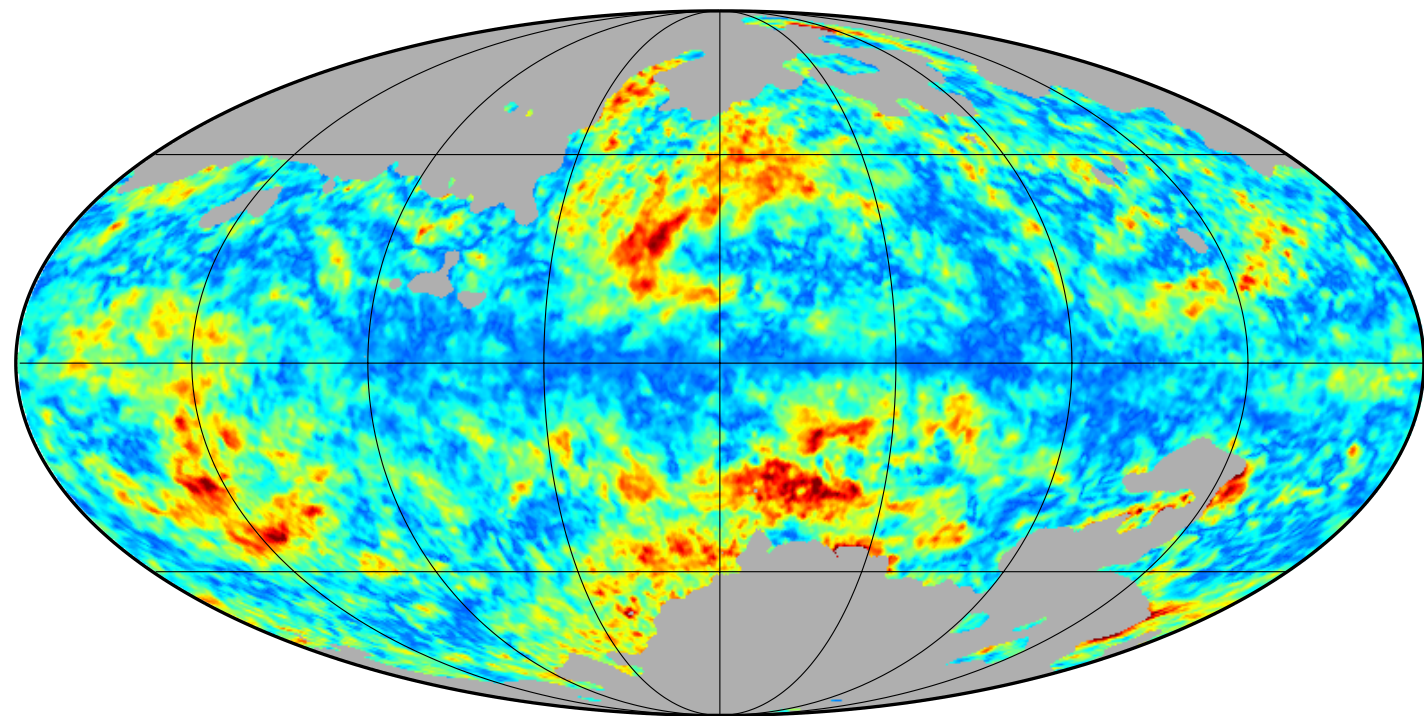
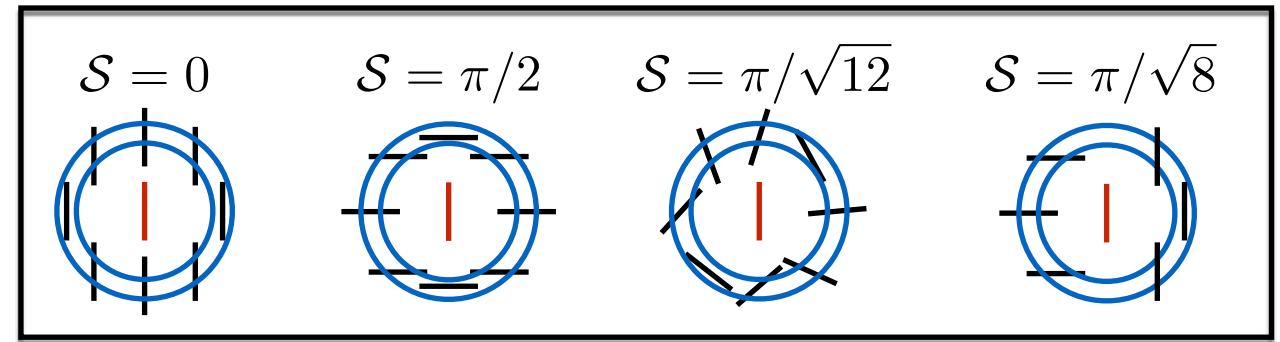


- Strongly anti-correlated with the polarization fraction
- Low polarization fractions found where the polarization angle direction changes abruptly
- Increased lag δ flattens the anti-correlation

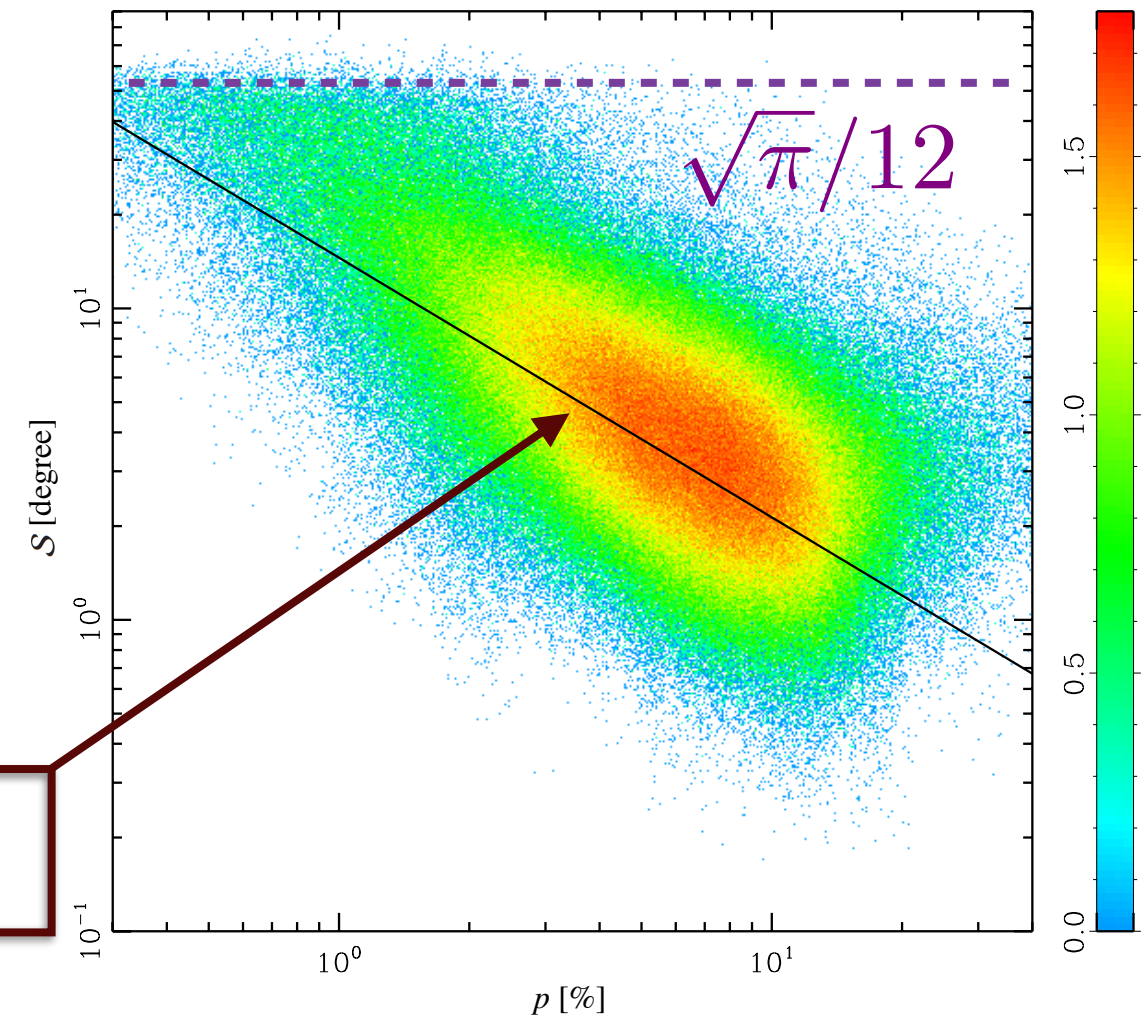
Spatial structure of the polarization angle map

Polarization angle dispersion function

$$\mathcal{S}(r, \delta) = \sqrt{\frac{1}{N} \sum_{i=1}^N [\psi(\mathbf{r} + \boldsymbol{\delta}_i) - \psi(\mathbf{r})]^2}$$

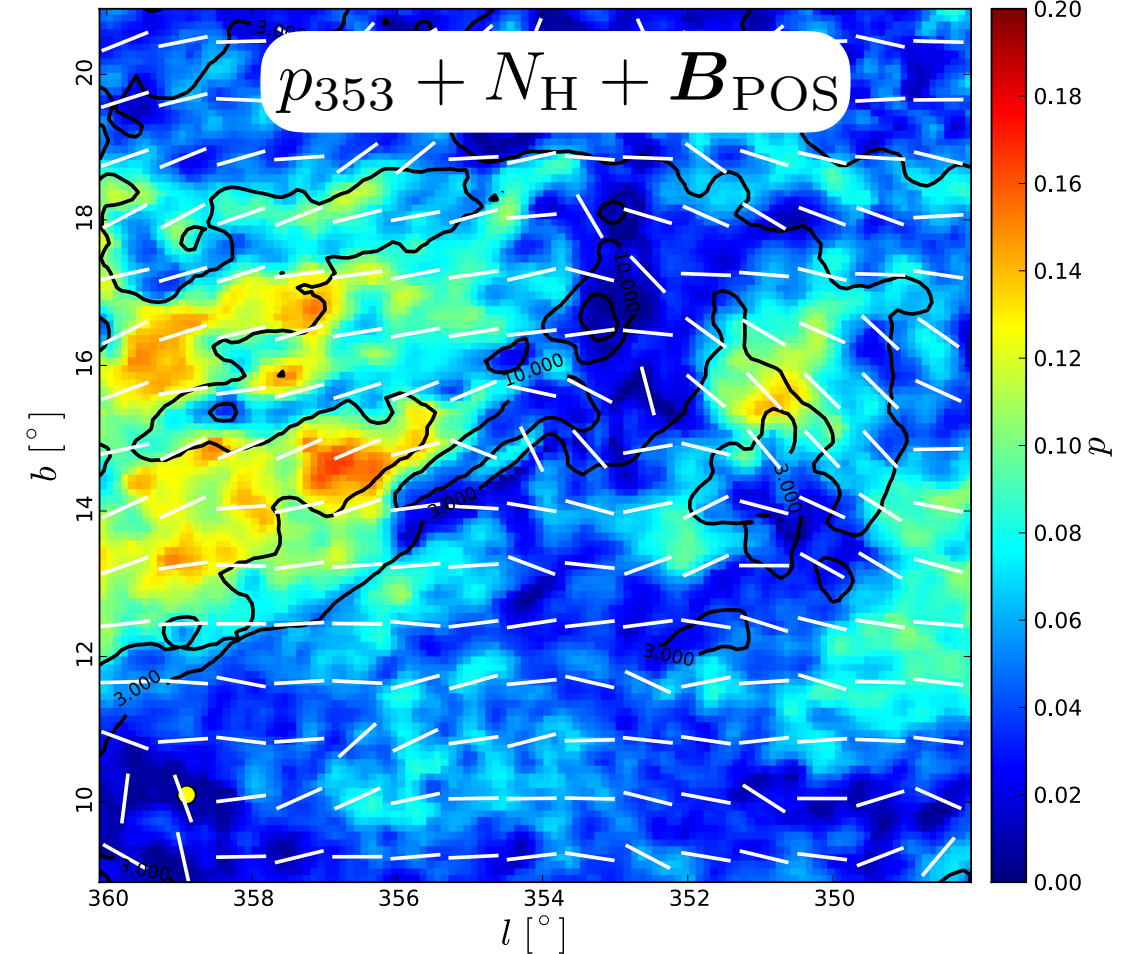
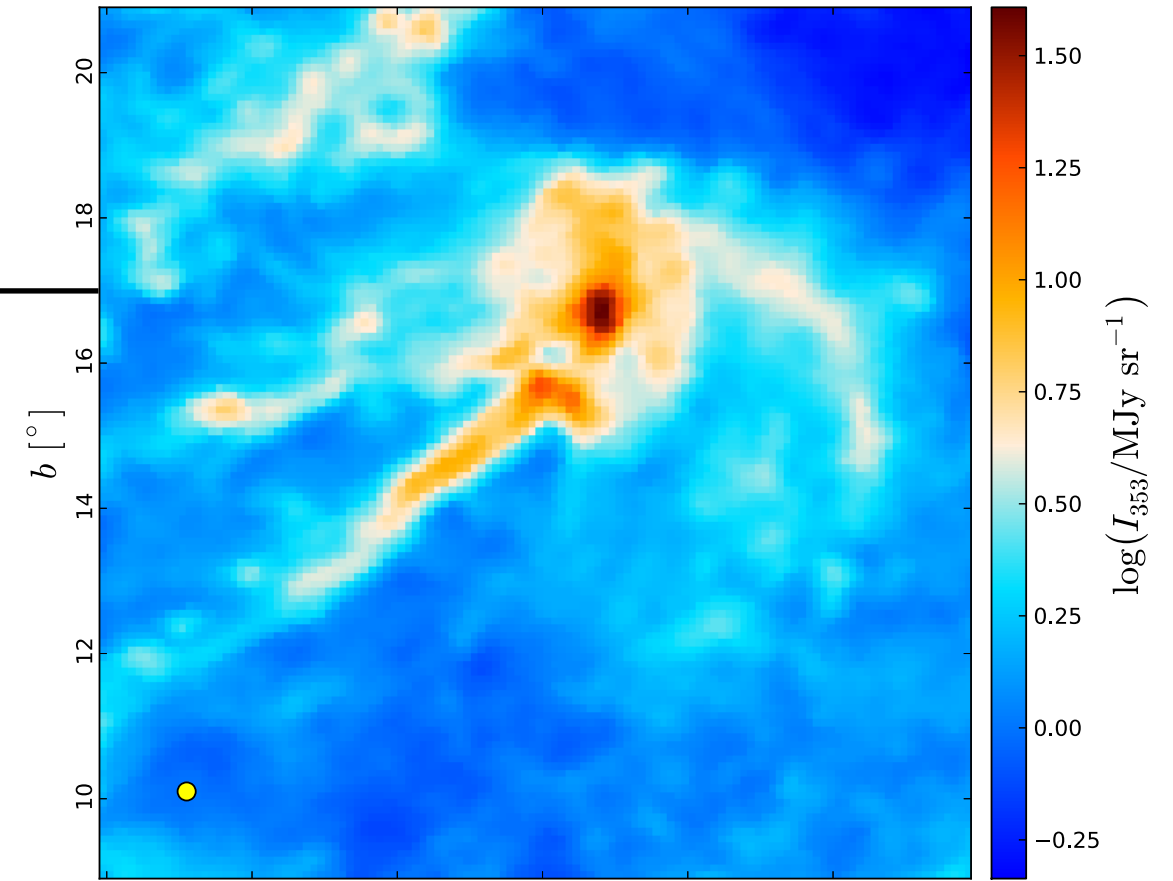
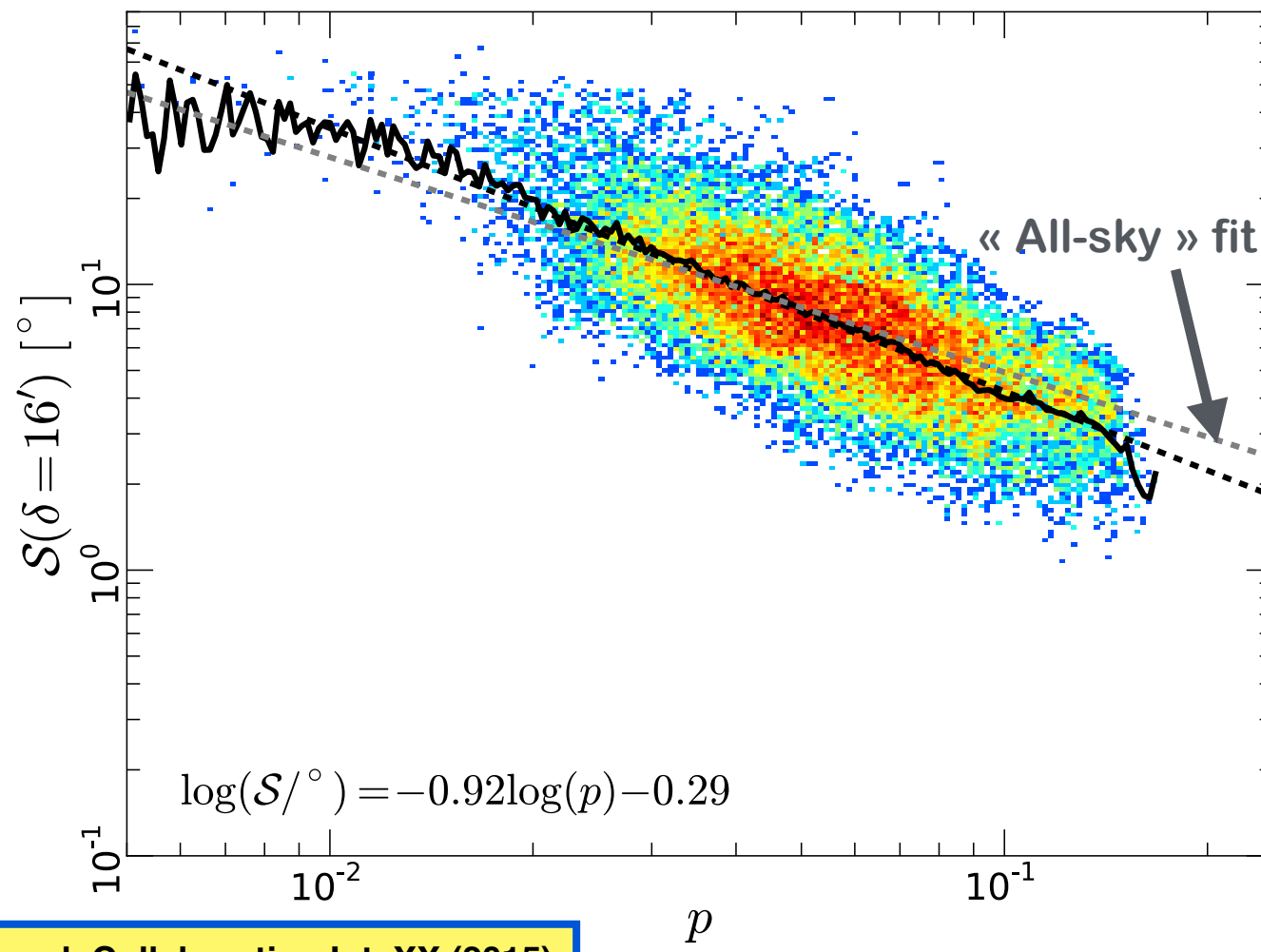
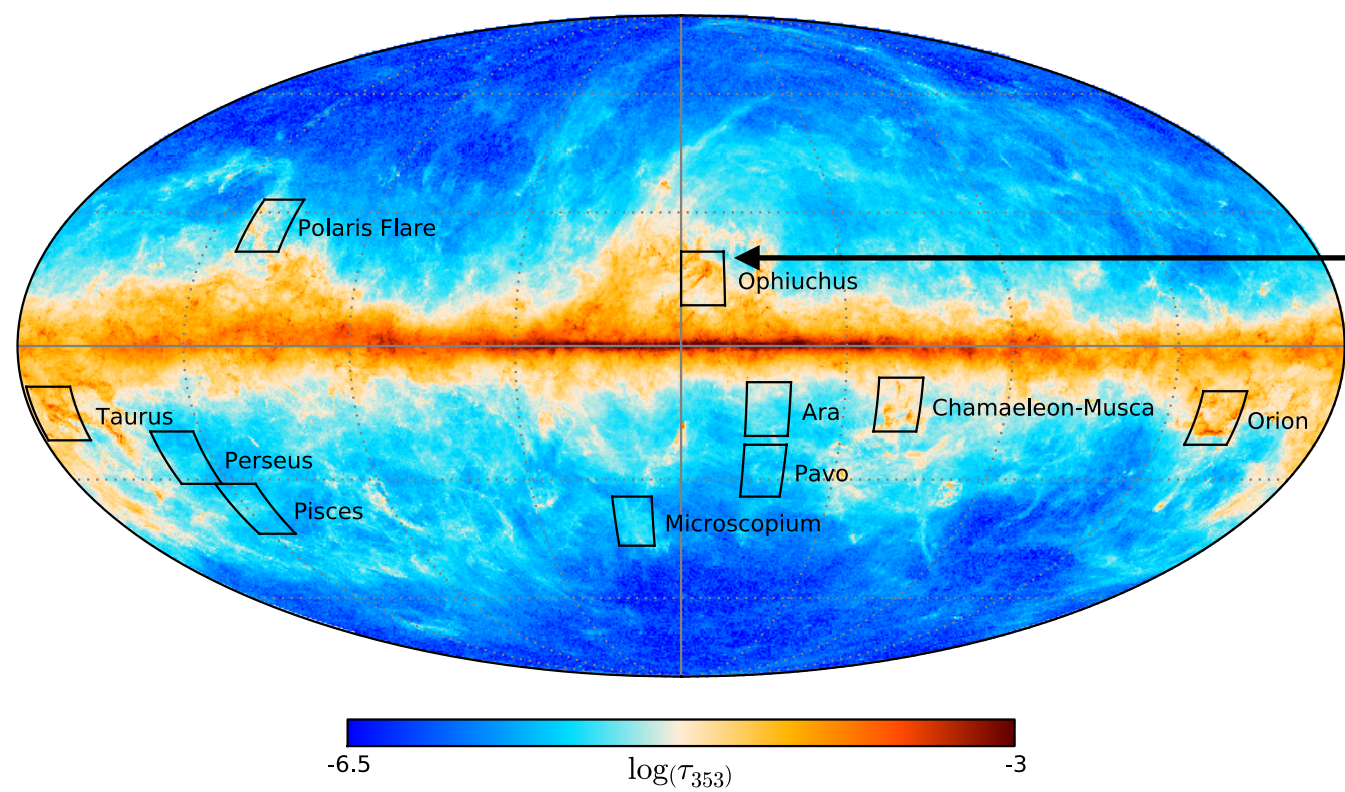


$$\log(\mathcal{S}/\text{deg}) = -0.834 \log p - 0.504$$

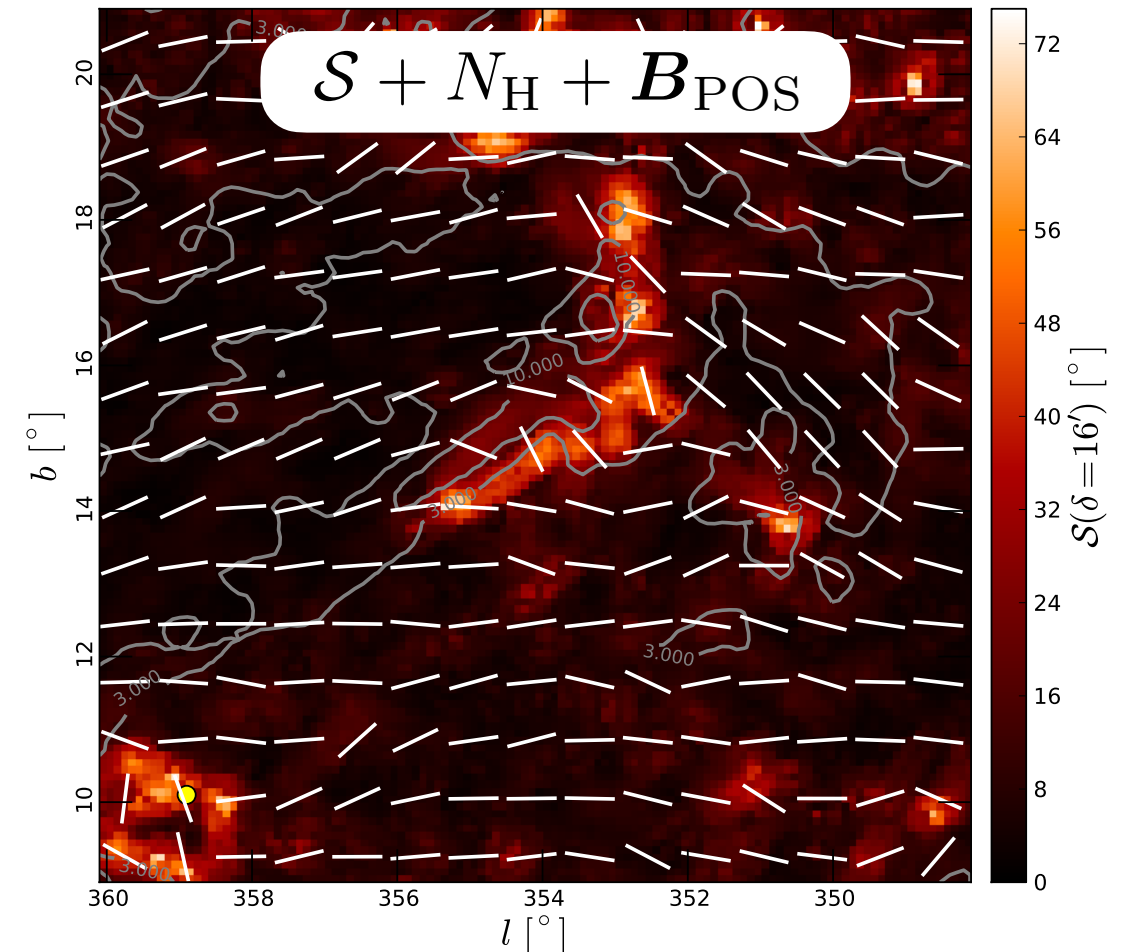
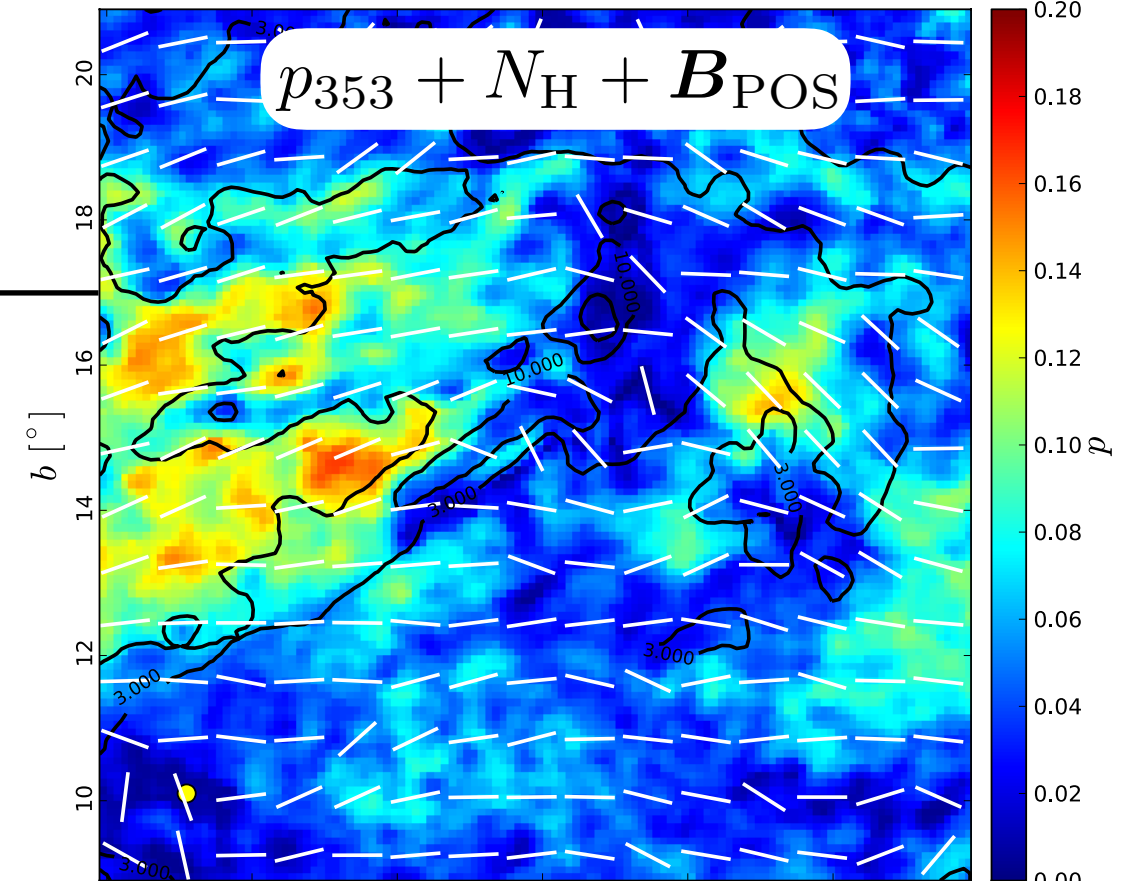
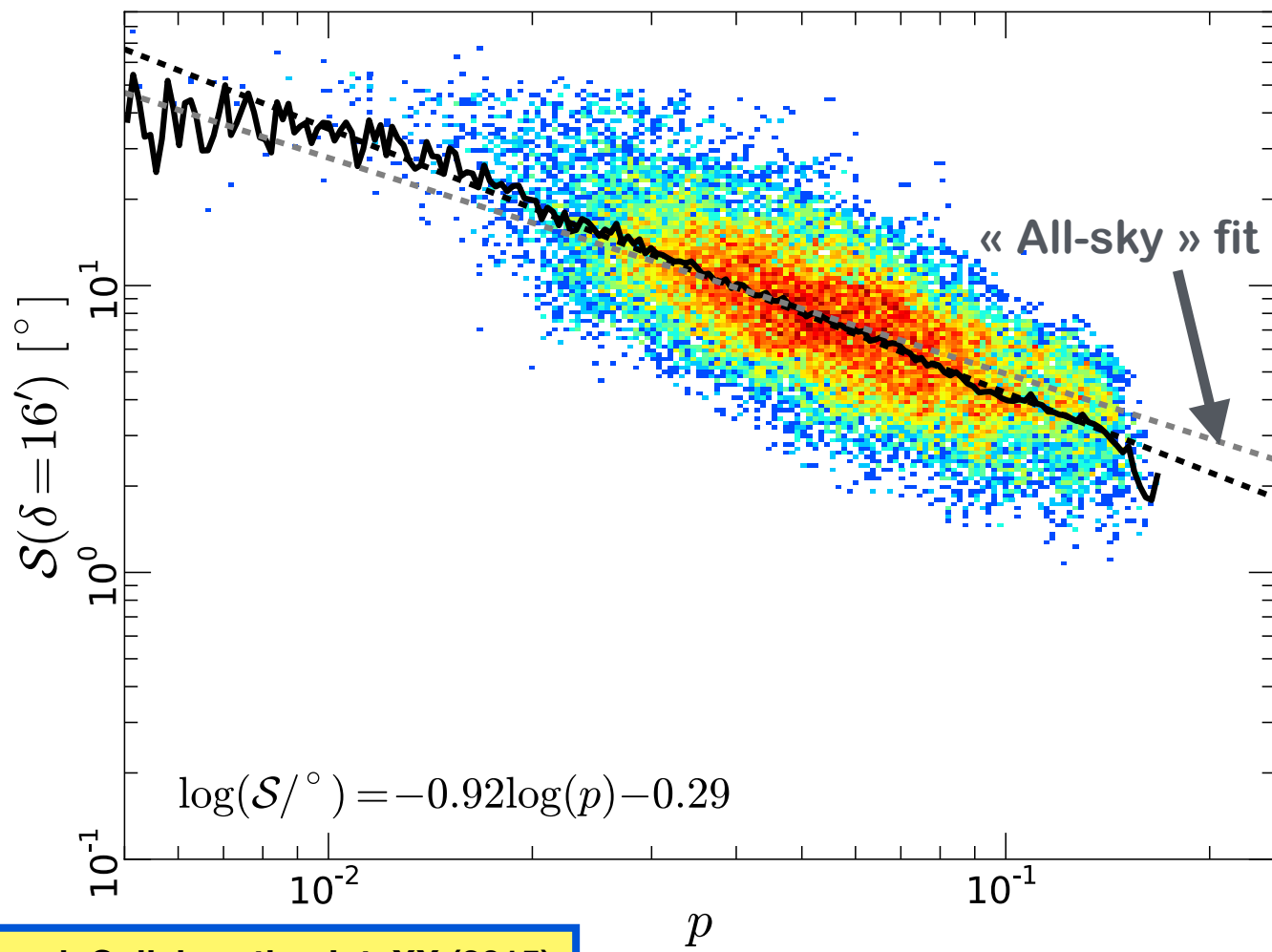
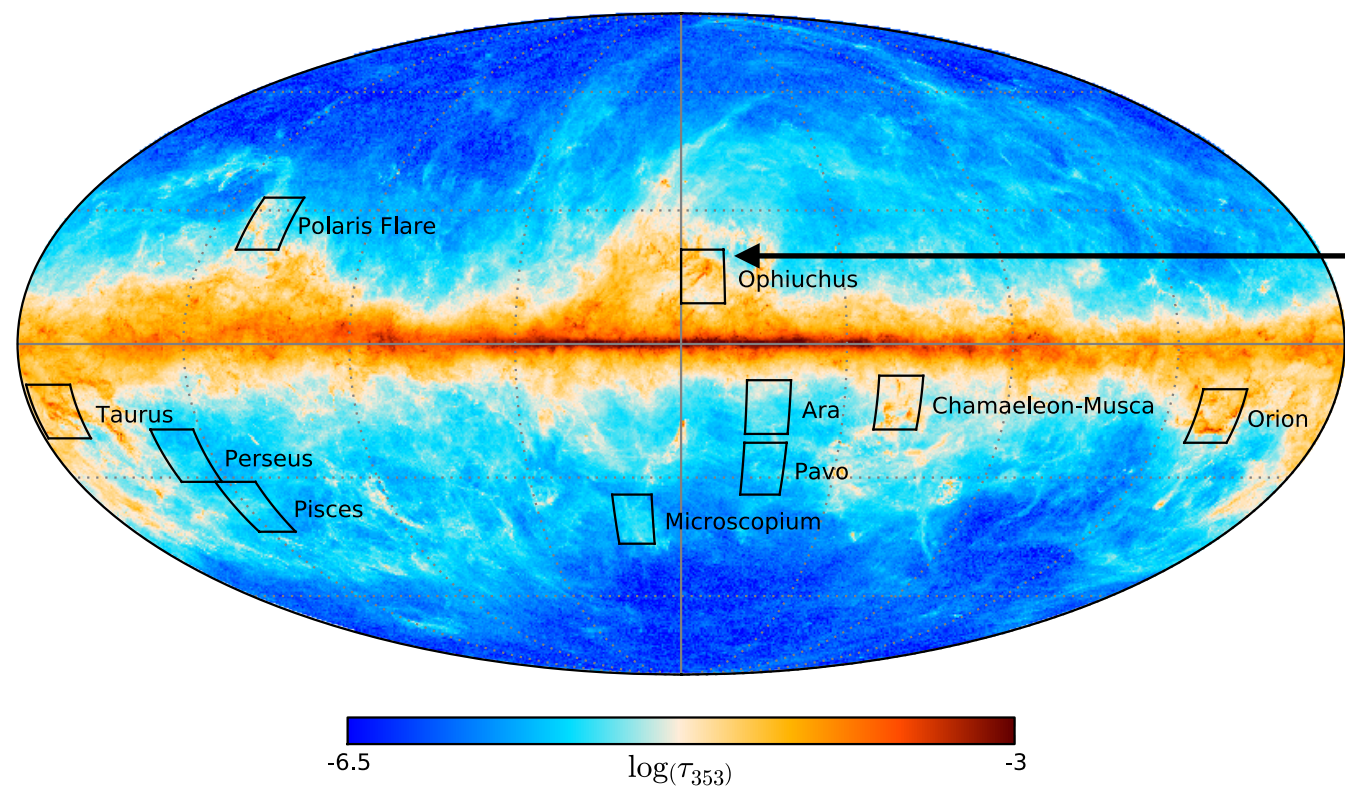


- Strongly anti-correlated with the polarization fraction
- Low polarization fractions found where the polarization angle direction changes abruptly
- Increased lag δ flattens the anti-correlation

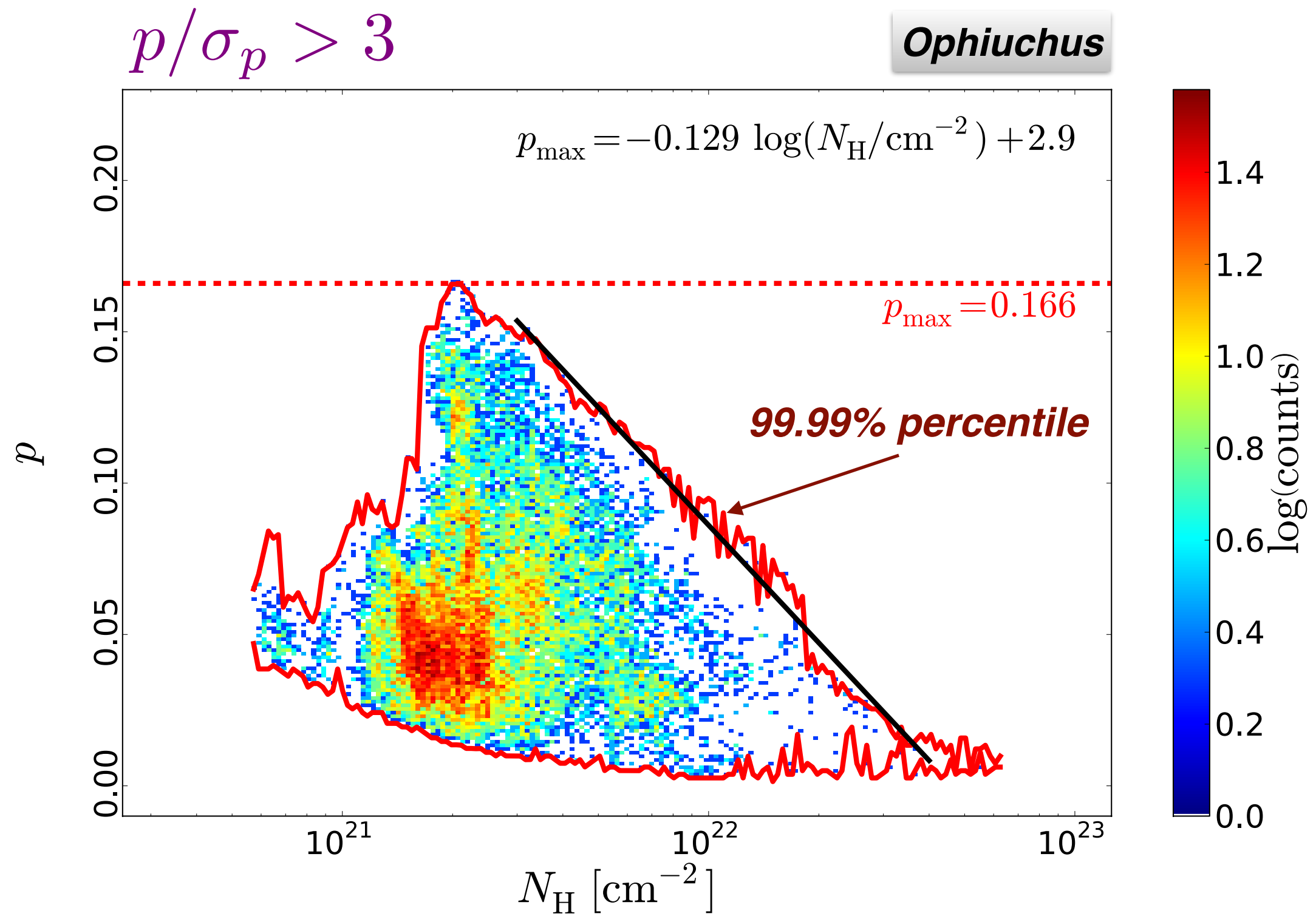
Thermal dust polarization towards molecular clouds



Thermal dust polarization towards molecular clouds

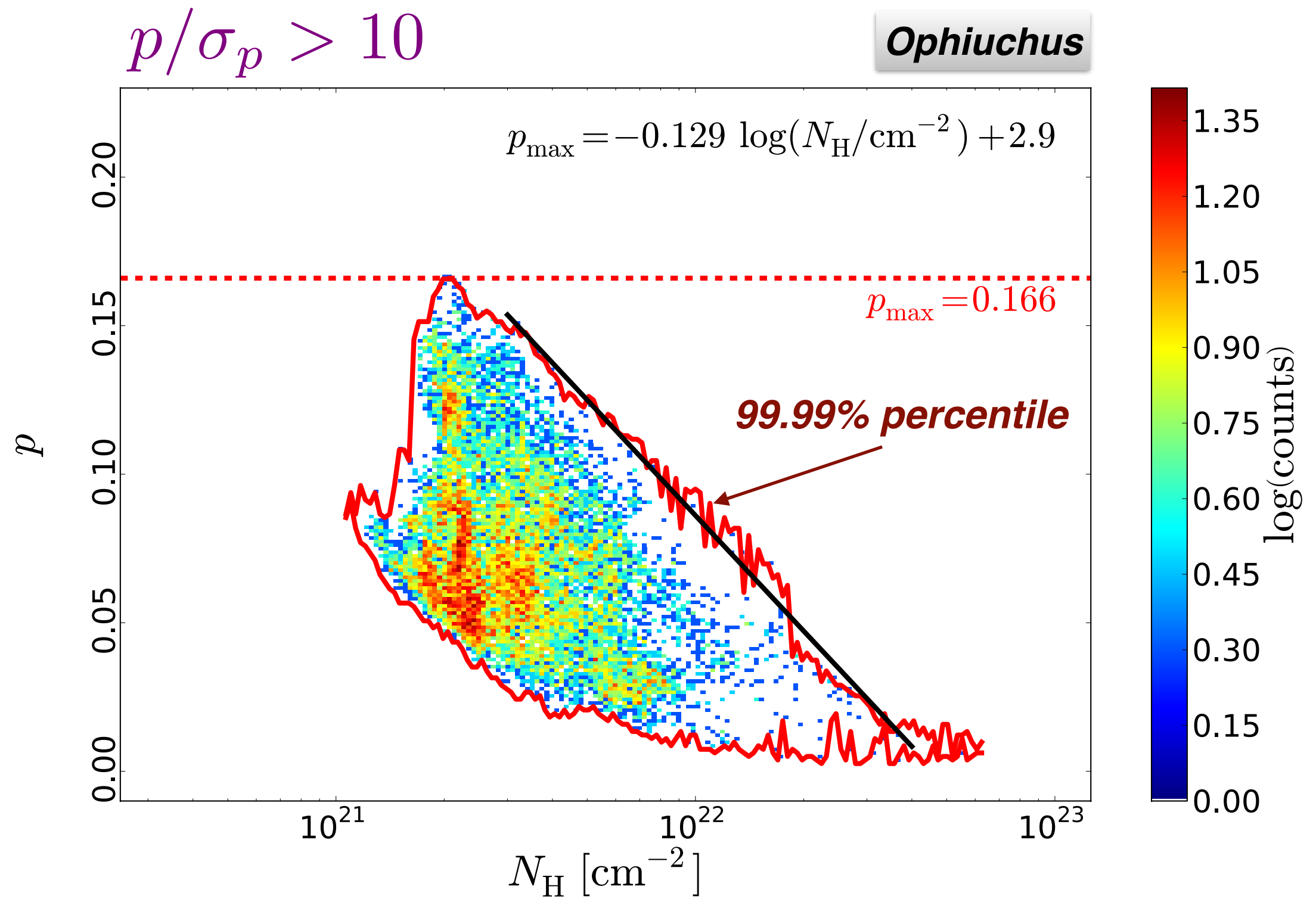


Maximum polarization fraction vs. column density



Anti-correlation robust with respect to polarization S/N

Maximum polarization fraction vs. column density



Anti-correlation robust with respect to polarization S/N

Comparison with a simulation of anisotropic MHD turbulence

- MHD turbulence simulation with self-gravity using RAMSES
- An 18 pc subset of a 50 pc simulation cube
- Converging flows of magnetized warm gas
- Mean magnetic field along the flows
- Rotation of the cube, placed at 100 pc distance
- Uniform dust temperature and intrinsic polarization
- Simulated Stokes maps at 353 GHz smoothed at 15'

starformat.obspm.fr

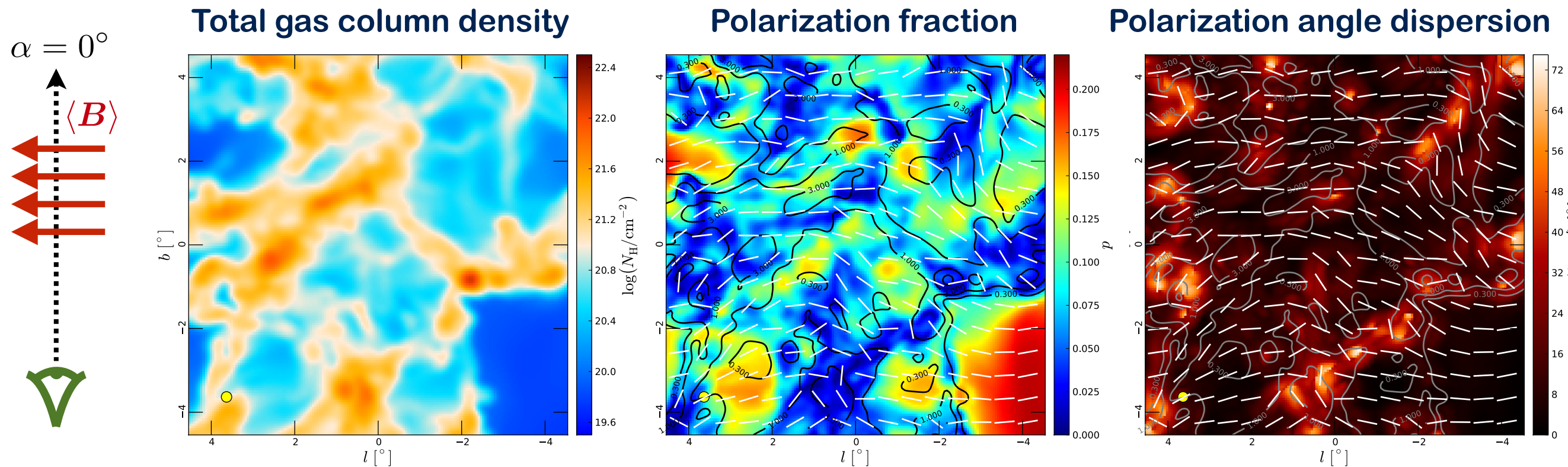
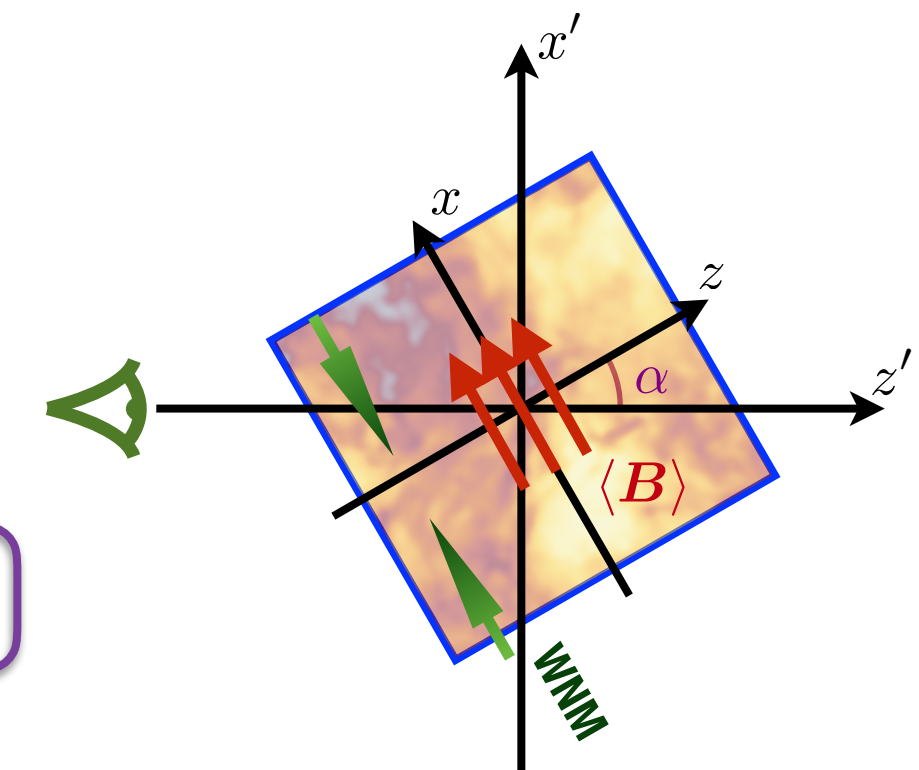
Hennebelle et al. (2008)

$$I = \int S_\nu e^{-\tau_\nu} \left[1 - p_0 \left(\cos^2 \gamma - \frac{2}{3} \right) \right] d\tau_\nu$$

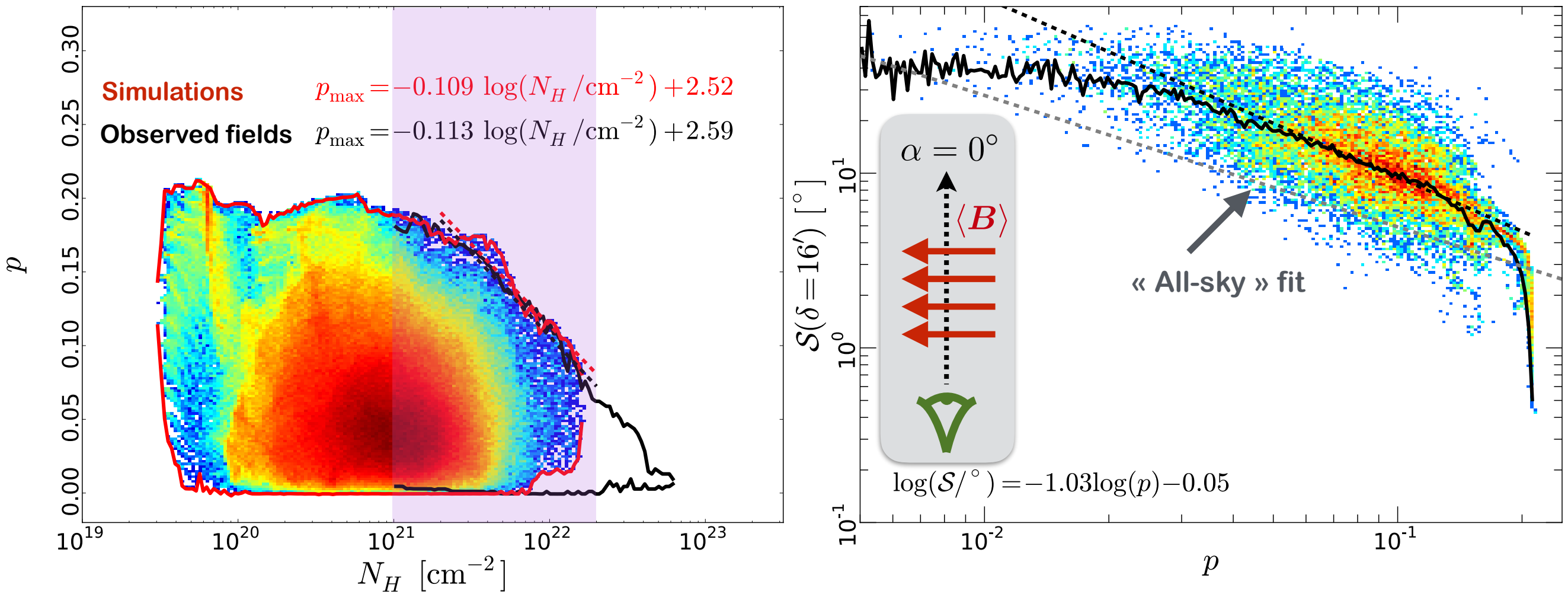
$$Q = \int p_0 S_\nu e^{-\tau_\nu} \cos(2\phi) \cos^2 \gamma d\tau_\nu$$

$$U = \int p_0 S_\nu e^{-\tau_\nu} \sin(2\phi) \cos^2 \gamma d\tau_\nu$$

$p_0 = 0.20$

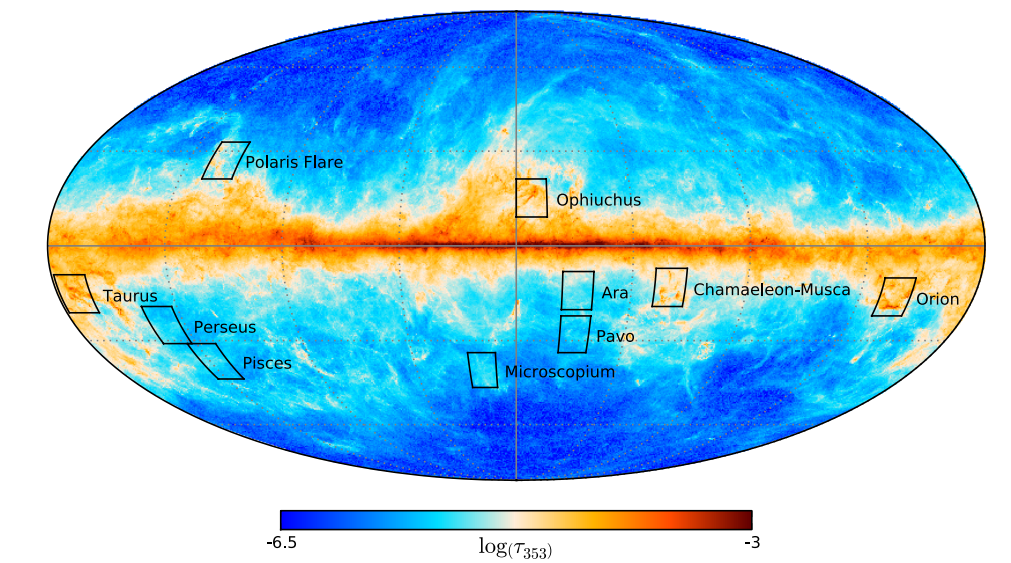
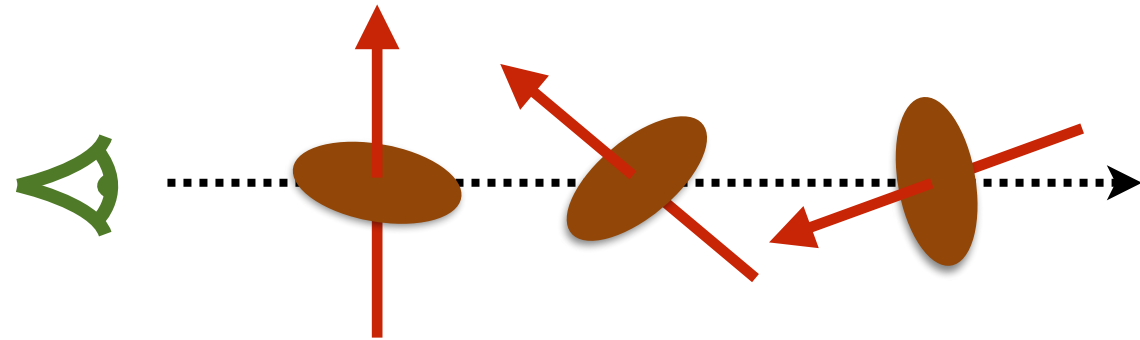


Comparison with a simulation of anisotropic MHD turbulence



- Simulations reproduce the decrease of the maximum polarization fraction with N_H in that range
- The global anti-correlation with the polarization angle dispersion function is reproduced, with a shift

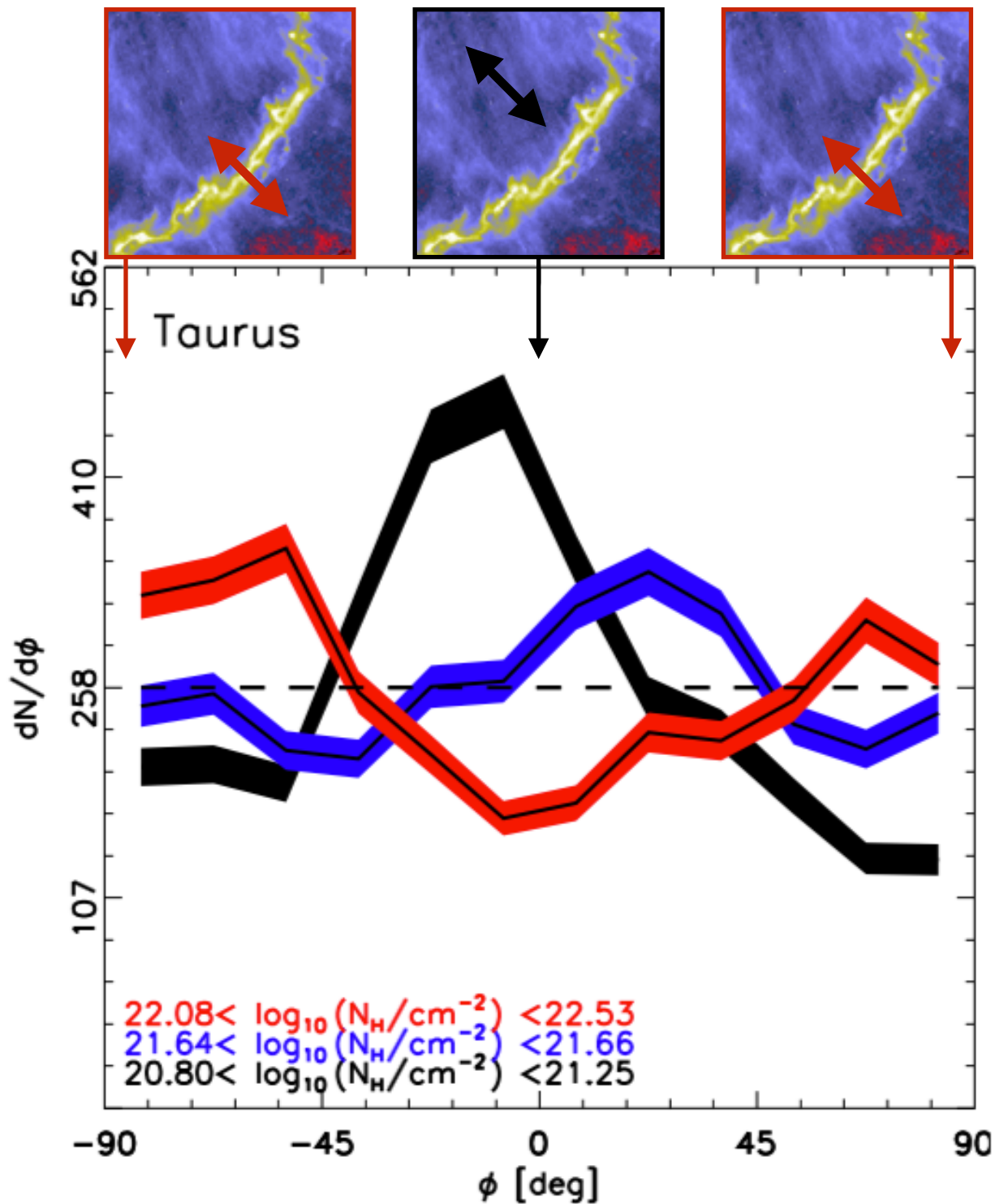
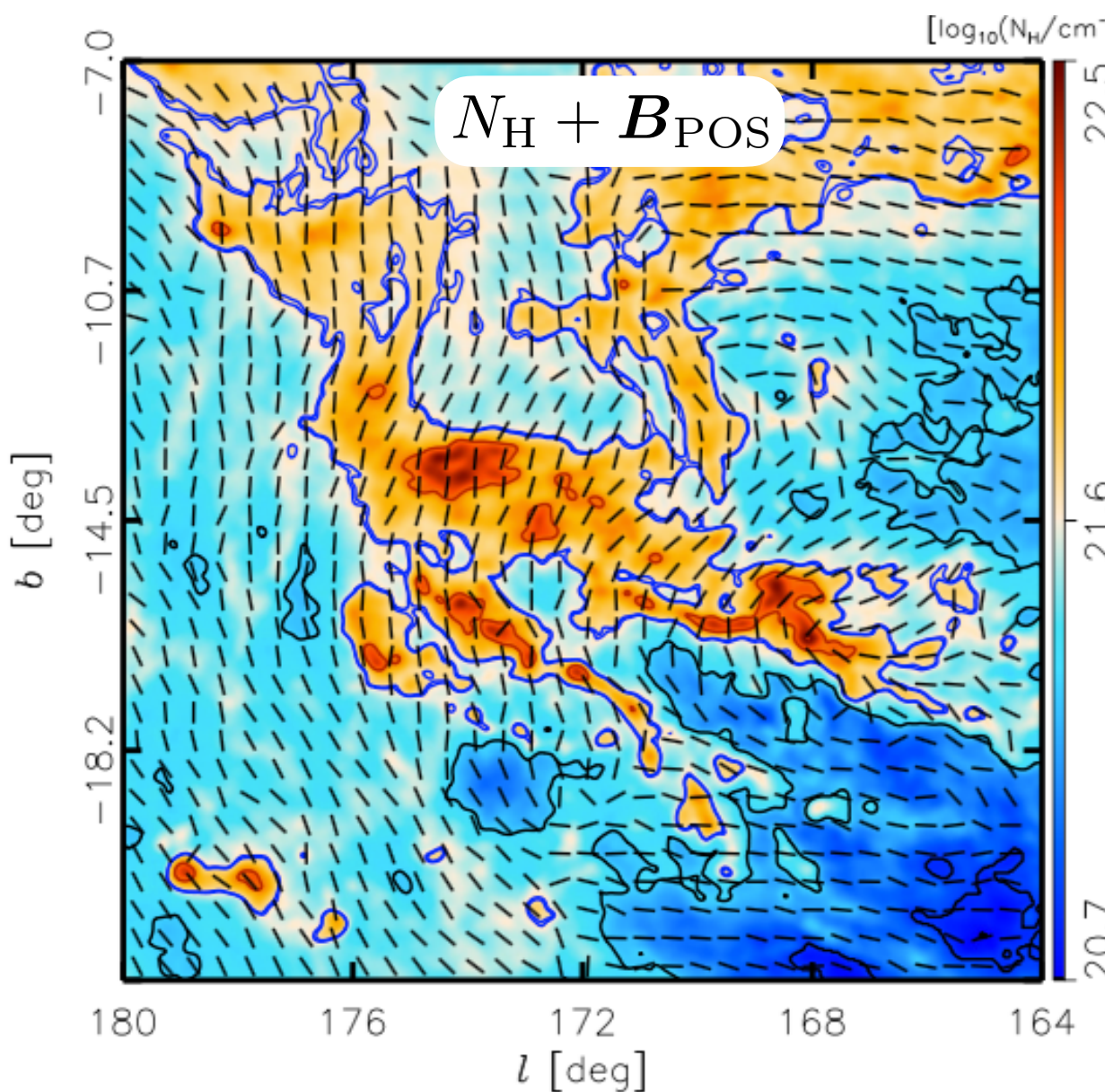
An effect of magnetic field tangling on the line of sight...



Magnetic field orientation with respect to structures of matter

- In nearby molecular clouds, using the Histogram of Relative Orientations (HRO) Soler et al. (2013)
- Change of relative orientation as column density increases
- Consistent with sub- and trans-Alfvénic simulations of MHD turbulence (strong magnetic field)
- Estimates of B from the Davis-Chandrasekhar-Fermi method Chandrasekhar & Fermi (1953), Hildebrand et al. (2009)

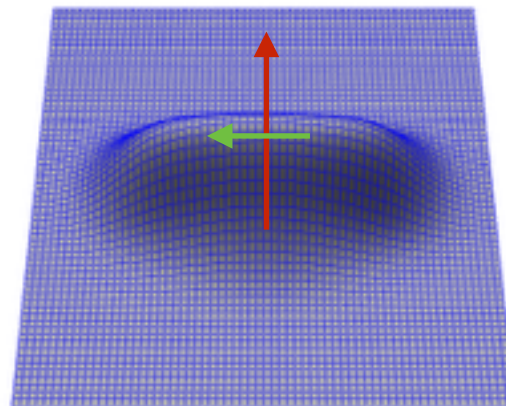
$$B_{\text{POS}} \sim 10 - 50 \mu\text{G}$$



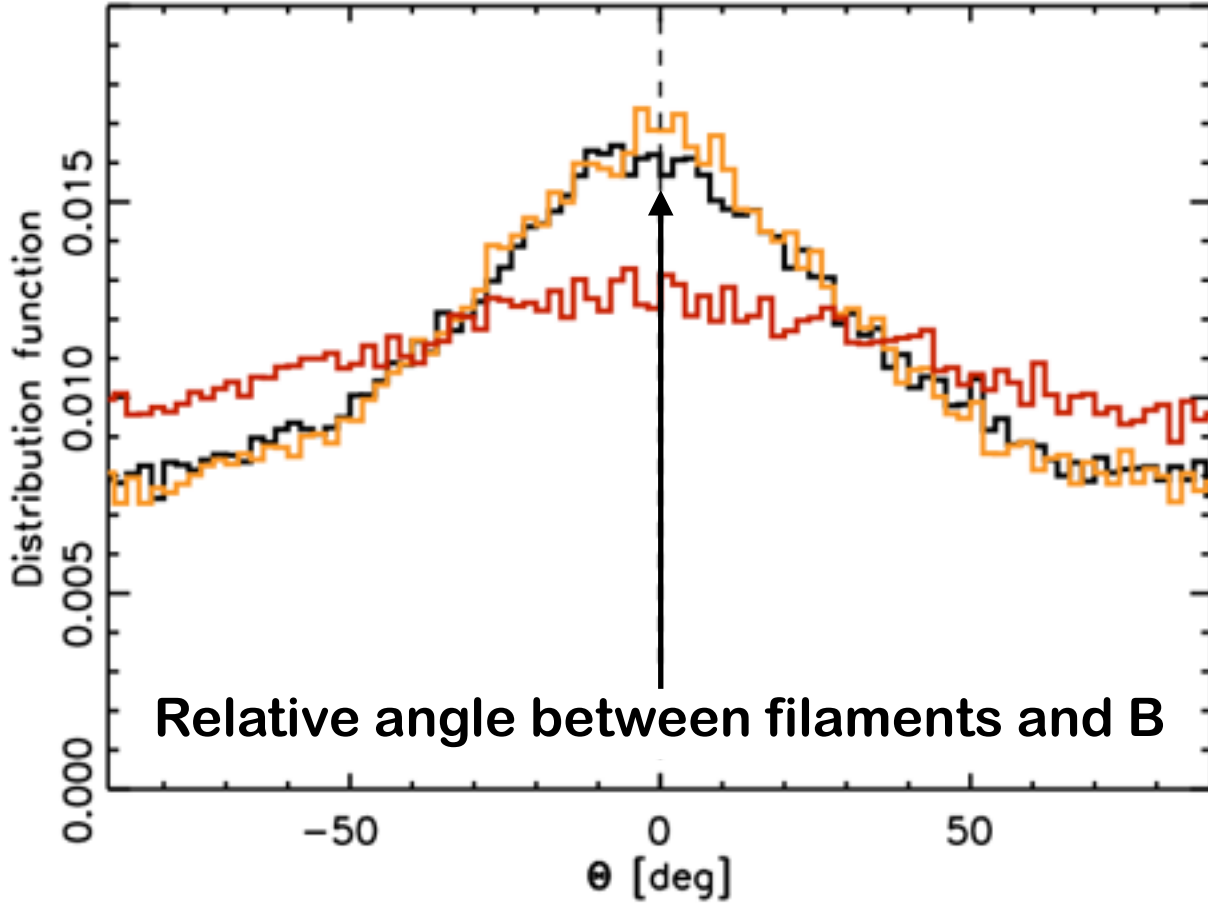
Magnetic field orientation with respect to structures of matter

- At intermediate and high Galactic latitudes, using the eigenvalues and eigenvectors of the Hessian
- Relative angle between filaments and magnetic field shows preferred alignment

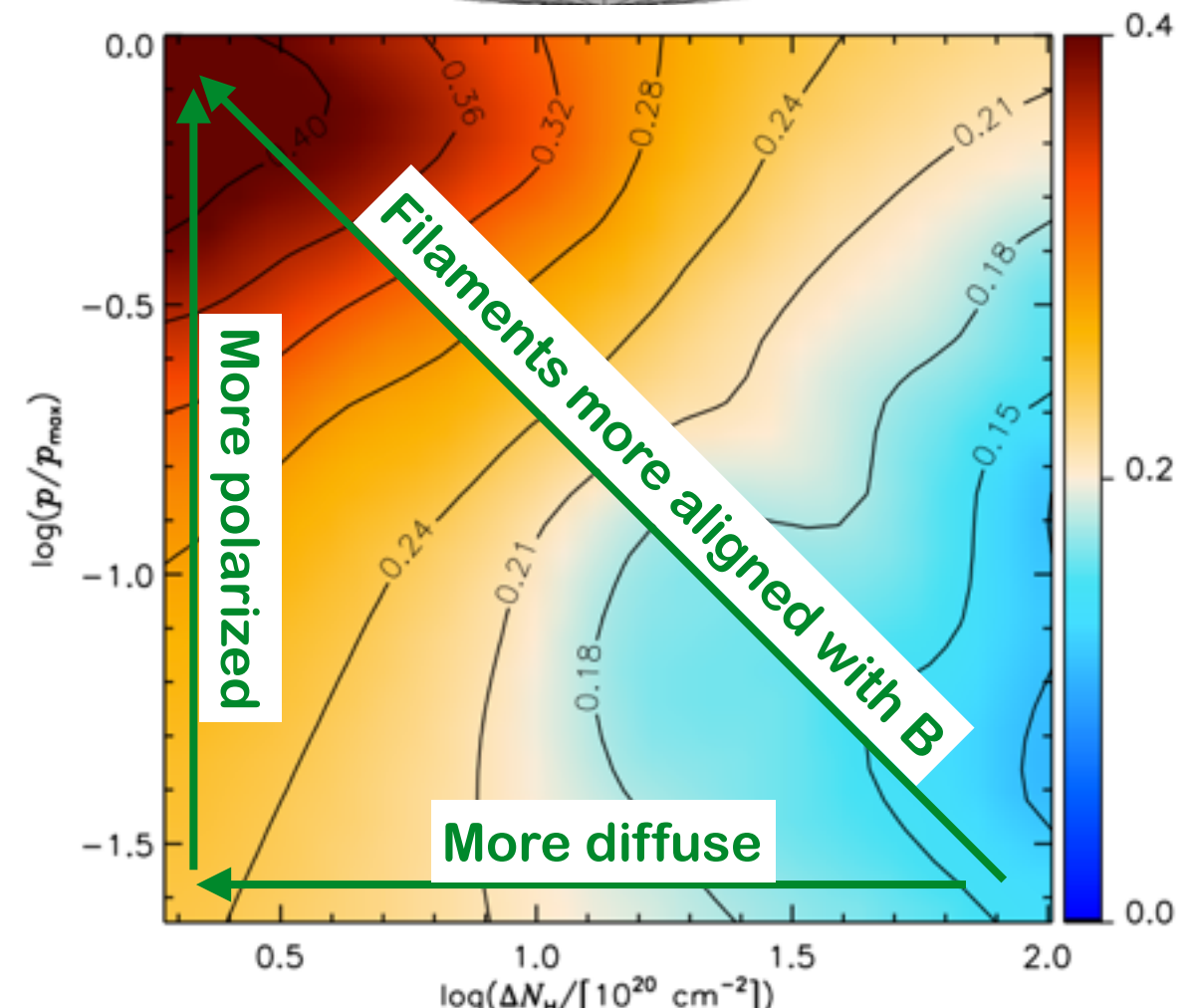
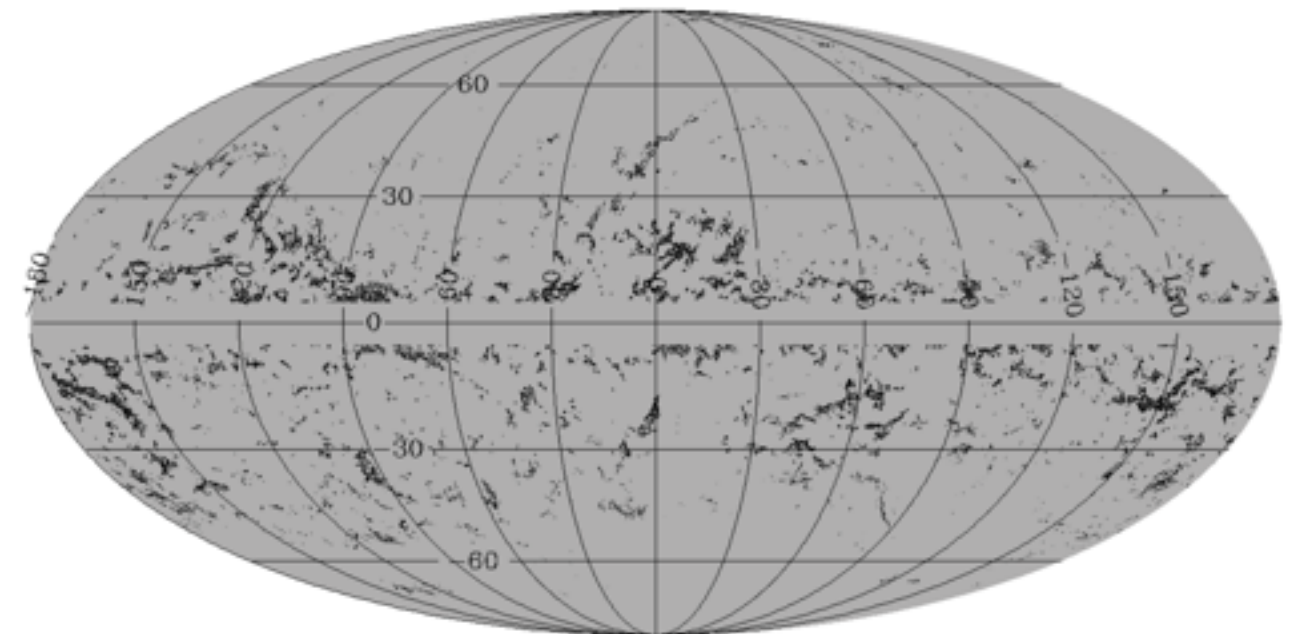
$$\mathbf{H} = \begin{bmatrix} \partial_{xx}^2 D_{353} & \partial_{xy}^2 D_{353} \\ \partial_{xy}^2 D_{353} & \partial_{yy}^2 D_{353} \end{bmatrix}$$



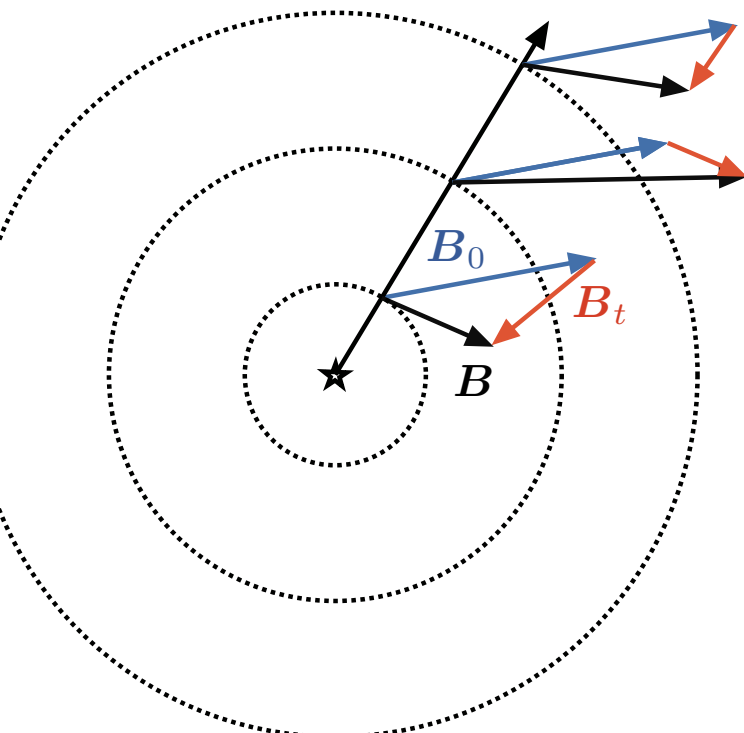
$$\langle p \rangle = 12 \pm 1\%$$



Map of the most negative eigenvalue



A Gaussian model of the polarized sky

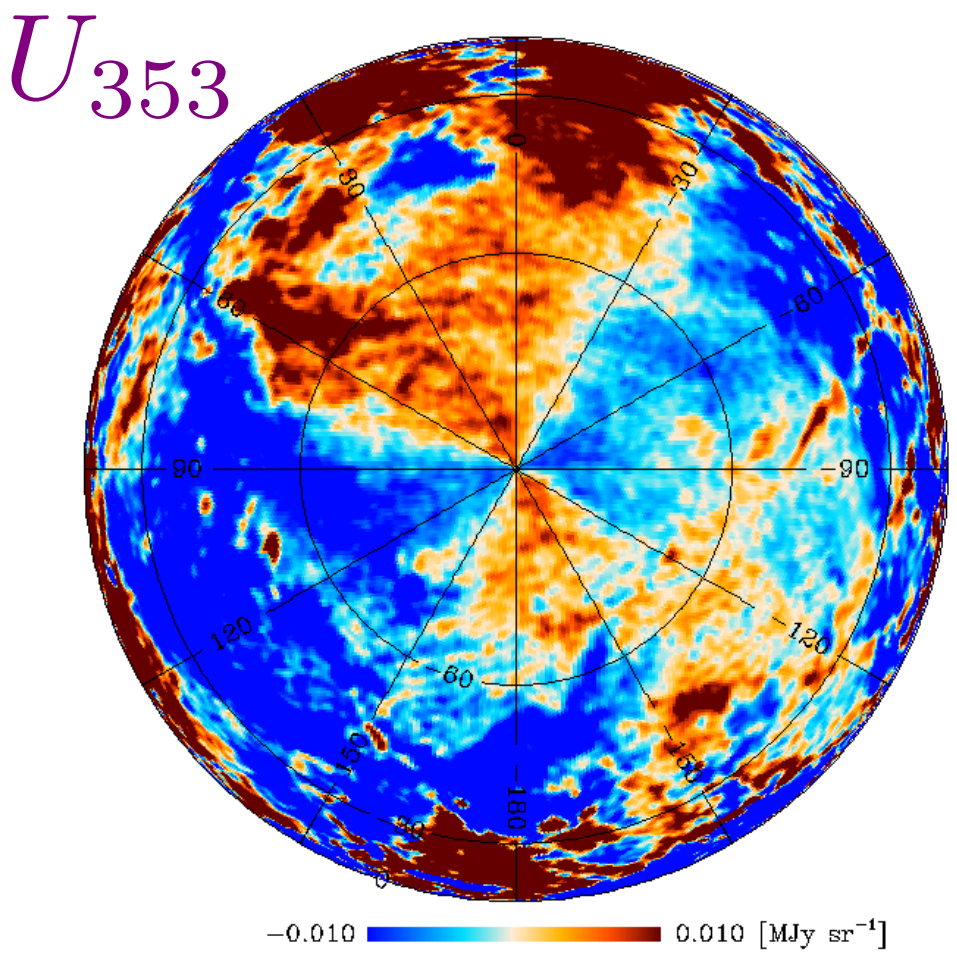


Magnetic field $B = B_0 + B_t$

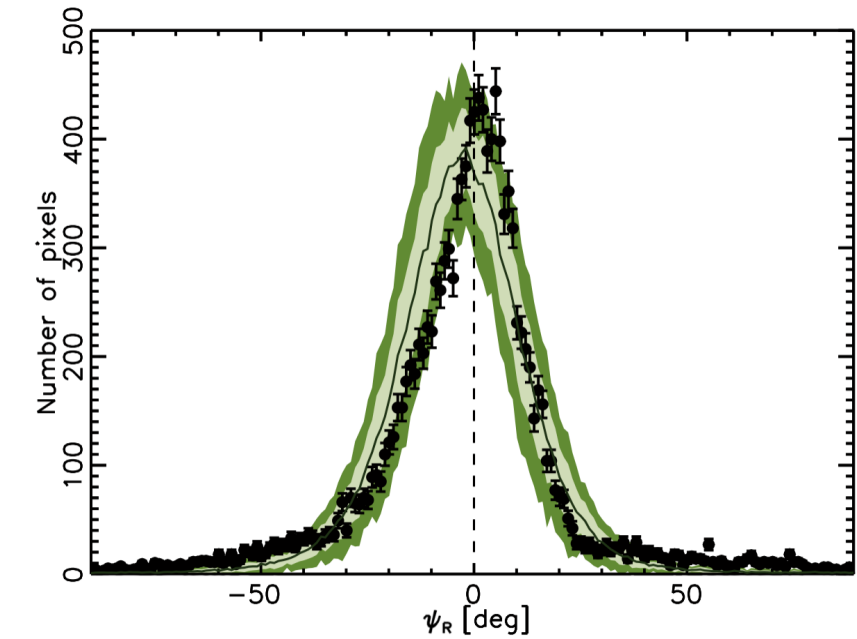
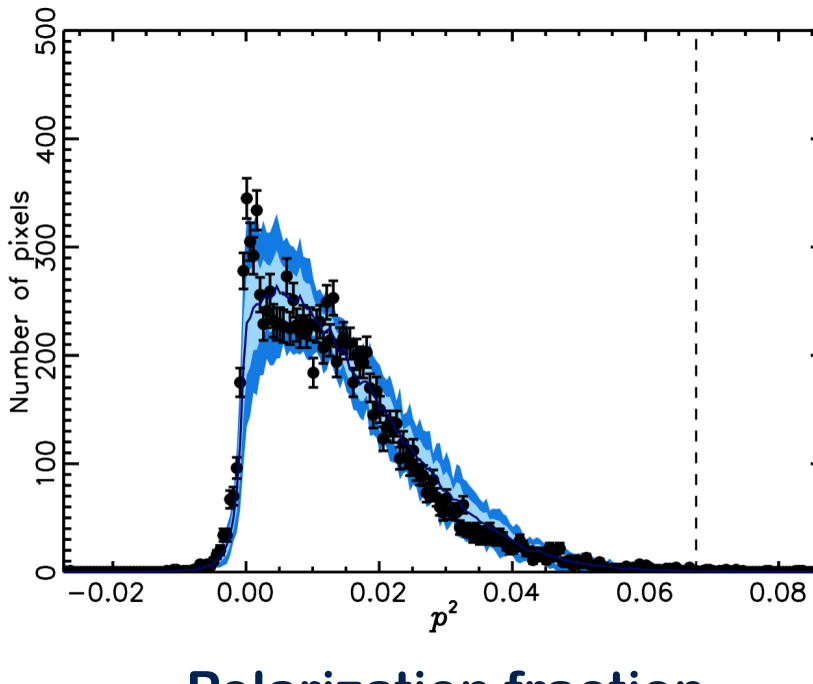
Uniform field Uniform field

Turbulent field Turbulent field

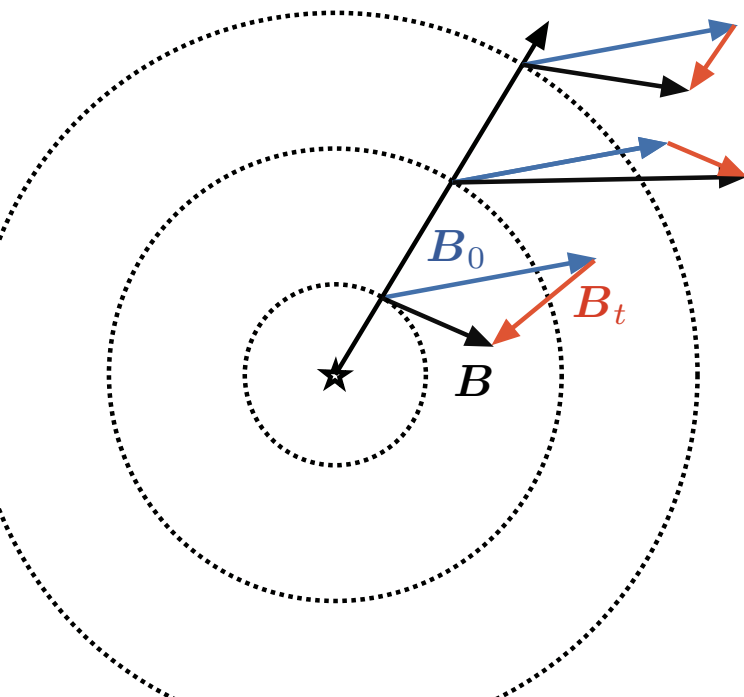
- A superposition of variously polarized layers (turbulent cells ?)
- Turbulent field : 3D Gaussian random variable
- Analysis of the Southern Galactic cap
 - Spatial power spectrum unconstrained $C_\ell \propto \ell^{\alpha_M}$
 - Direction of the large-scale field $(l_0, b_0) = (70 \pm 5^\circ, 24 \pm 5^\circ)$
 - Turbulent-to-mean ratio $f_M = 0.9 \pm 0.1$
 - Number of layers $N = 7 \pm 2$
 - Intrinsic polarization fraction $p_0 = 26 \pm 3\%$



Observations (black dots) vs. Simulations (colored regions)

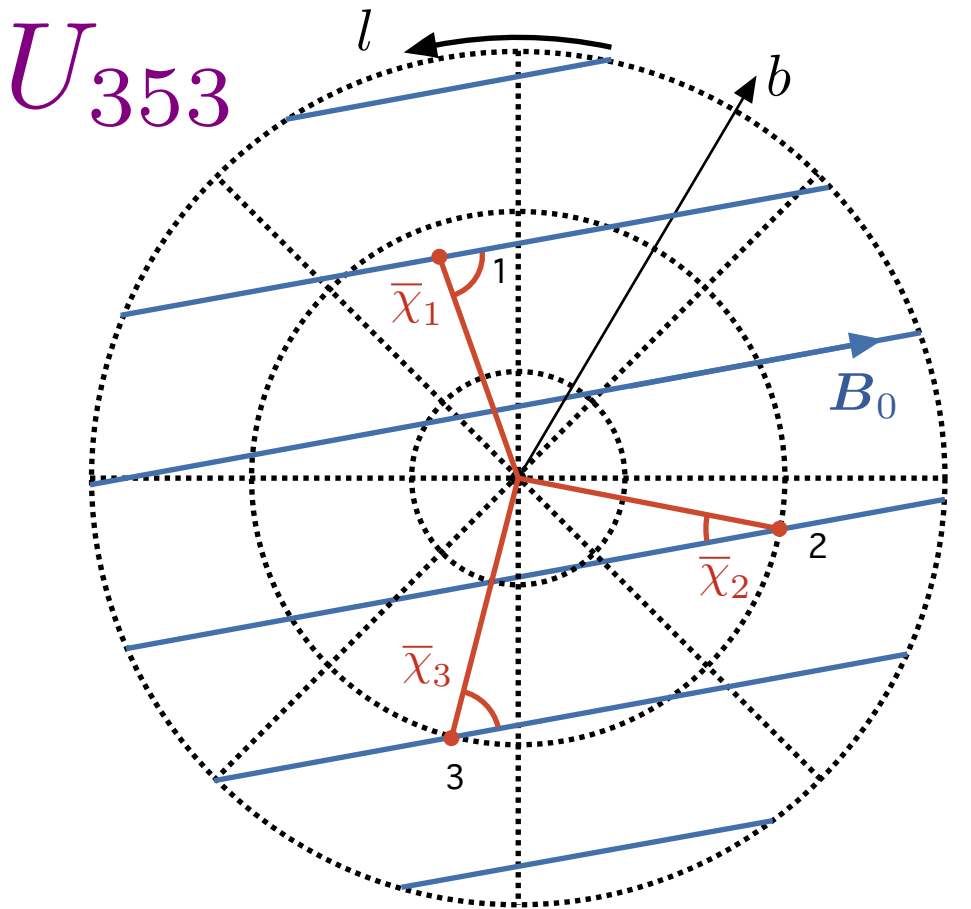


A Gaussian model of the polarized sky

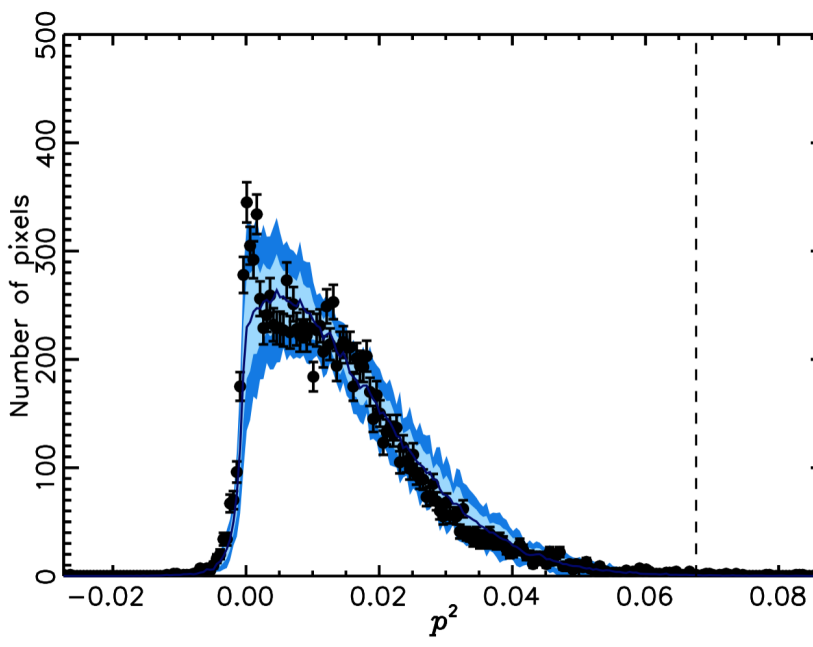


- A superposition of variously polarized layers (turbulent cells ?)
- Turbulent field : 3D Gaussian random variable
- Analysis of the Southern Galactic cap

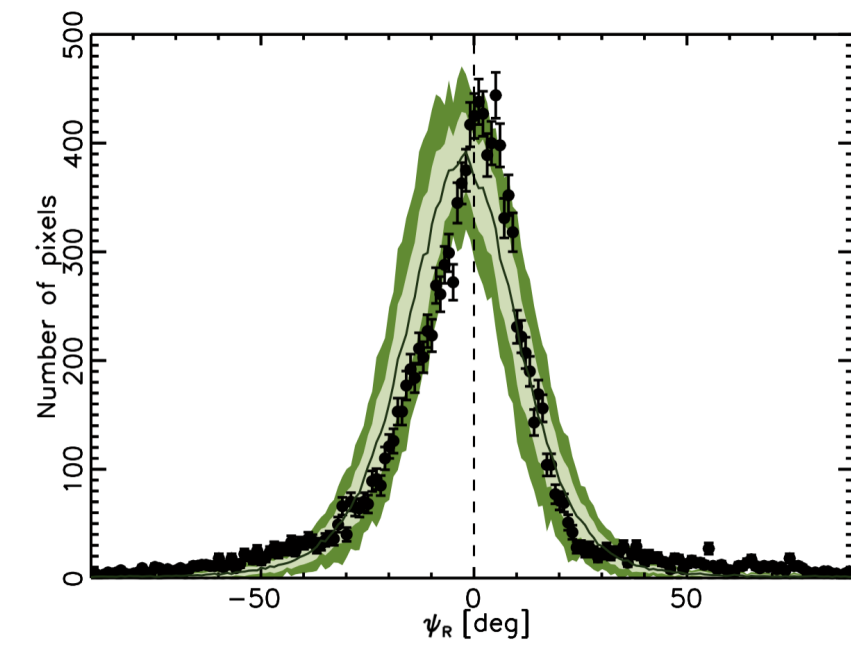
- Spatial power spectrum unconstrained $C_\ell \propto \ell^{\alpha_M}$
- Direction of the large-scale field $(l_0, b_0) = (70 \pm 5^\circ, 24 \pm 5^\circ)$
- Turbulent-to-mean ratio $f_M = 0.9 \pm 0.1$
- Number of layers $N = 7 \pm 2$
- Intrinsic polarization fraction $p_0 = 26 \pm 3\%$



Observations (black dots) vs. Simulations (colored regions)



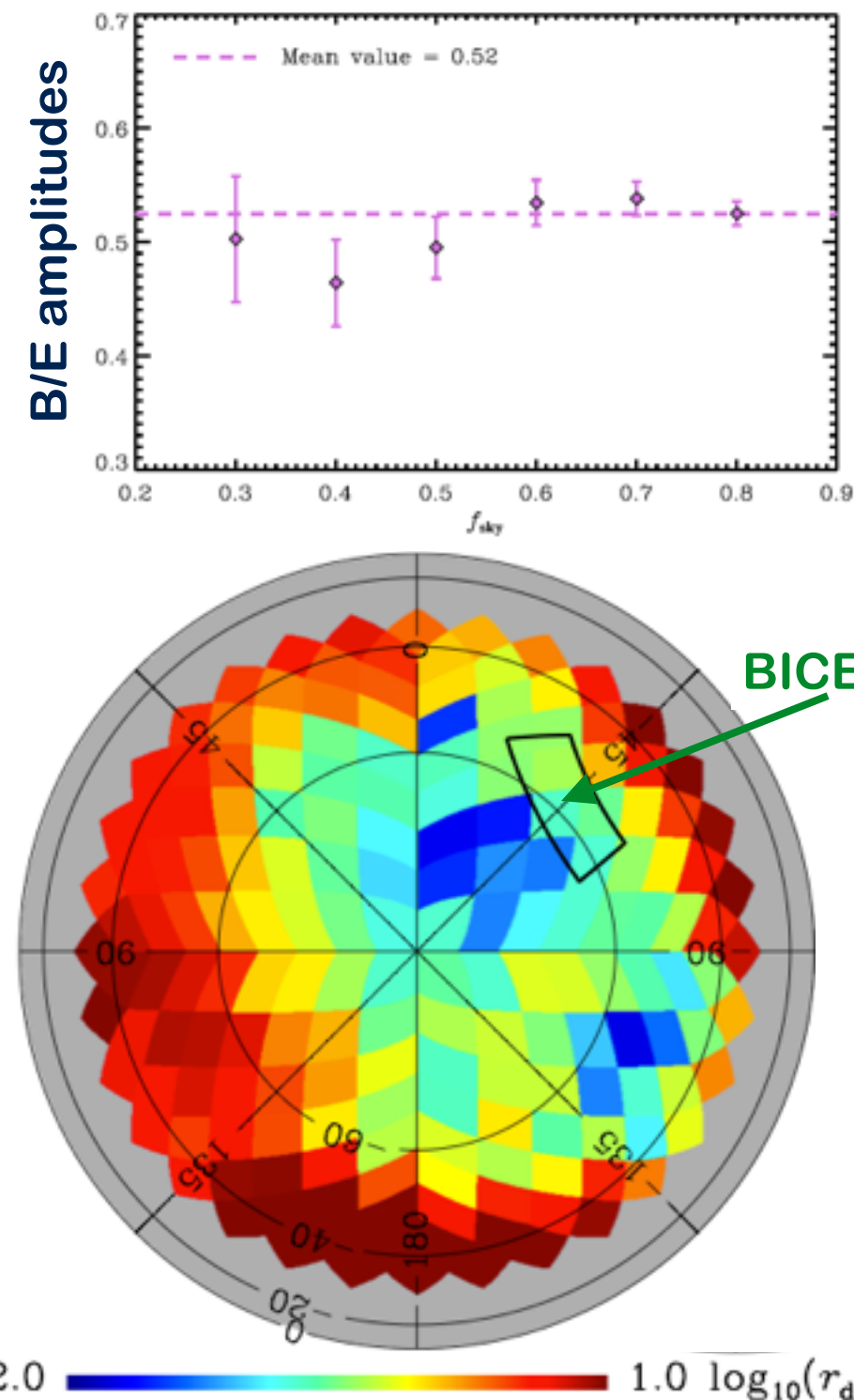
Polarization fraction



Polarization angle relative
to the large-scale field

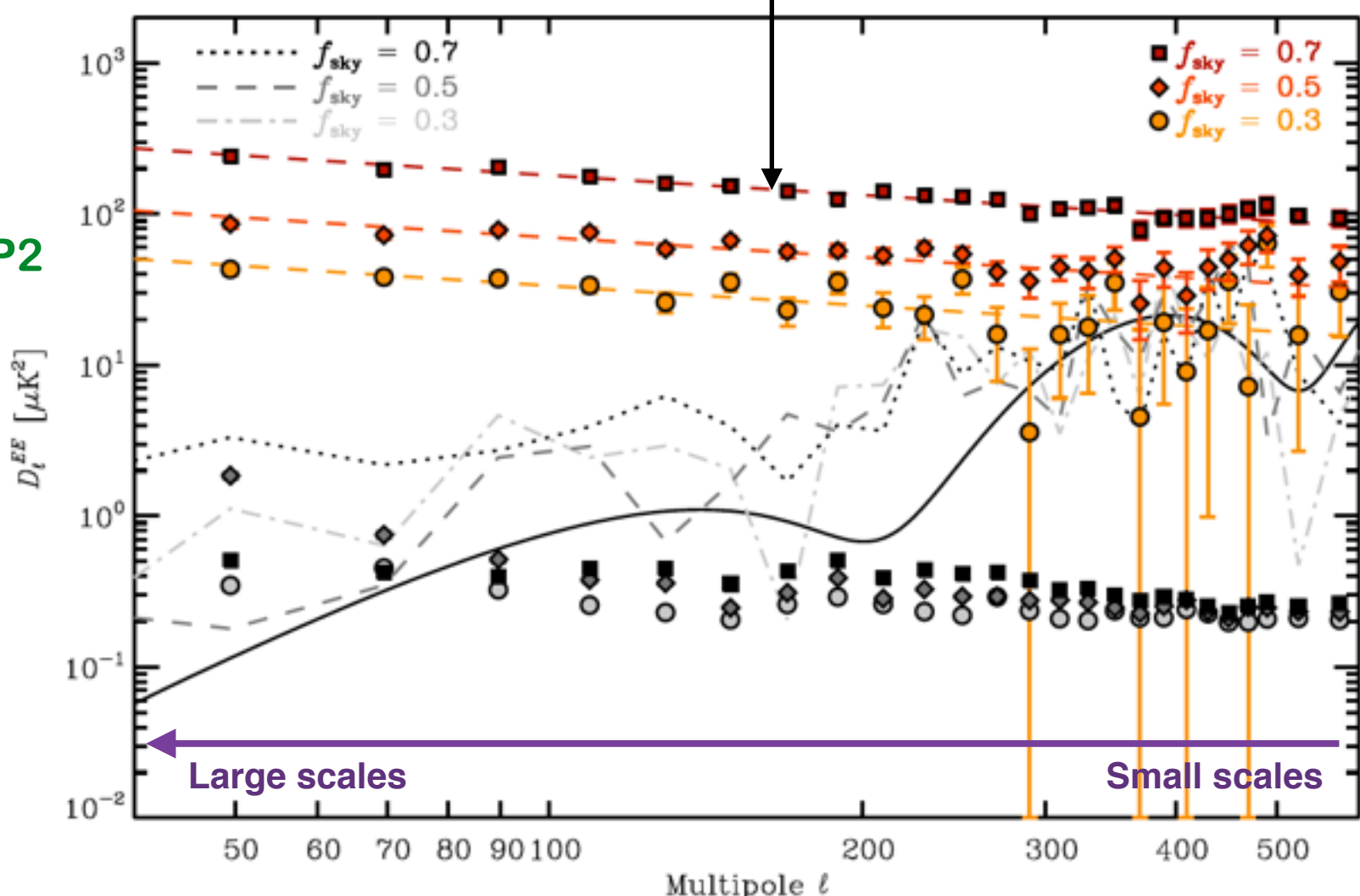
The angular power spectrum of polarized thermal dust emission

- E and B thermal dust emission angular power spectra outside the Galactic plane well fit by power laws
- Amplitudes vary approximately as the square of average dust brightness in the selected region
- Asymmetry in the E and B modes : twice as much power in E modes
- B mode power attributable to dust in the BICEP2 field compatible with reported detection



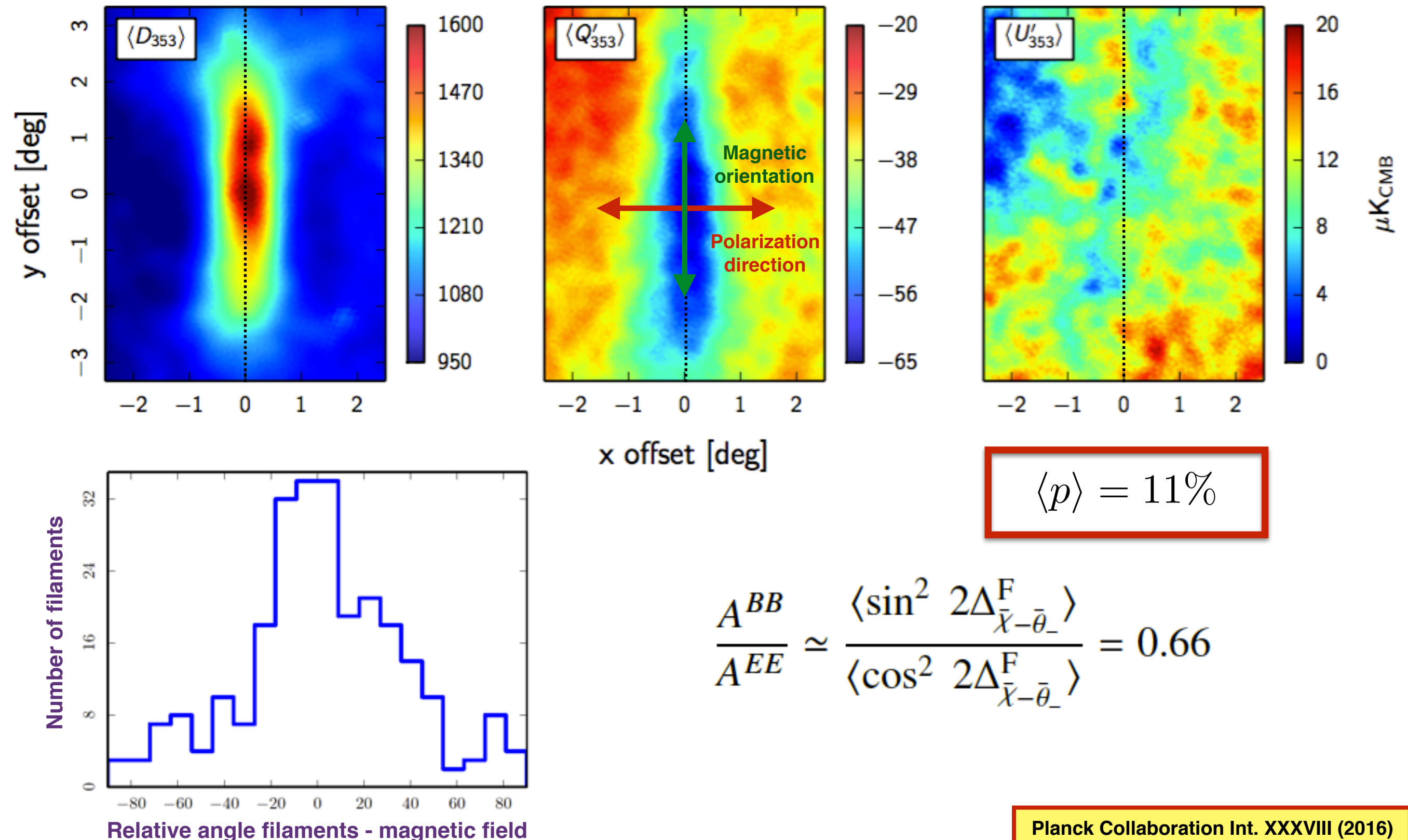
BICEP2 Collaboration (2014)

$$\mathcal{D}_\ell = \frac{\ell(\ell+1)}{2\pi} C_\ell$$



Origin of the E/B power asymmetry

- Identification of 259 matter filaments longer than 2° in the high Galactic latitude sky using the Hessian
- Preferential alignment of the filaments with the magnetic field
- Stacking of Stokes parameter maps rotated along the filaments leads to mean polarization fraction
- E/B asymmetry may be accounted for by this preferential alignment



Frequency dependence of dust polarized emission

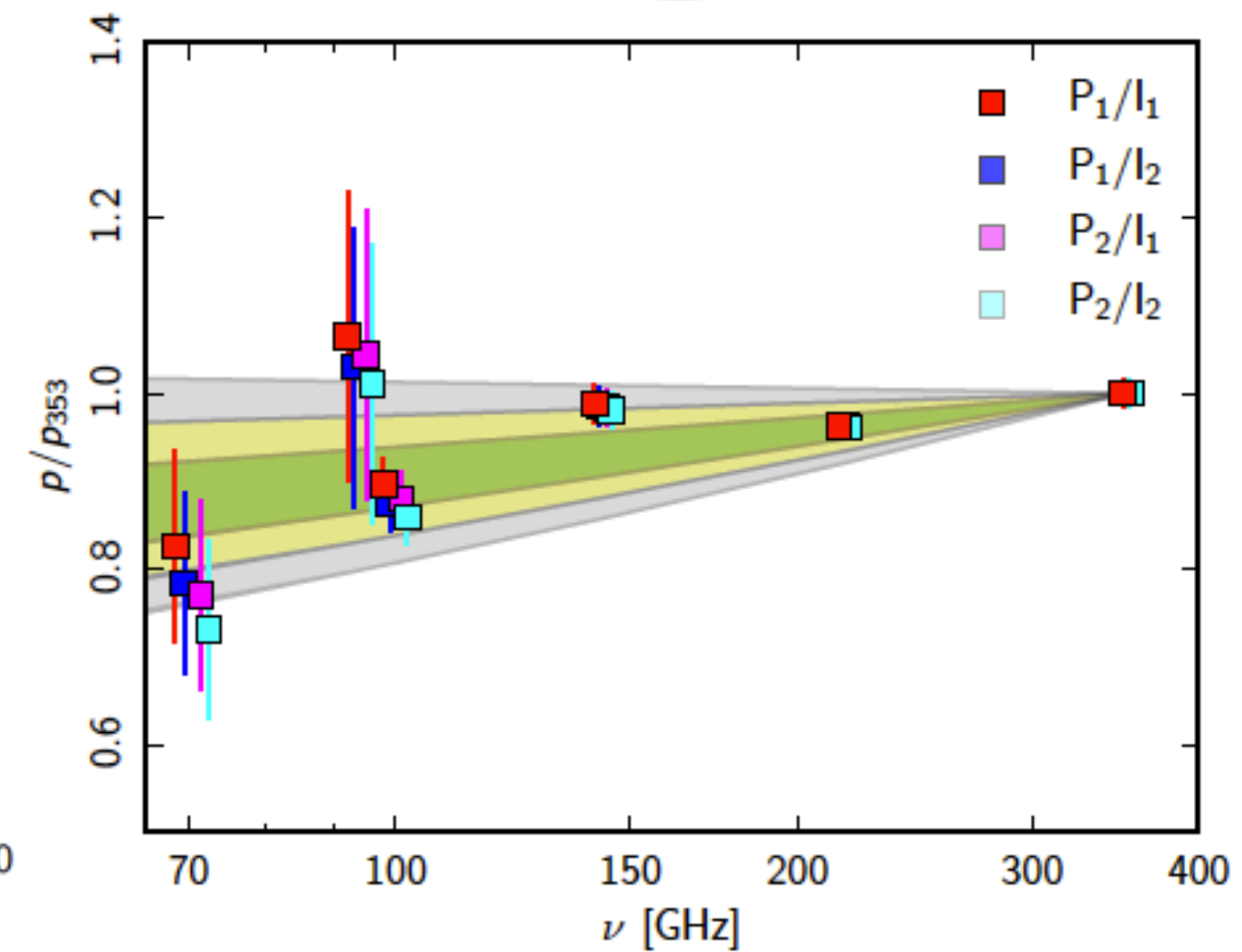
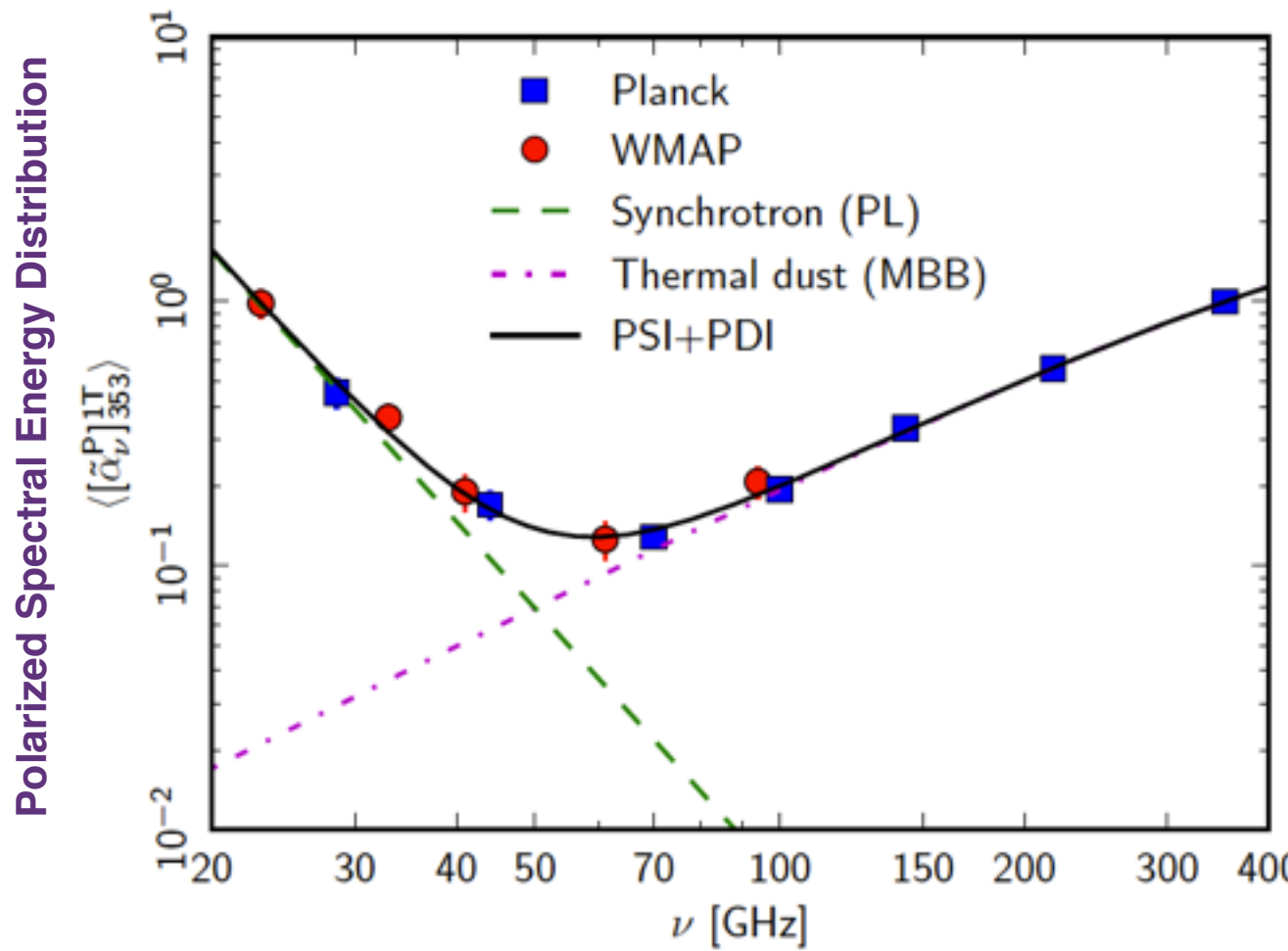
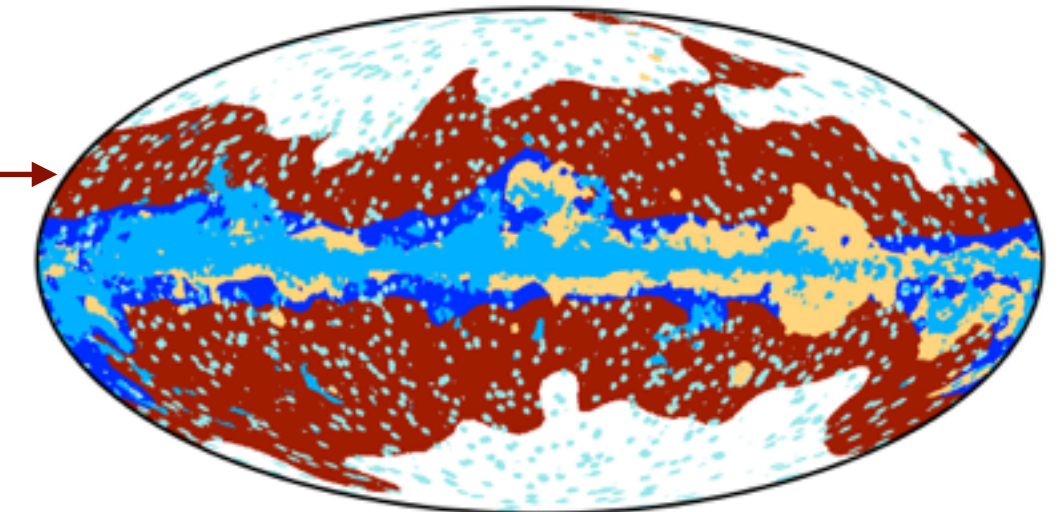
- Cross-correlation of 353 GHz Stokes maps (dust templates) with Planck and WMAP [23-353 GHz]
- Spectral indices of dust emission in total intensity and polarization over 10° radius patches
- Mean dust spectral energy distribution (SED) shows an increase below 60 GHz
- Polarization fraction of dust emission is found to decrease from 353 GHz to 70 GHz

$$T_d = 19.6 \text{ K}$$

$$\beta_I = 1.51 \pm 0.01$$

$$\beta_P = 1.59 \pm 0.02$$

Regions used →

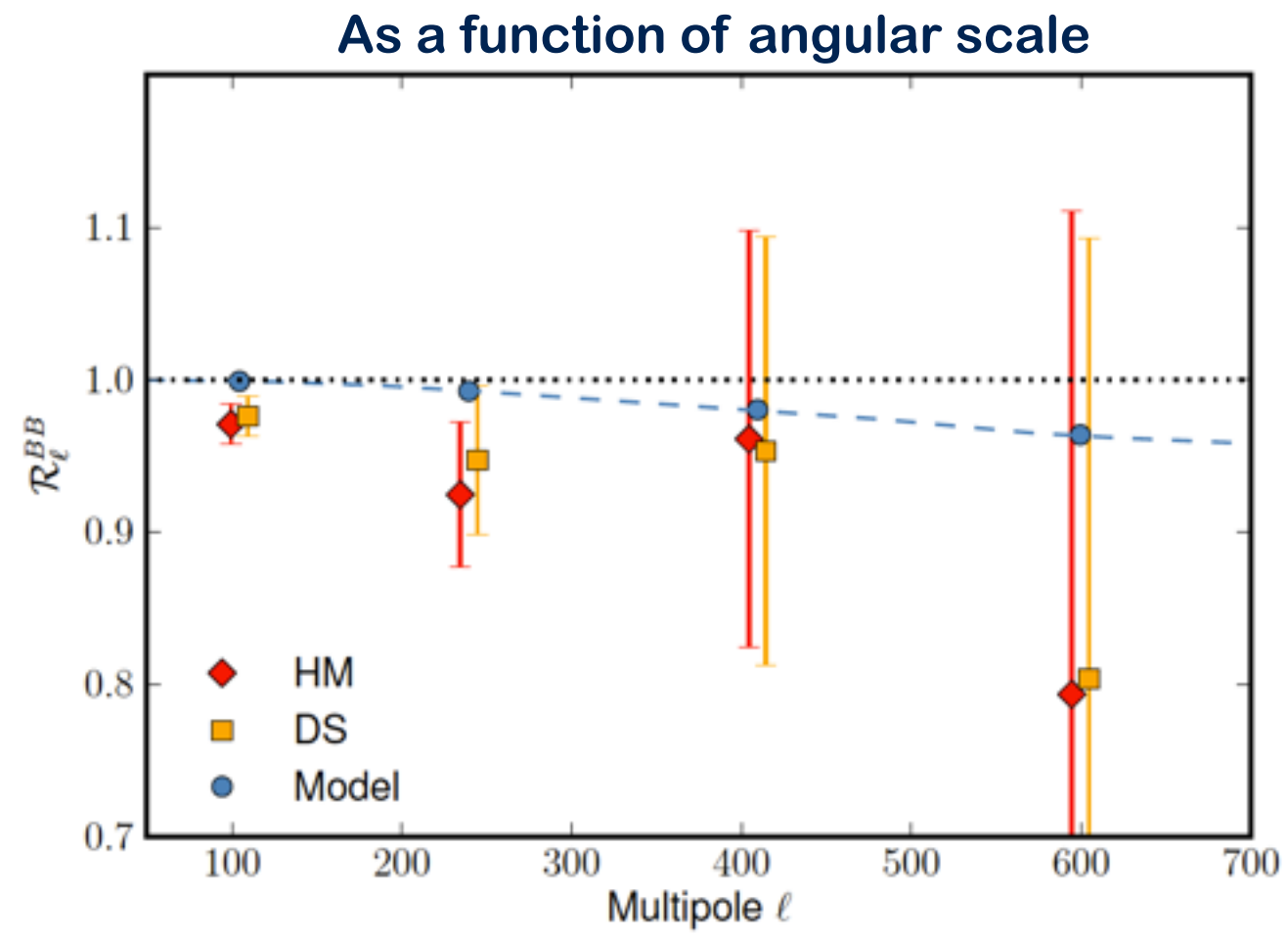
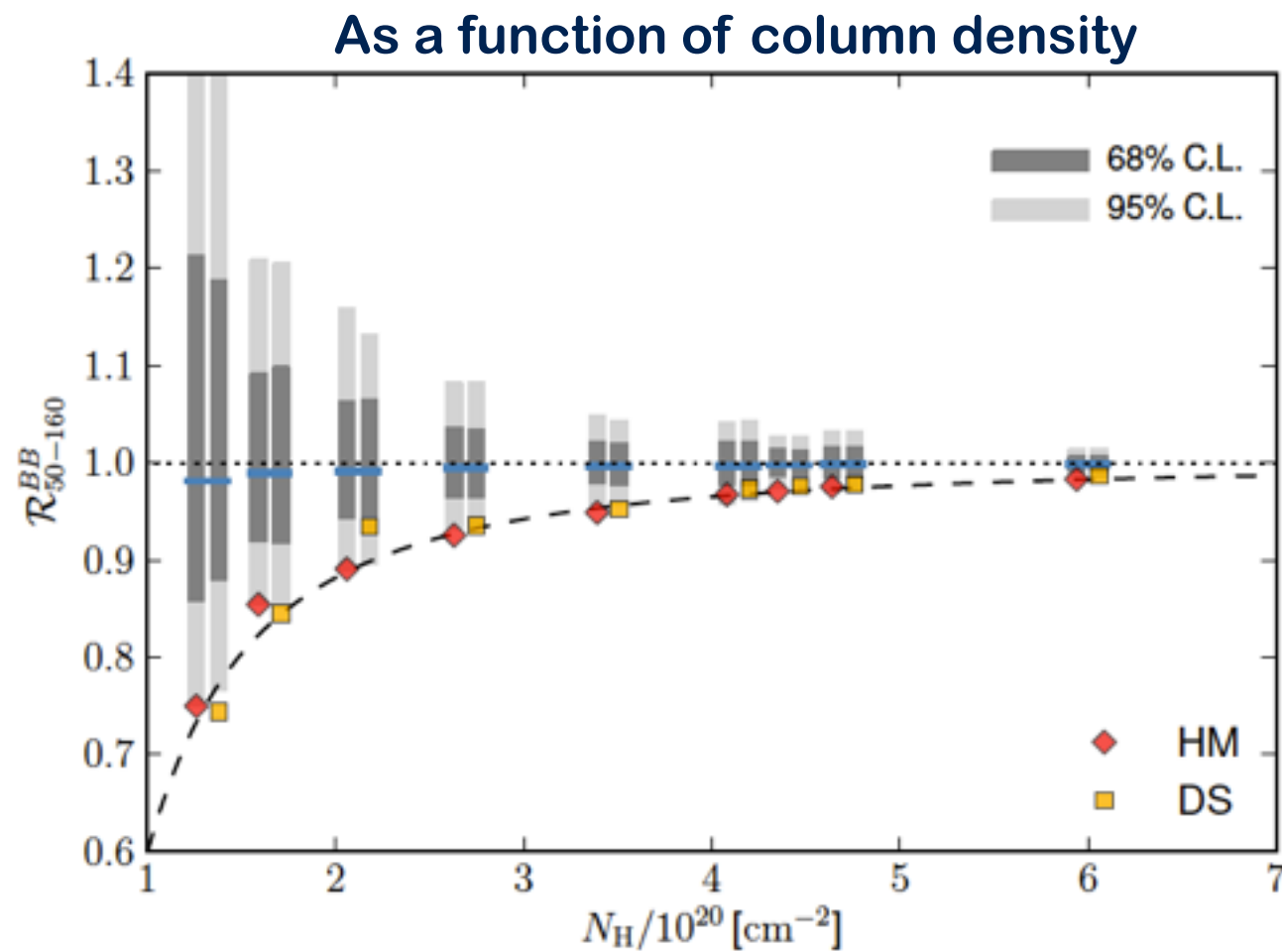


Spatial decorrelation of polarized emission across frequencies

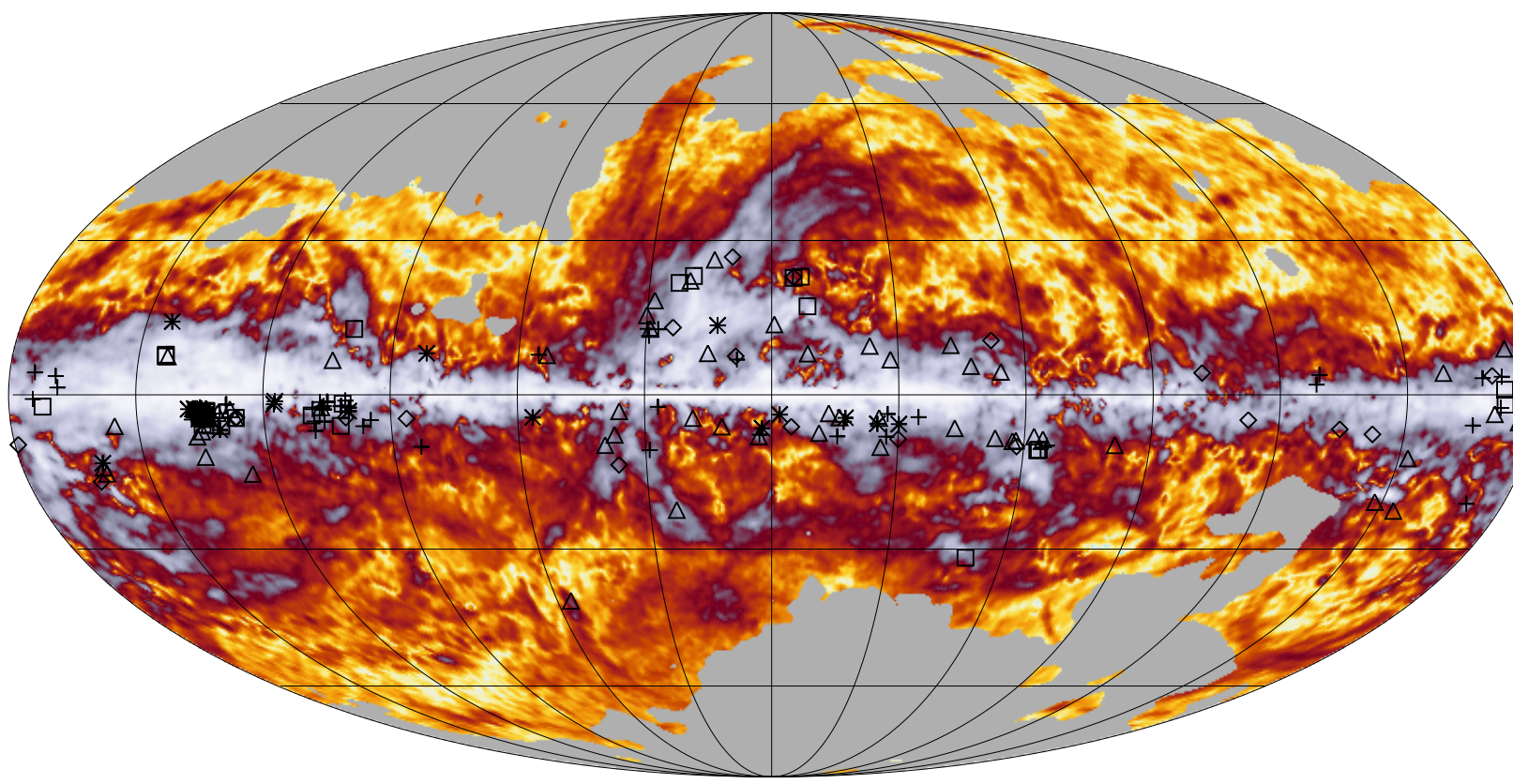
- Correlation ratio of 353 and 217 GHz E and B modes lower than expected
- Decorrelation stronger in more diffuse regions and at smaller scales, possibly very variable on the sky
- Spatial variations of the polarized SED spectral index or of the polarization angle
- Fundamental issue when extrapolating dust emission templates from high frequency to CMB channels

Correlation ratio

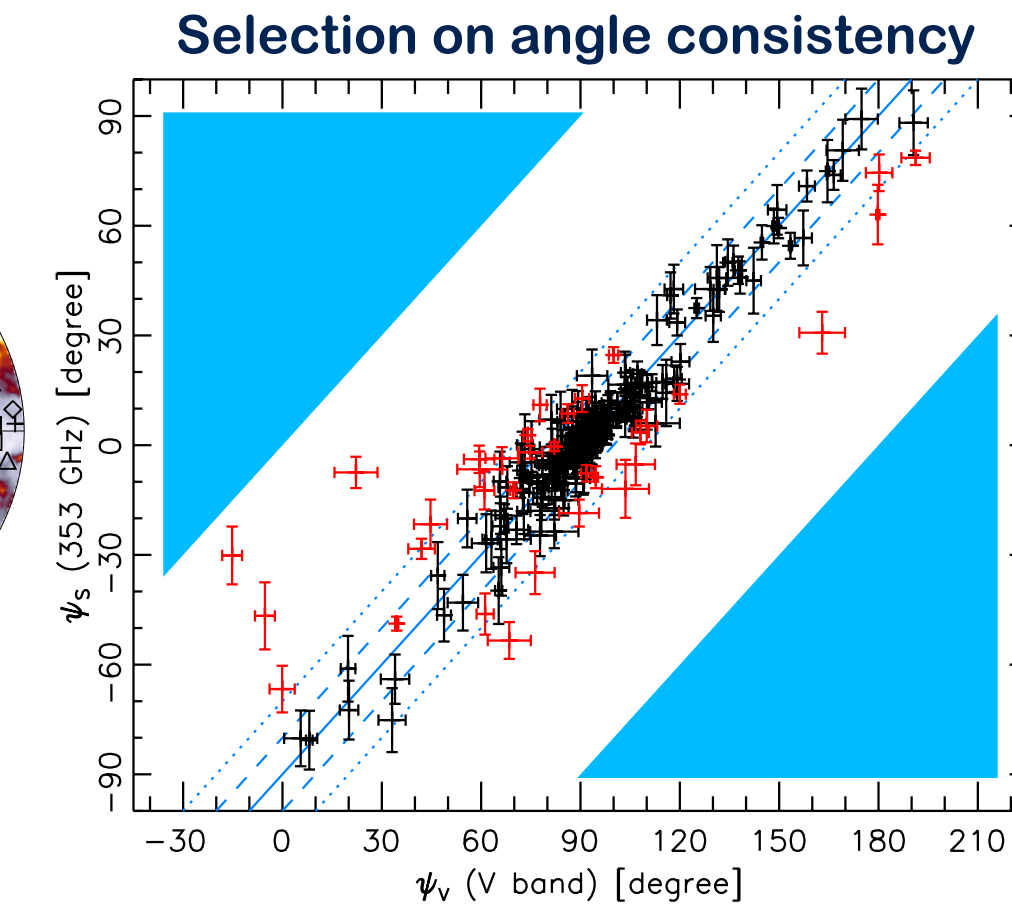
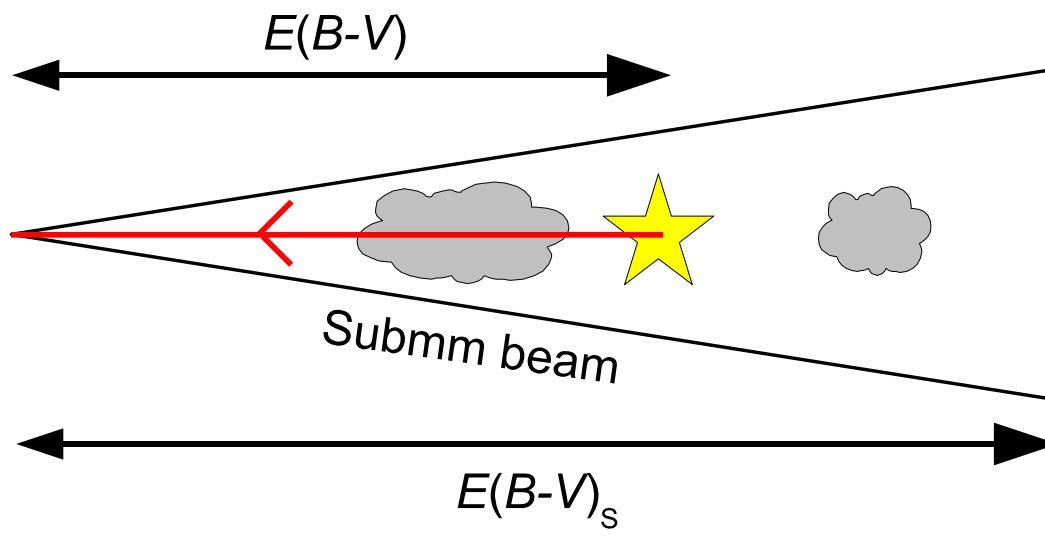
$$\mathcal{R}_\ell^{XX} \equiv \frac{C_\ell^{XX}(353 \times 217)}{\sqrt{C_\ell^{XX}(353 \times 353) C_\ell^{XX}(217 \times 217)}} \quad X \in \{E, B\}$$



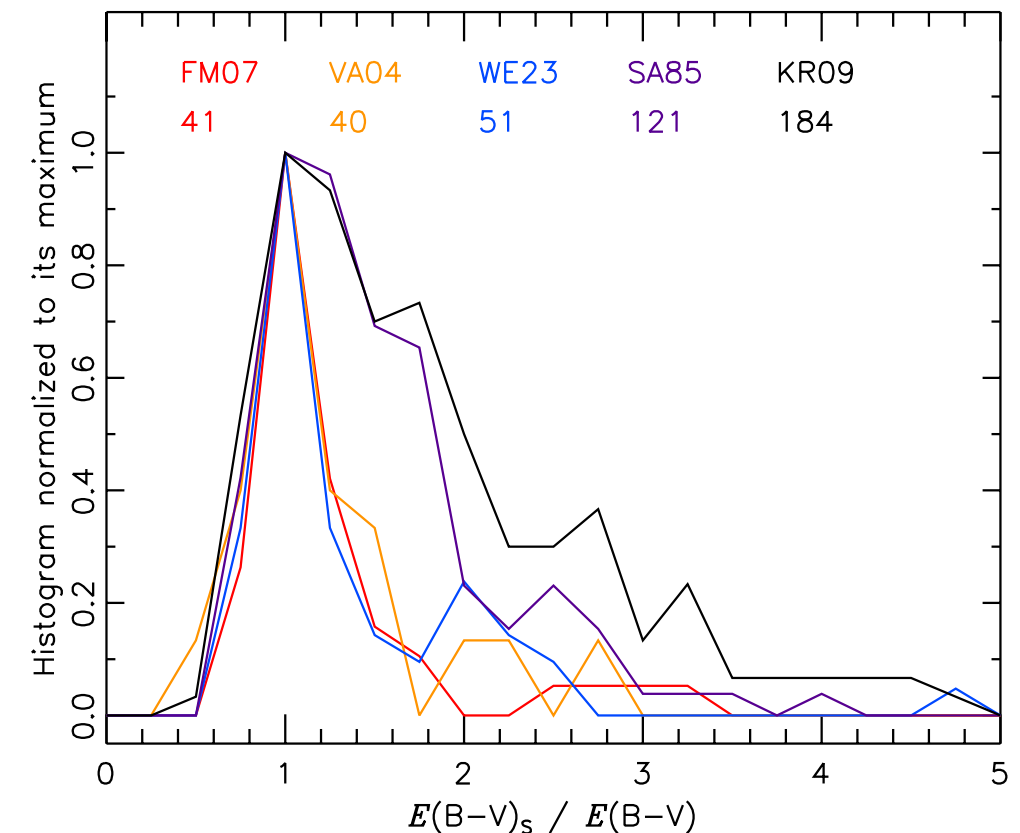
Comparison with starlight polarization in extinction



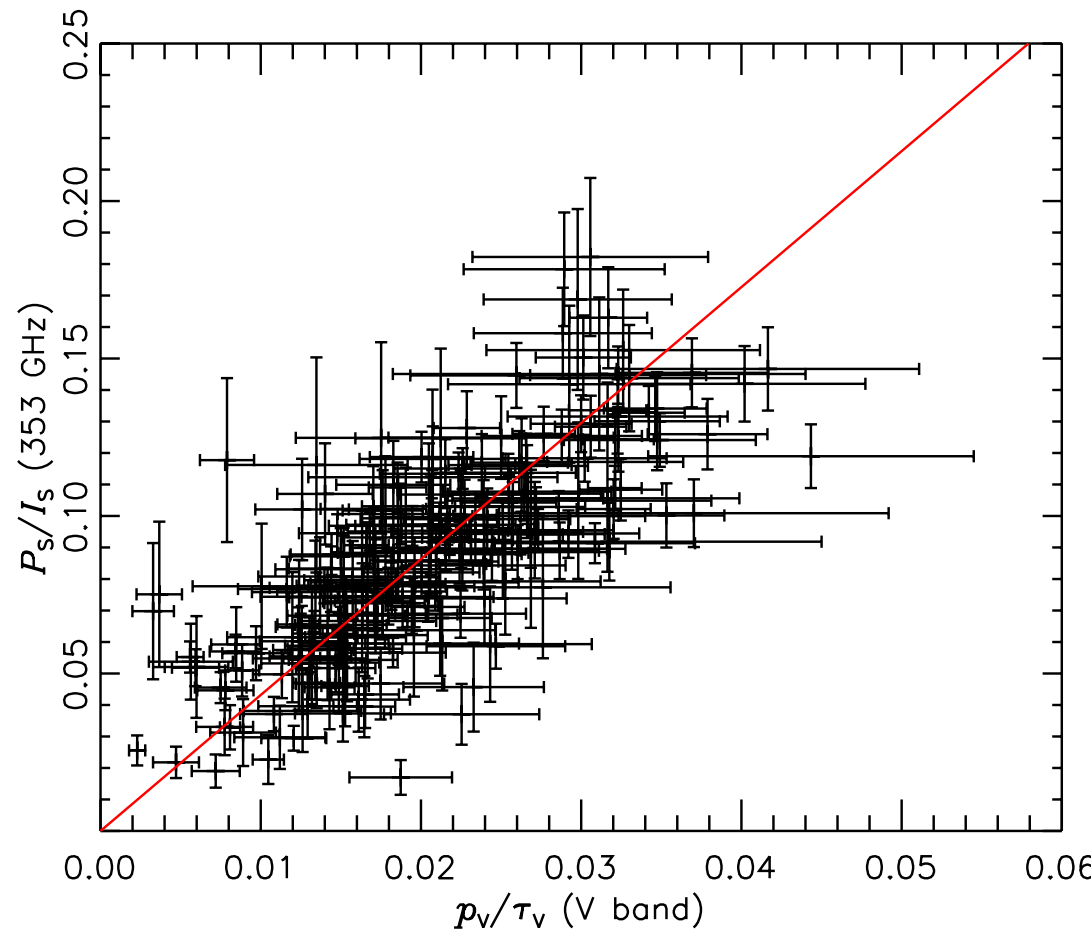
Selection of 206 stars with optical polarization measurements with consistent polarization angles and column densities



Selection on reddening ratio

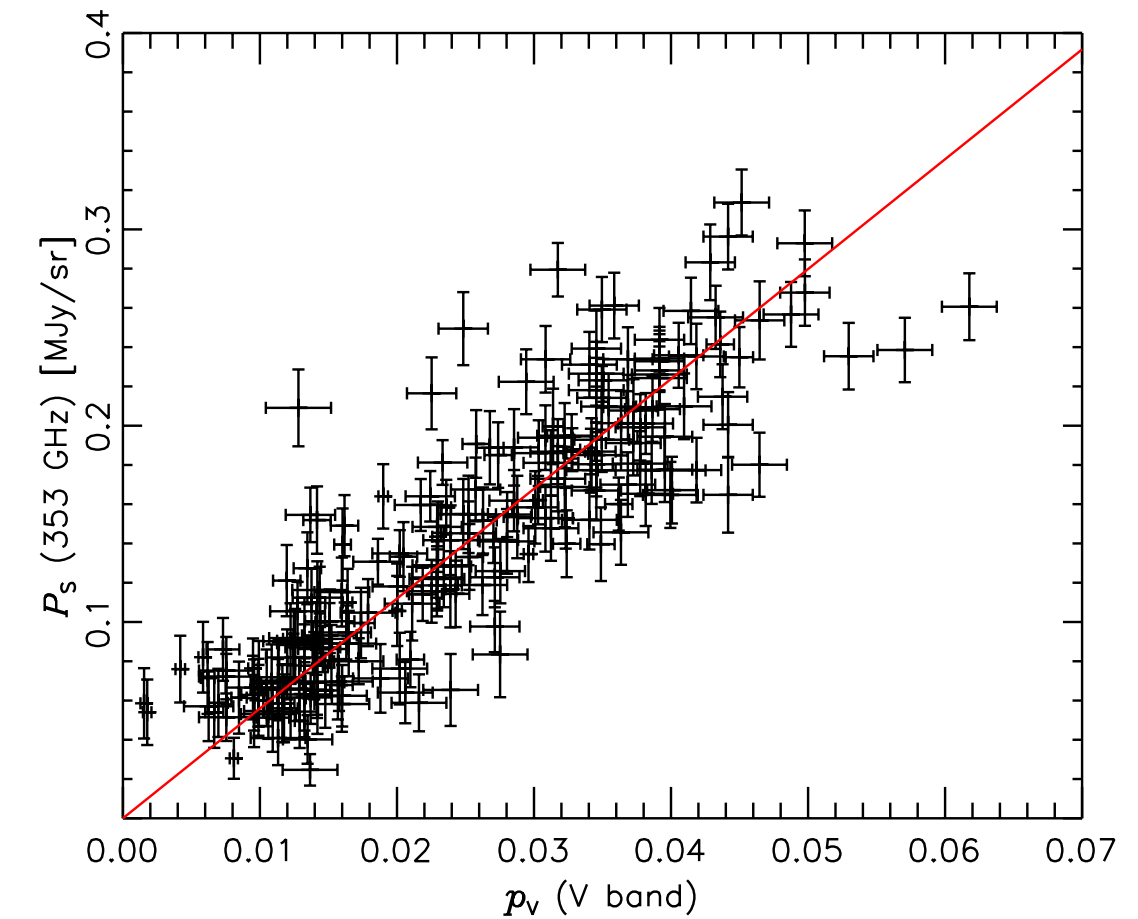


Comparison with starlight polarization in extinction



$$R_{S/V} = \frac{P_S/I_S}{p_V/\tau_V} = 4.2 \pm 0.2 \pm 0.3 \quad (\text{Stat}) \quad (\text{Syst})$$

- Reasonably compatible with current dust models
- Not very discriminating

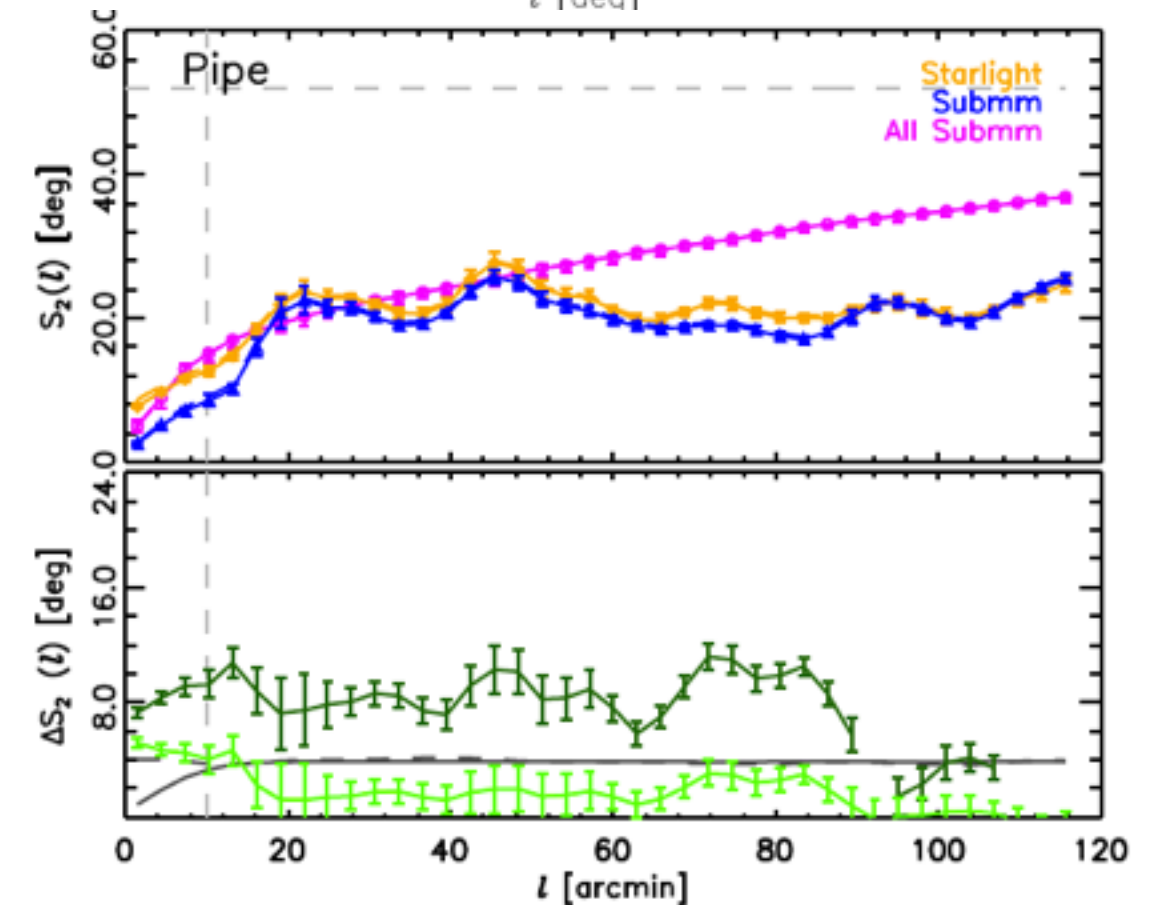
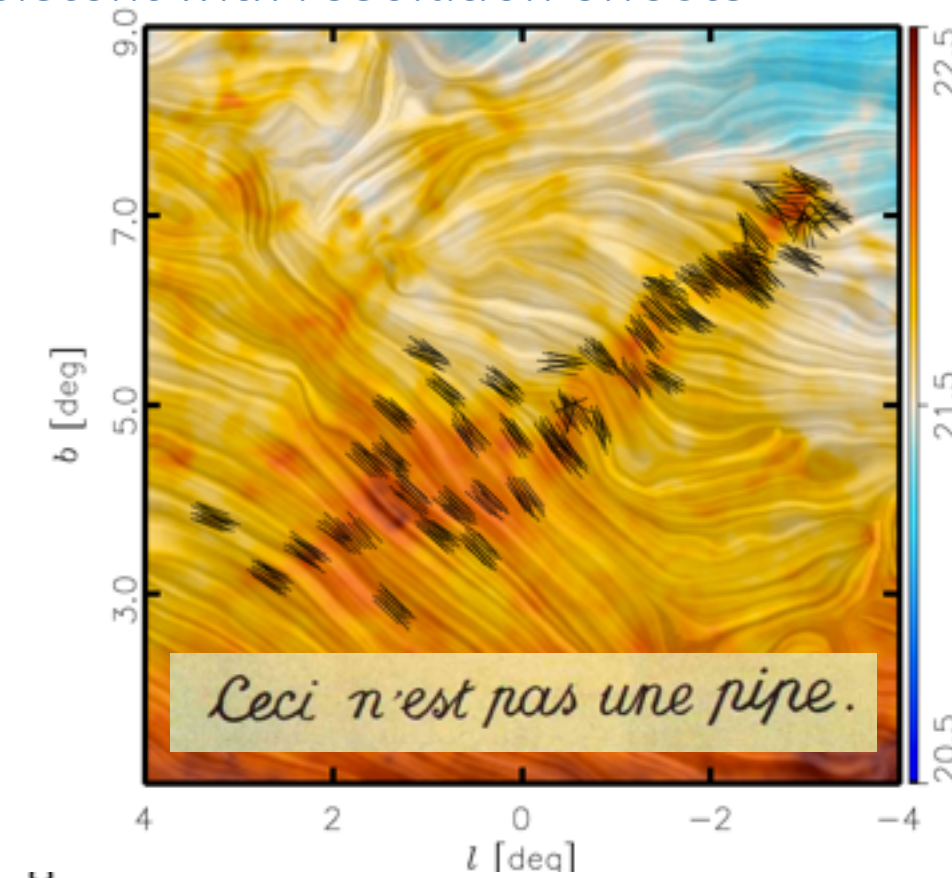
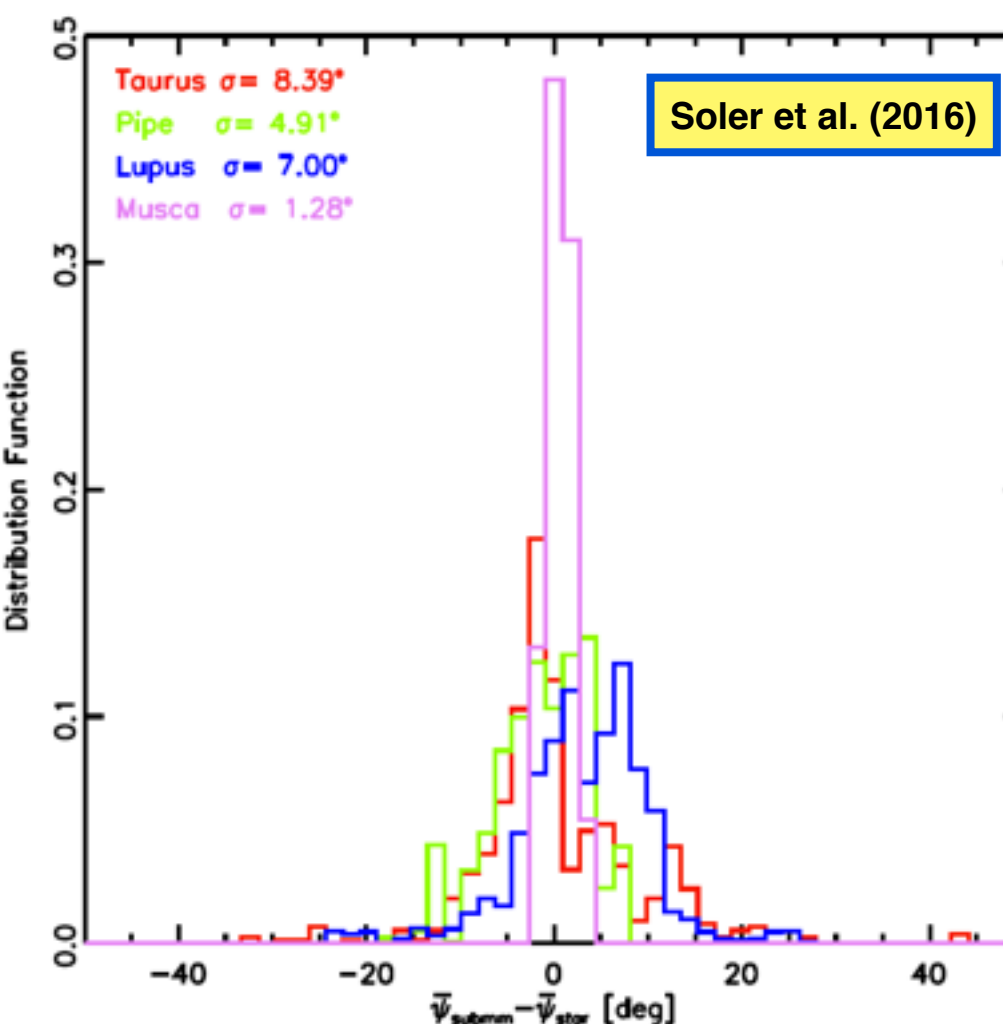
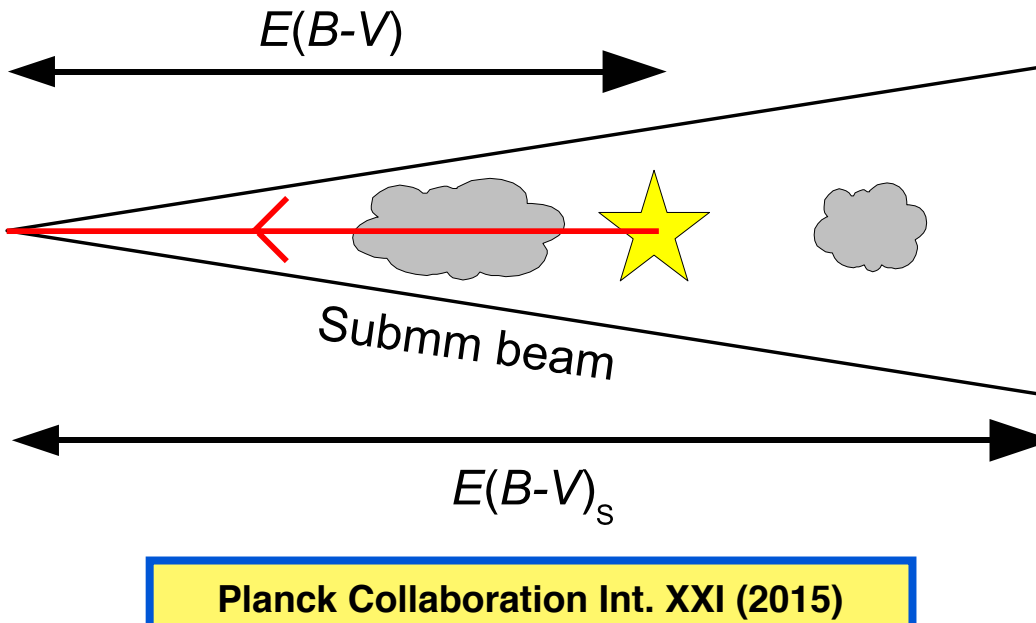


$$R_{P/p} = \frac{P_S}{p_V} = 5.4 \pm 0.2 \pm 0.3 \text{ MJy sr}^{-1} \quad (\text{Stat}) \quad (\text{Syst})$$

- Much more discriminating diagnostic
- Current dust models predict a value lower by a factor 2.5

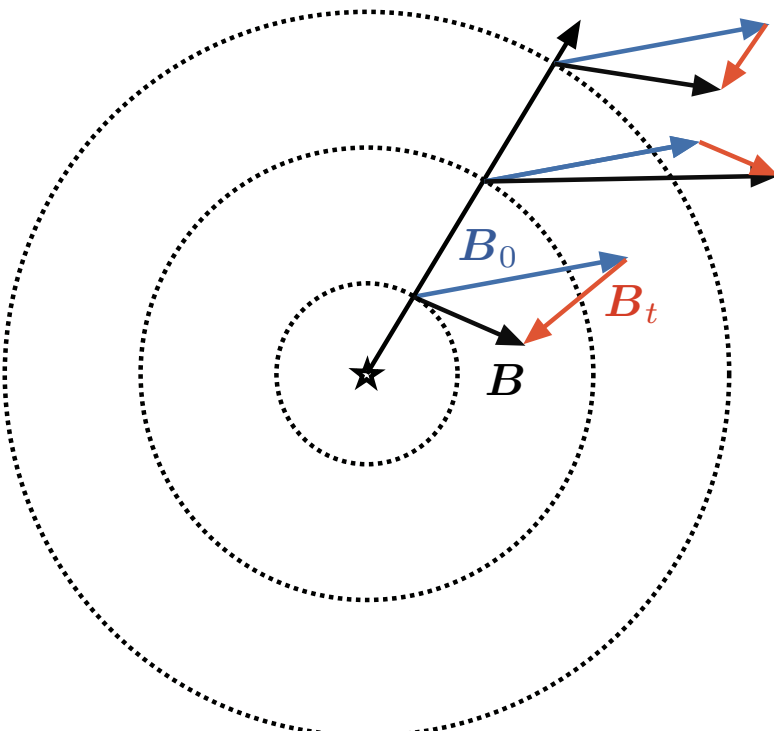
Comparison with starlight polarization in extinction

- Starlight polarization in extinction in NIR/visible probes much smaller scales than Planck data
- Differences in polarization angles are small and consistent with resolution effects



Perspectives on modelling polarized thermal dust emission

- Stacking of a small number of polarized emission layers, with POS spatial correlations



$$B = B_0 + B_t$$

Uniform field Turbulent field

Turbulent-to-mean ratio $f_M = \frac{\sigma_B}{B_0}$

Spectral index of the turbulent component $C_\ell \propto \ell^{\alpha_M}$

Molecular clouds $f_M = 0.5 \pm 0.2$

Planck Collaboration Int. XXXV (2016)

Diffuse ISM at high and intermediate latitudes $f_M = 0.8 \pm 0.2$

Planck Collaboration Int. XXXII (2016)

Southern Galactic cap $f_M = 0.9 \pm 0.1$

Planck Collaboration Int. XLIV (2016)

$$\alpha_M \in [-2, -3]$$

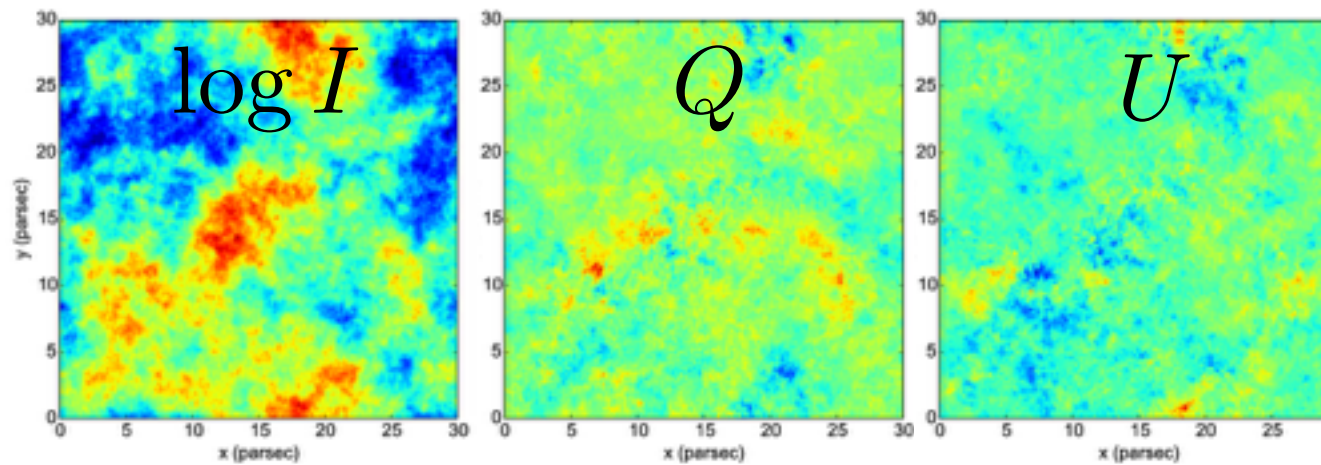
- Turbulent magnetic field modelled along the LOS, no POS correlation from pixel to pixel

WMAP 23 GHz polarized synchrotron data Miville-Deschénes et al. (2008)

Models of polarized thermal dust emission at 150 GHz O'Dea et al. (2012)

Modelling polarized thermal dust emission with fBm fields

- Dust density and magnetic field modelled by 3D fields with realistic spatial correlations
- Parameters are spectral indices, fluctuation levels, angle of the mean field and depth on the LOS
- Simulated polarization maps characterized by PDFs, power spectra, and correlations
- Monte-Carlo Markov Chain exploration of parameter likelihood given input polarization maps



$$\alpha_M = -2.53^{+0.13}_{-0.12}$$

$$f_M = 0.87^{+0.06}_{-0.08}$$

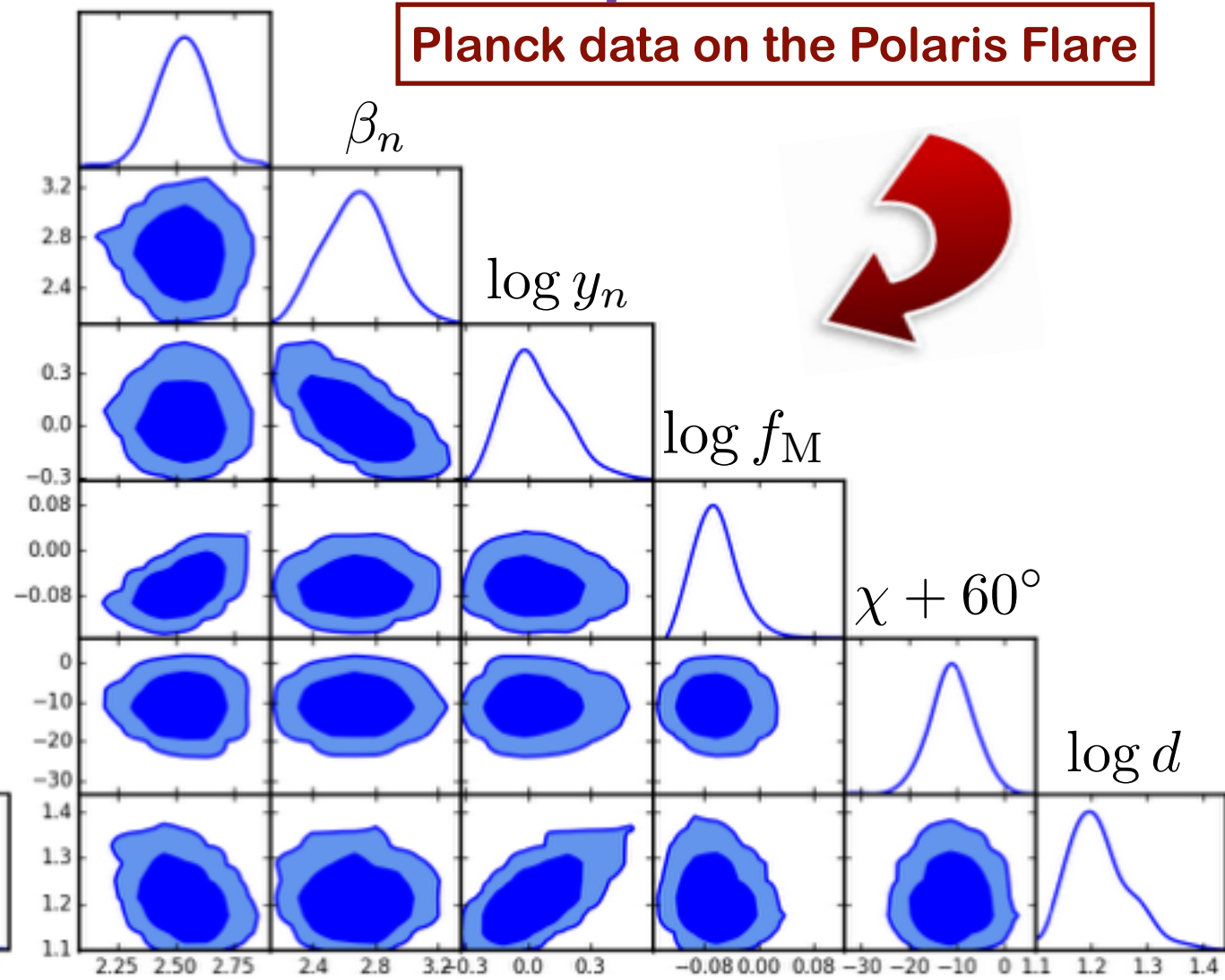
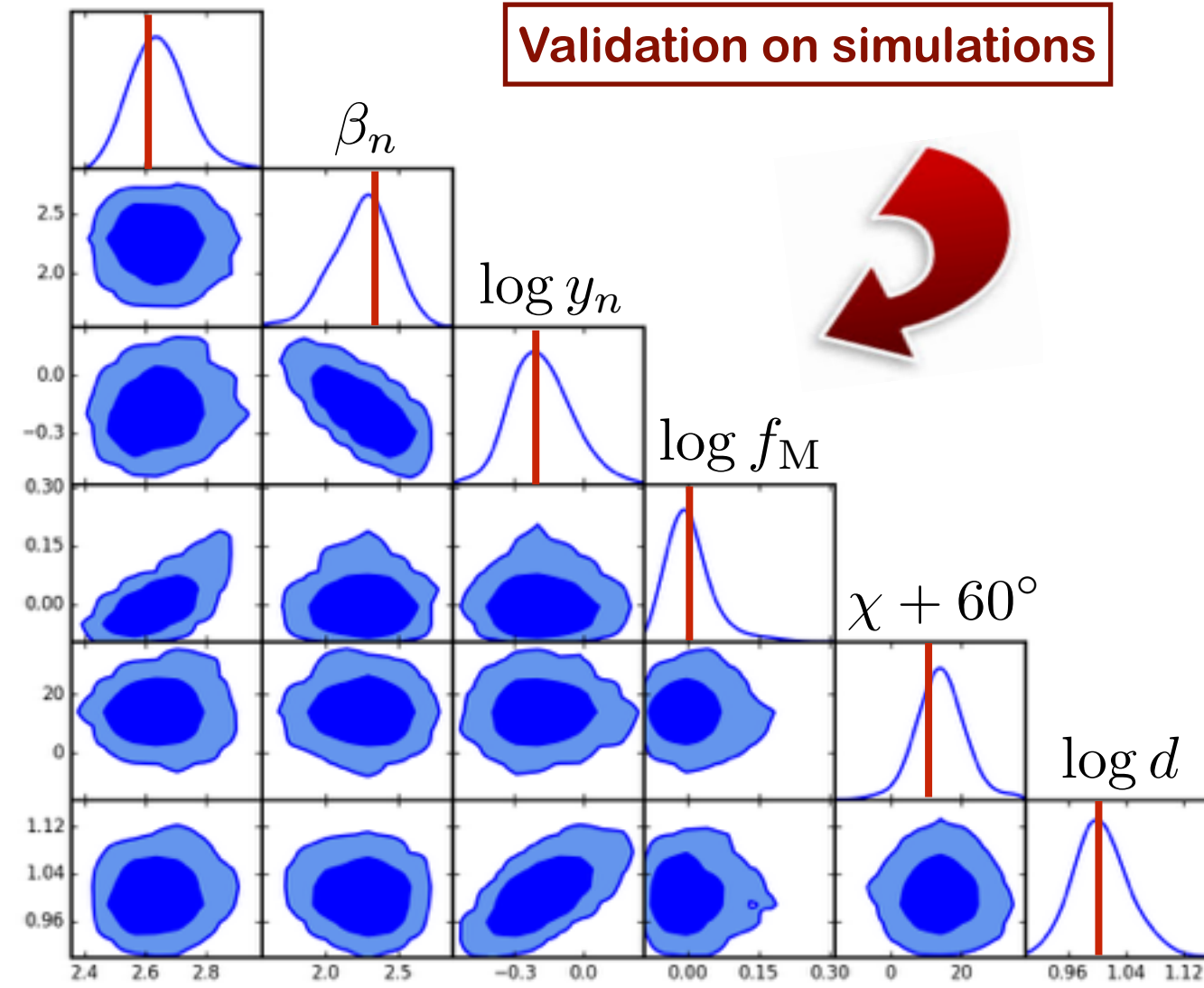
Levrier et al. (in prep)

$-\alpha_M$

Validation on simulations

$-\alpha_M$

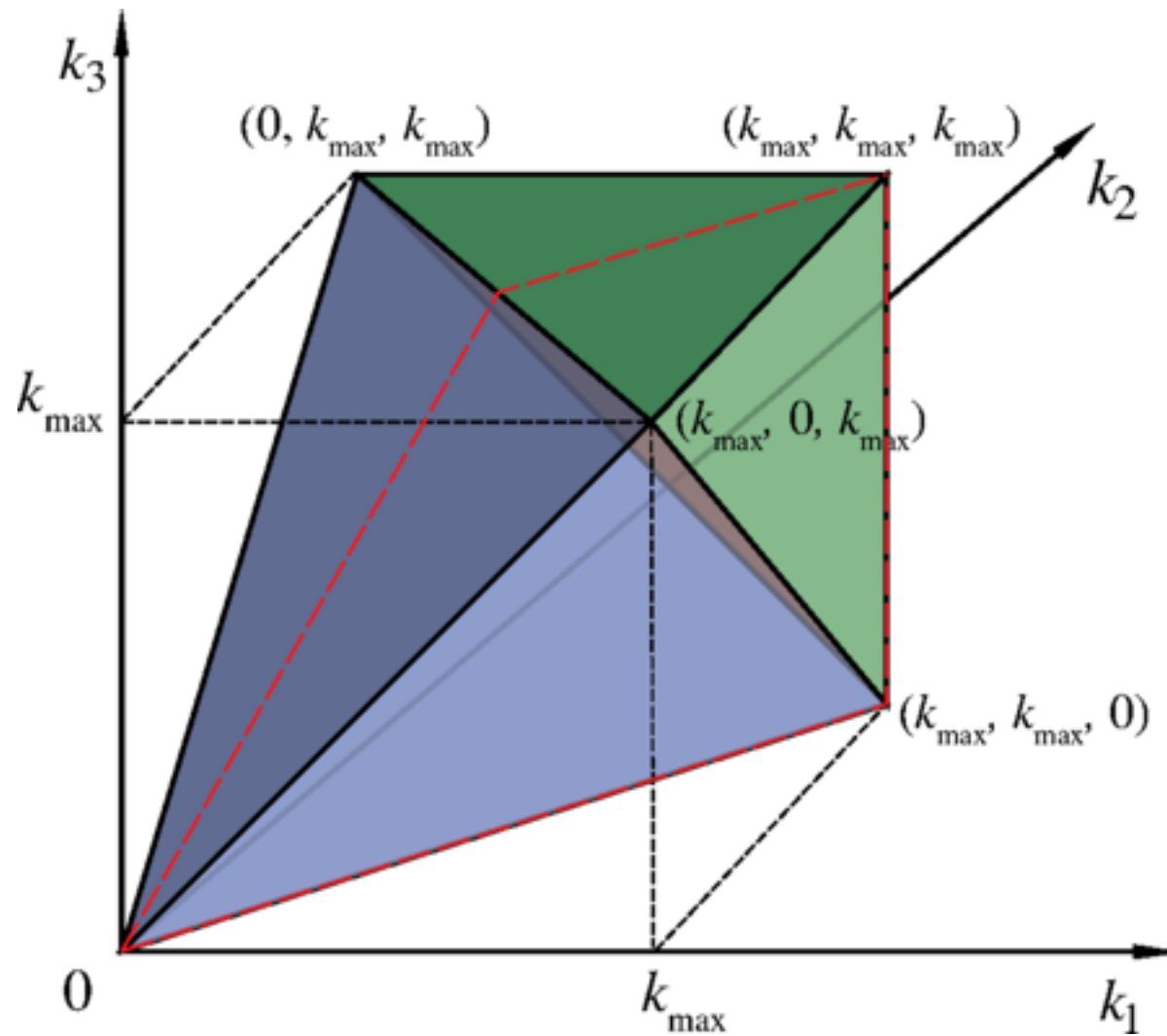
Planck data on the Polaris Flare



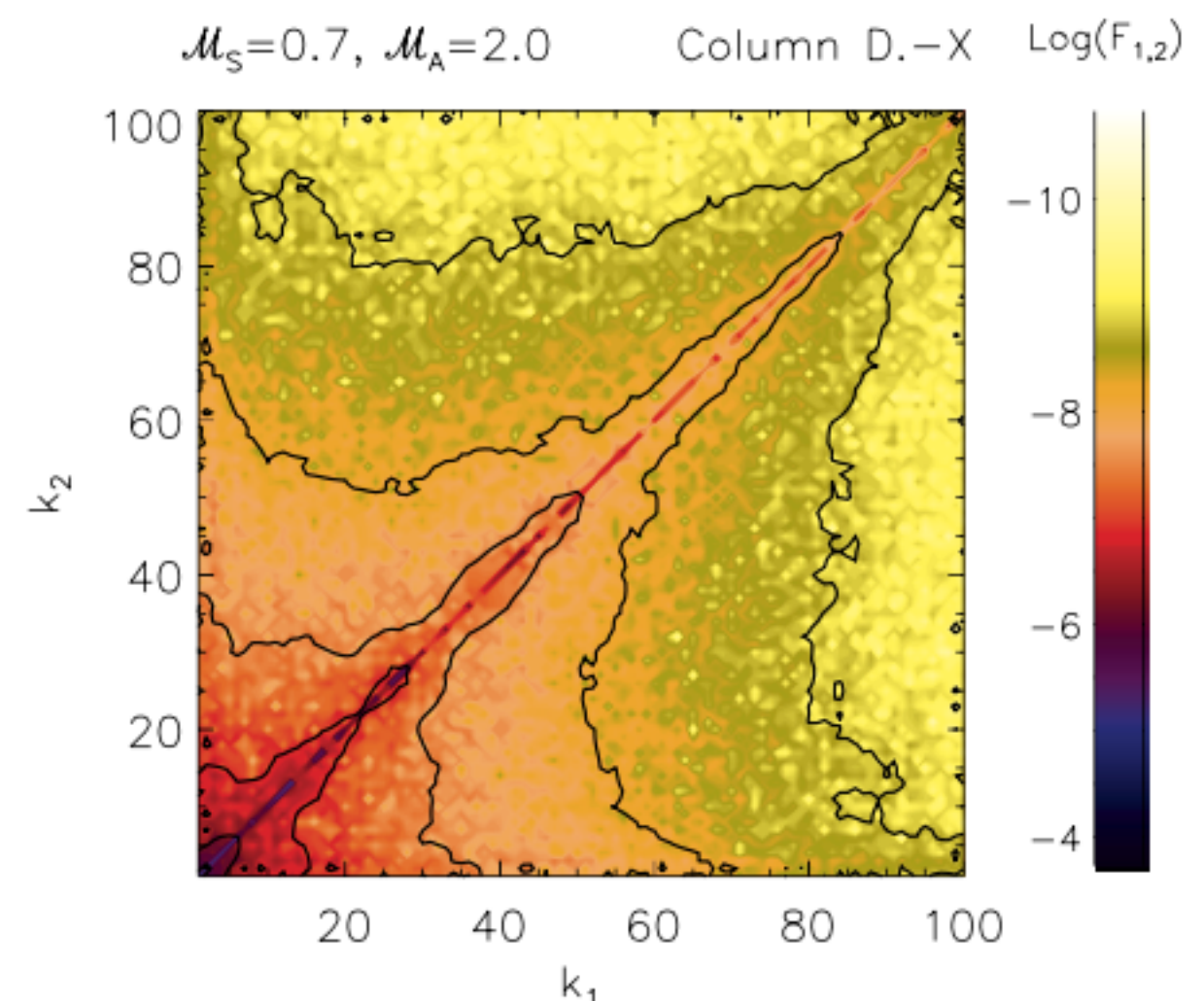
Higher-order statistical tools

- So far, one- and two-point statistical diagnostics (PDFs, power spectra)
- Using higher-order tools such as bispectra is the next step
- Will allow characterization of non-Gaussianities in the polarized dust emission maps

$$\langle \Phi(\mathbf{k}_1)\Phi(\mathbf{k}_2)\Phi(\mathbf{k}_3) \rangle = (2\pi)^3 \delta^{(3)}(\mathbf{k}_1 + \mathbf{k}_2 + \mathbf{k}_3) B_\Phi(\mathbf{k}_1, \mathbf{k}_2, \mathbf{k}_3)$$



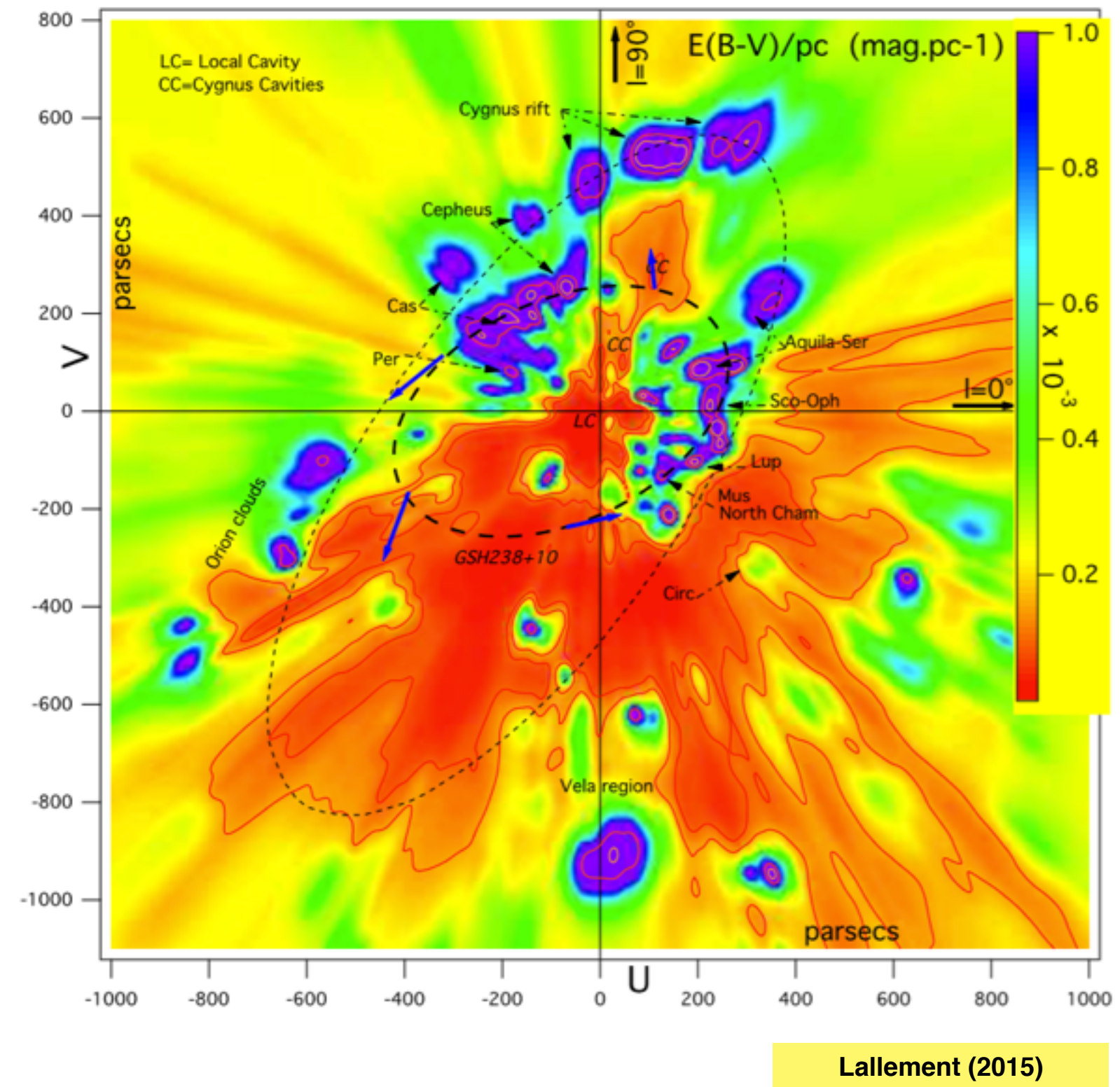
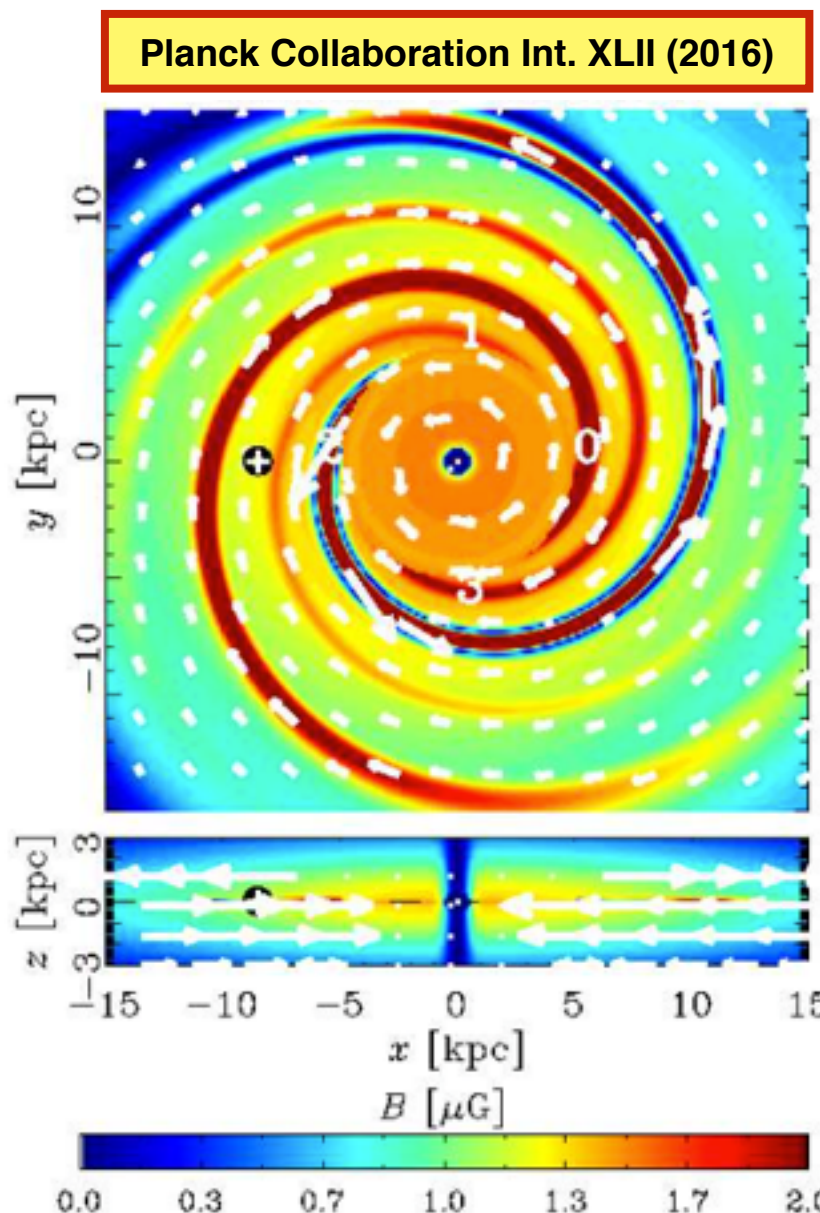
Lazanu et al. (2015)



Burkhart et al. (2009)

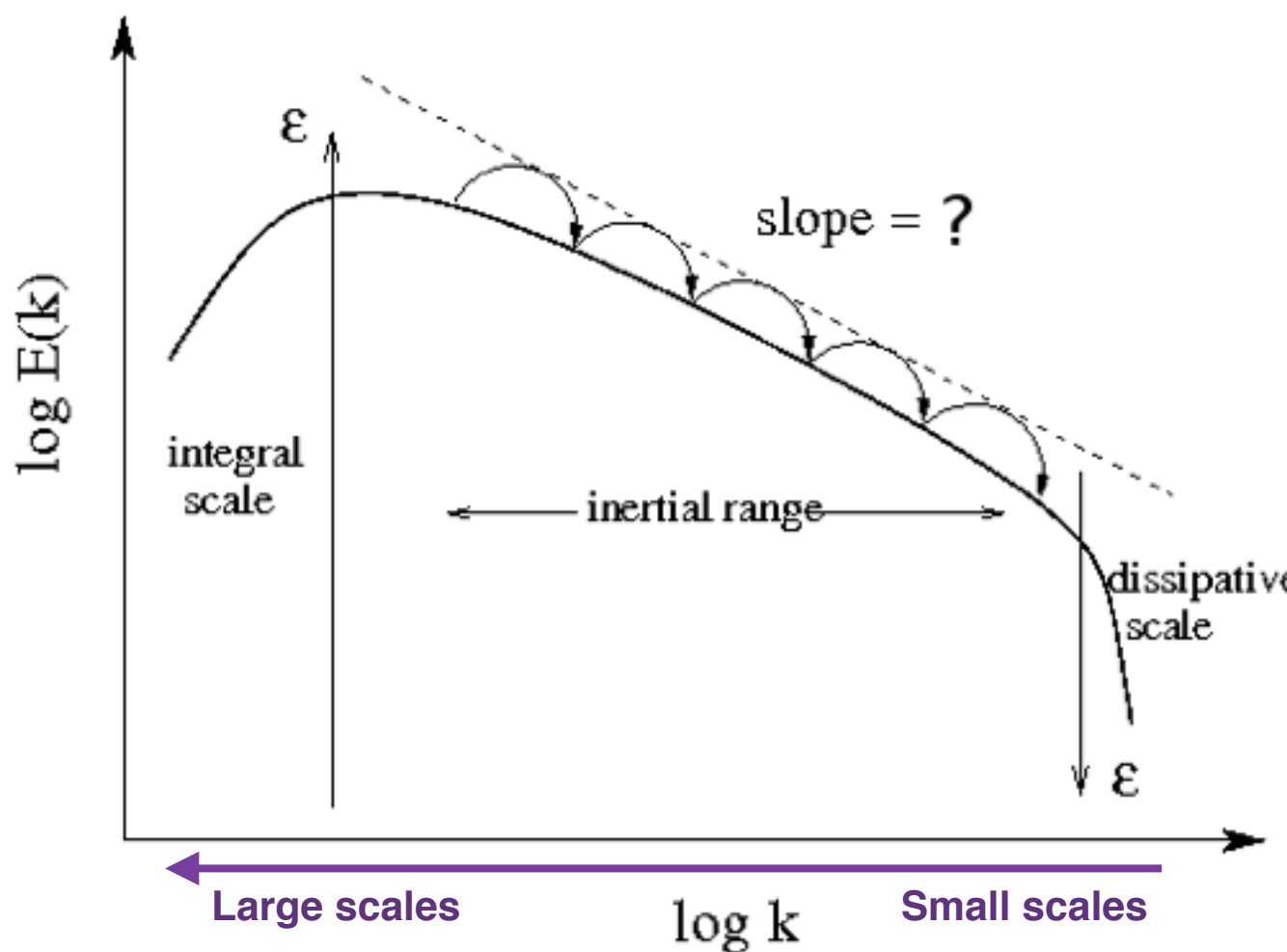
Modelling of the large-scale field

- The large-scale magnetic field is not uniform, unless at high latitude and in small fields of view
- Use large-scale field models of Janson & Farrar or Jaffe
- Local bubble modelling using the Lallement model of dust distribution



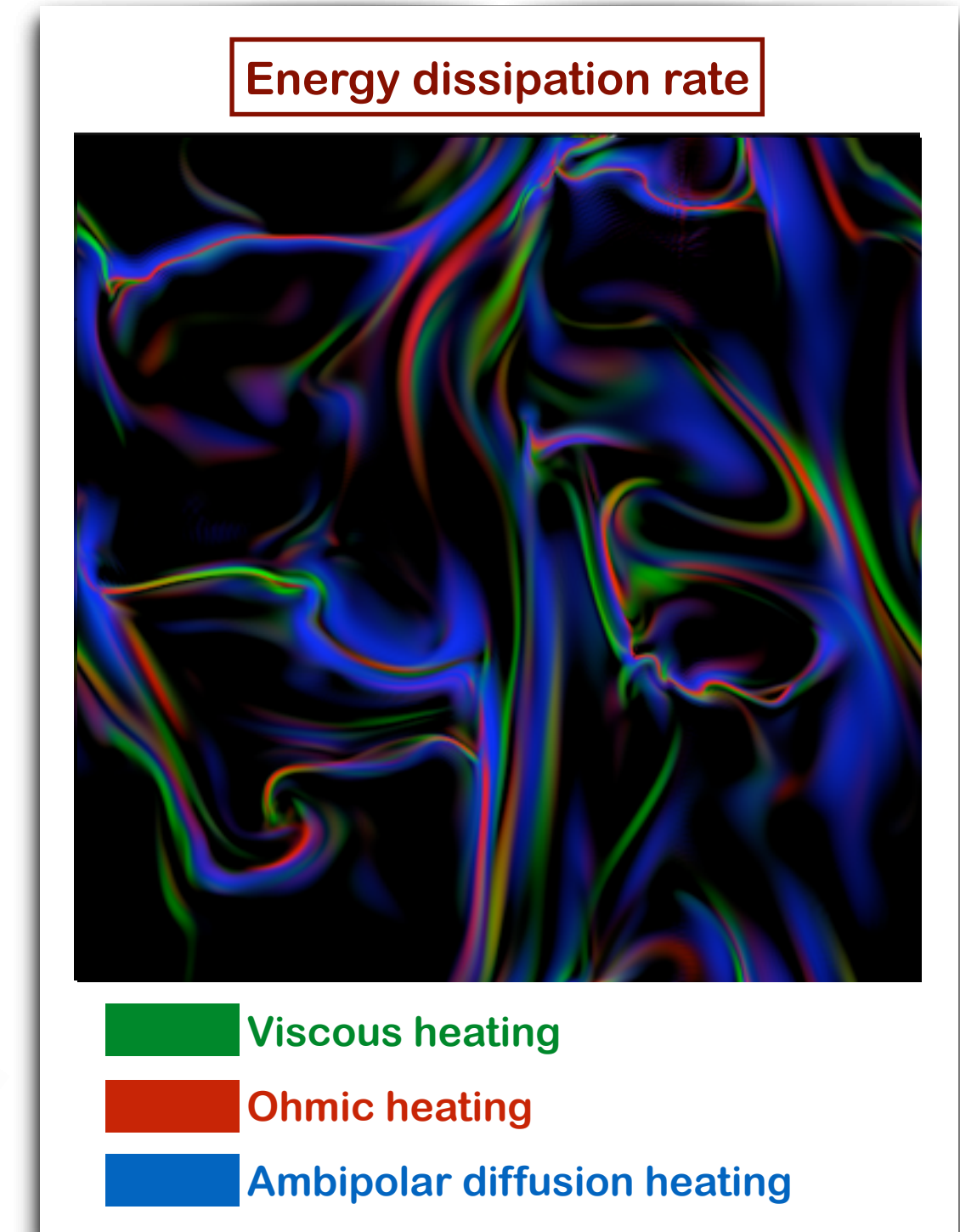
Injection and dissipation scales

- More realistic turbulent magnetic field models should not be fully scale-invariant
- Phenomenological cut-offs at large and small scales : injection and dissipation scales
- Dissipation comes in several guises...



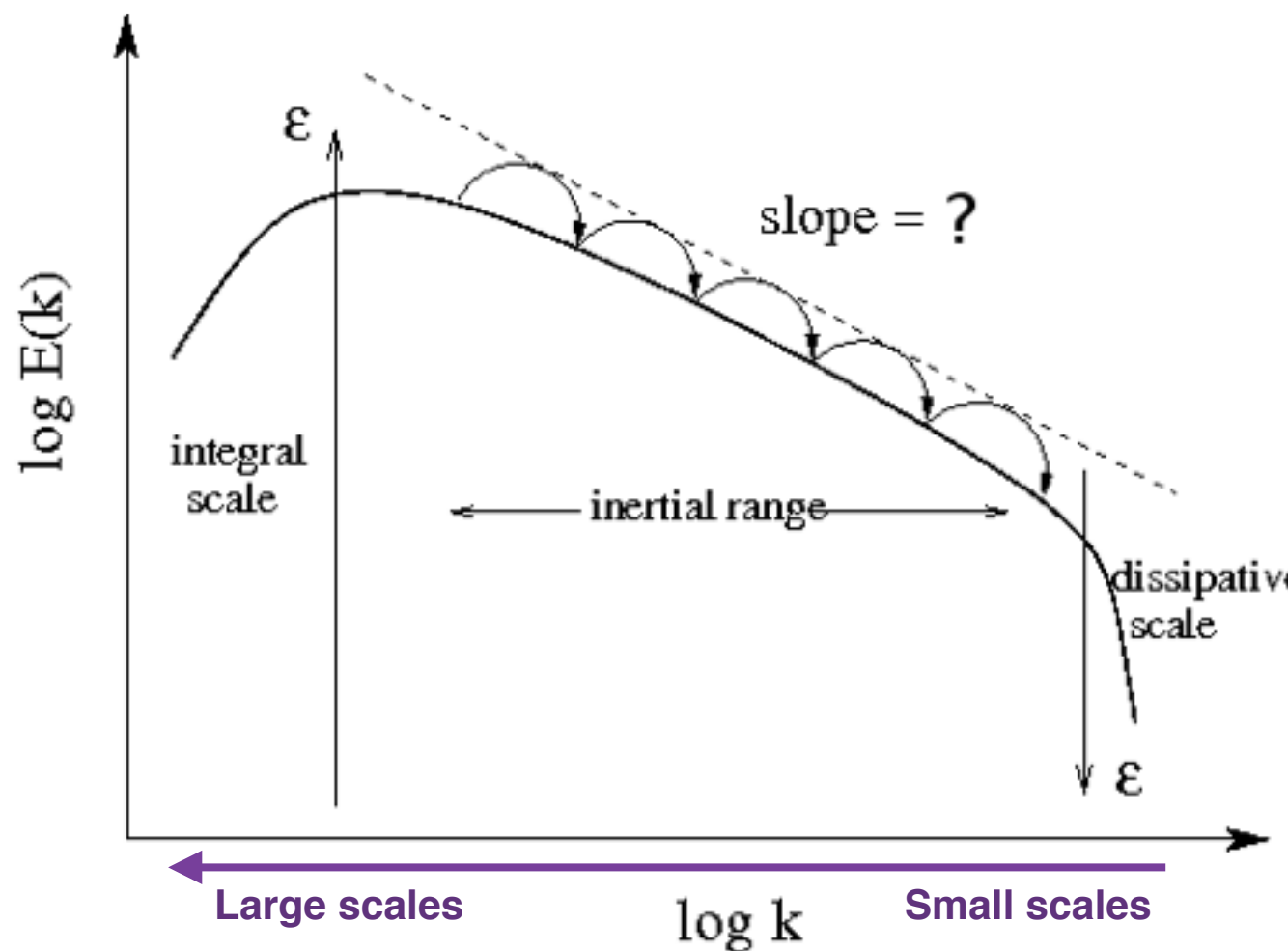
2D cut through a 512^3 incompressible MHD turbulence simulation

Momferratos et al. (2014)



Injection and dissipation scales

- More realistic turbulent magnetic field models should not be fully scale-invariant
- Phenomenological cut-offs at large and small scales : injection and dissipation scales
- Dissipation comes in several guises...

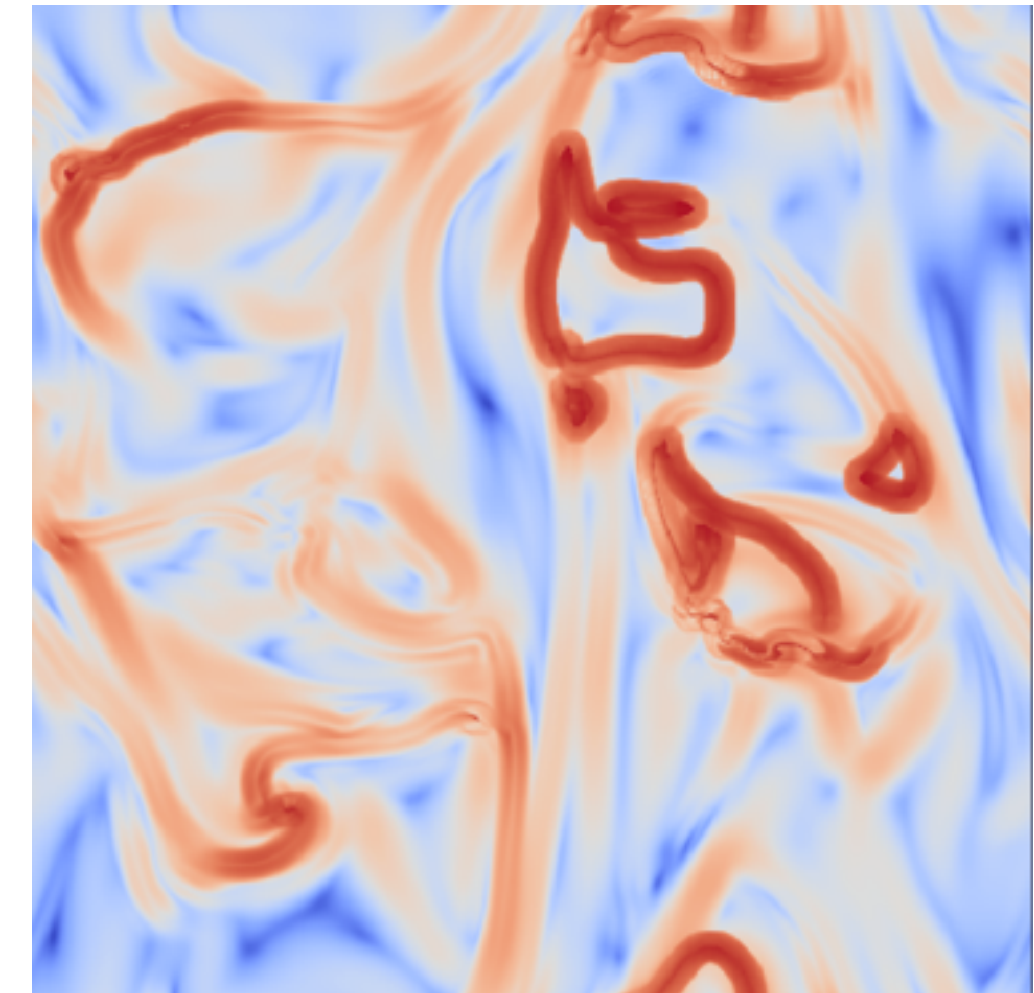


2D cut through a 512^3 incompressible MHD turbulence simulation

Momferratos et al. (2014)



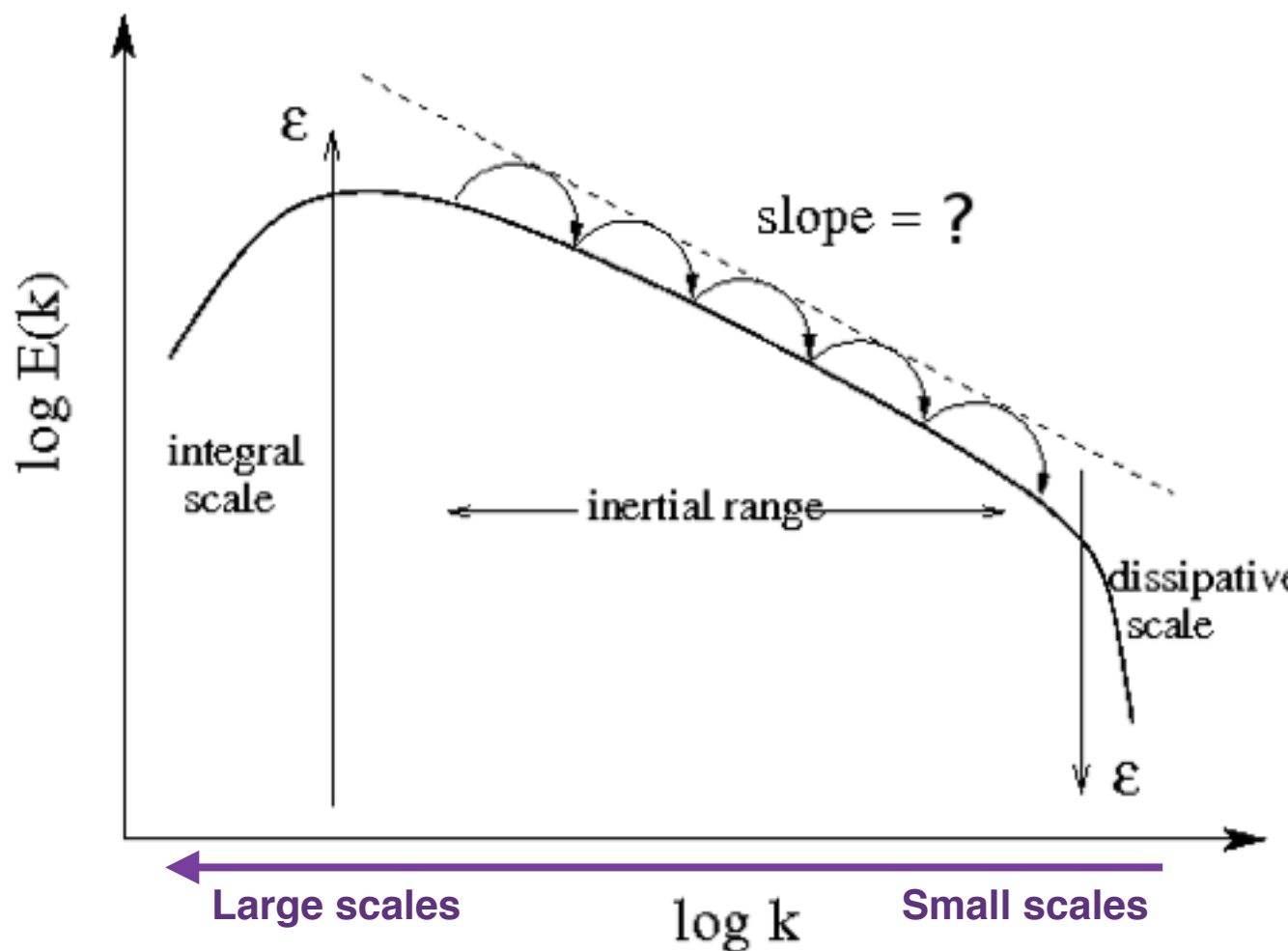
POS B field angular dispersion



Dissipation occurs in regions with sharp changes of the magnetic orientation

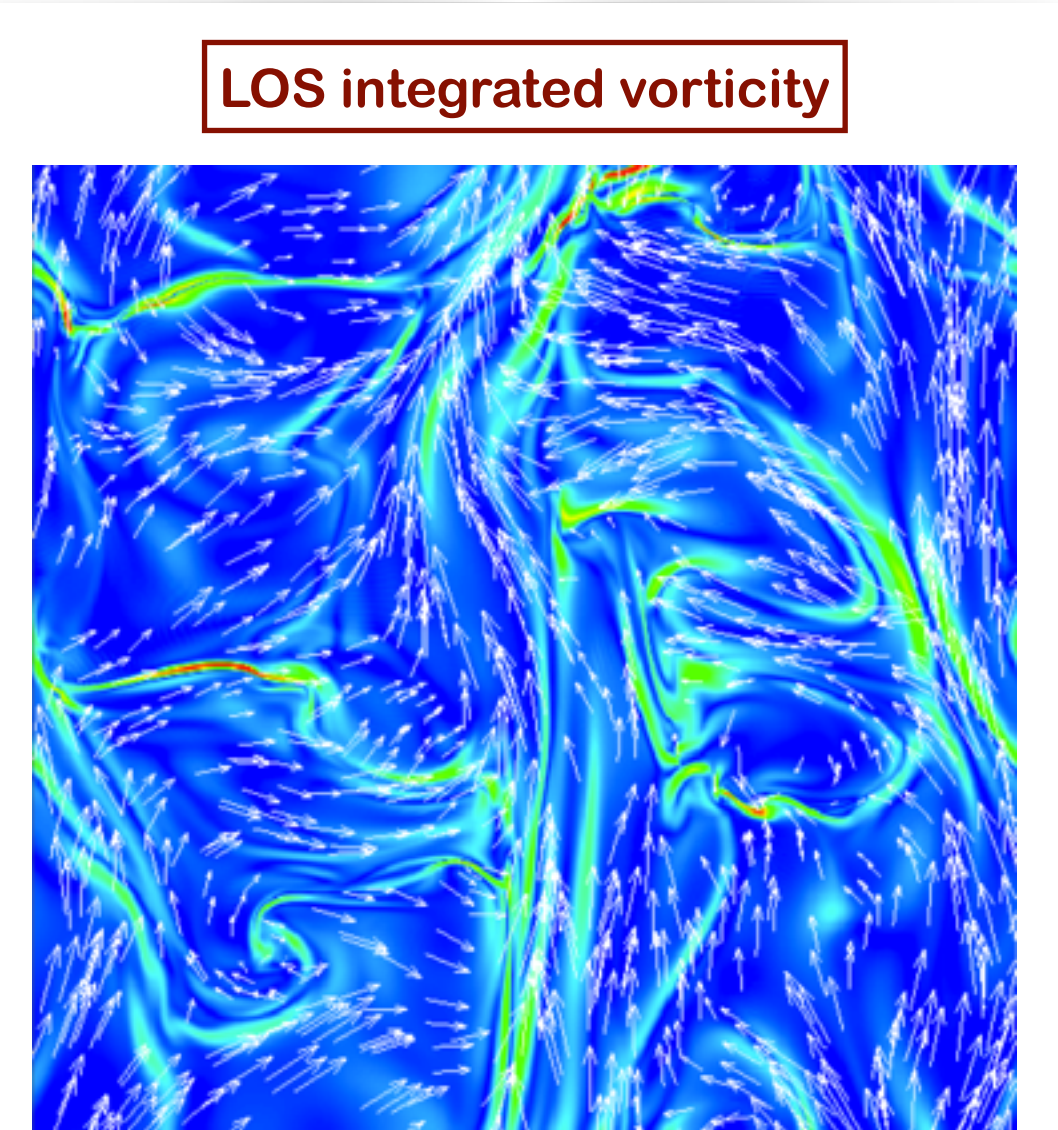
Injection and dissipation scales

- More realistic turbulent magnetic field models should not be fully scale-invariant
- Phenomenological cut-offs at large and small scales : injection and dissipation scales
- Dissipation comes in several guises...

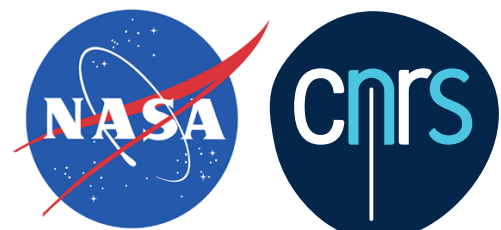


2D cut through a 512^3 incompressible MHD turbulence simulation

Momferratos et al. (2014)



... and they correspond to regions of large vorticity of the velocity field



DTU Space
National Space Institute



Science & Technology
Facilities Council



DLR Deutsches Zentrum
für Luft- und Raumfahrt e.V.



planck

